Title

A Functional Toxicogenomics Approach to Characterize Genotoxicity Mechanisms of the Environmental Contaminant Trichloroethylene

Author

De La Rosa, Vanessa Yvette

Publication Date

2014

Peer reviewed|Thesis/dissertation

A Functional Toxicogenomics Approach to Characterize Genotoxicity Mechanisms of the Environmental Contaminant Trichloroethylene

By

Vanessa De La Rosa

A dissertation submitted in partial satisfaction of the requirements for the degree of

Doctor of Philosophy
In
Molecular Toxicology
in the
Graduate Division
of the
University of California, Berkeley

Committee in charge:

Christopher Vulpe
Daniel Nomura
David Drubin

Fall 2014

Abstract

A Functional Toxicogenomics Approach to Characterize the Genotoxicity Mechanisms of the Environmental Contaminant Trichloroethylene

by

Vanessa De La Rosa

Doctor of Philosophy in Molecular Toxicology

University of California, Berkeley

Professor Christopher Vulpe, Chair

Trichloroethylene (TCE) is an environmental contaminant and human carcinogen that remains an environmental health hazard decades after its introduction. While evidence from rodent and epidemiological studies suggests a mutagenic mode of action mediating TCE kidney carcinogenesis, there remains a lack of molecular evidence to support the association between TCE exposure, mutagenesis and cancer. A clearer understanding of the molecular mechanisms mediating TCE exposure and cancer will strengthen risk assessment analyses, exposure standards and policies regarding TCE cleanup. Advances in genomic technologies make a functional genomics approach in *Saccharomyces cerevisiae* an appealing platform for elucidating toxicity mechanisms for a range of environmental contaminants. The studies of this dissertaion aim to utilize functional profiling platforms in model organisms to (1) identify novel insights into heavy metal and TCE toxicity; (2) assess and characterize the genotoxicity of TCE; and (3) identify candidate human toxicant susceptibility genes.

Heavy metals are widely distributed environmental contaminants increasingly associated with a range of adverse health effects, including neurological disease, developmental abnormalities and cancer. We used functional profiling in yeast to identify ion specific and common molecular pathways that mediate heavy metal toxicity. Our studies with the metals cadmium, lead and zinc revealed that a common subset of pathways and processes, including intracellular trafficking, vacuolar function and protein catabolism are required in response to heavy metal exposure. In the presence of Pb, Cd, and Zn, mutants deficient in components of iron and copper metabolic pathways were hypersensitive, suggesting that metal toxicity is mediated by alterations in iron metabolism. Copper is required for iron uptake, suggesting iron deficiency may be a secondary effect of copper deficiency. Thus, some of the cytotoxic effects associated with these metals could result from disruption of metal homeostasis. These studies revealed the importance of metal homeostasis and identified additional mechanisms important in heavy metal toxicity.

A similar functional genomics approach in yeast was employed to profile trichloroethylene metabolites, including the implicated penultimate metabolite in the kidney, dichlorovinyl cysteine (DCVC). Specific DNA repair pathways such as 1) error prone translesion synthesis repair 2) nucleotide excision repair and 3) homologous recombination were required in response to DCVC exposure. The phenotypic profile generated by DCVC showed high similarity to those

of known DNA interstrand crosslinking agents, implicating direct DNA damage and mutagenic repair as a potential mechanism of renal toxicity. A combination of functional studies in the avian DT40 system and human cell lines deficient in DNA repair were conducted to confirm and further characterize the DNA damage repair response to DCVC. While DNA repair in eukaryotes is highly conserved, these platforms allowed for additional analysis of DNA repair systems not present in yeast. DT40 translesion synthesis mutants were hypersensitive to DCVC, as observed in yeast and supported a role for mutagenic DNA repair in TCE toxicity. This hypothesis was further supported by an increased frequency of point mutations, insertions and deletions at low DCVC exposure levels. Interestingly, strains defective in the Fanconi anemia (FA) repair pathway and homologous recombination were unaffected and hyper-resistant, respectively, to DCVC exposure. This finding is in contrast to prior studies describing the repair of ICL agents and suggests a recombination independent mechanism for repairing DCVC induced DNA damage. Taken together these *in vitro* studies provide mechanistic evidence supporting a mutagenic mode of action for TCE that is mediated by the metabolite DCVC.

Table of Contents

Dedication

This work is dedicated to those I love the most- Alyssa, Chris, Dad, Mamasita and the Reynas

List of Figures

Chapter 5.

Abbreviations

ADH- alcohol dehydrogenase
ALDH- aldehyde dehydrogenase
ANOVA – analysis of variance
ATSDR – Agency for Toxic Substances and Disease Registry
AUC – area under the curve
CGDP- cysteine glutamyl dipeptidase
CH- chloral hydrate
CYP- cytochrome P450
DCA- dichloroacetic acid
DCVC- dichlorovinyl cysteine
DCVG- dichlorovinyl glutathione
DCVT- dichlorovinyl thiolate
DSB- double strand break
DSSA- Differential strain sensitivity analysis
DT40- avian lymphoblast cell line
EPA- Environmental Protection Agency
FA- Fanconi anemia
GFP – green fluorescent protein
GGT- gamma glutamyl transpepdidase
Gluc- glucuronide
GO – Gene Ontology
GSH- glutathione S-transferase
HR- homologous recombination
IARC- International Agency for Research on Cancer
ICL- interstrand crosslink
KIM-1- kidney injury molecule-1
MN- micronucleus
NER- nucleotide excision repair
NHANES – National Health and Nutrition Examination Surveys
PCNA- proliferating cell nuclear antigen
PDA- parallel deletion analysis
ROS- reactive oxygen species
TCA- trichloroacetic acid
TCE- trichloroethylene
TCOH- trichloroethanol
TK- thymidine kinase
TLS- translesion synthesis
TS- template switching
Ub- ubiquitin
UGT- uridinediphosphoglucuronyl transferase
VHL- von Hippel Lindau
WES- whole exome sequencing
WS- Werner's syndrome
WT – wild-type
YPD – yeast extract-peptone-dextrose

Acknowledgments

Chris Vulpe- I have gone through this heels dragging. Thank you for your continued support and enthusiasm. You have helped me to grow not just as a scientist, but as an educator and mentor. I am grateful for the abundant opportunities you have given me to see the world, pursue my passions and find new ones.
Mani, Jonathan, Leona, David and Brandon. Each of you made lab a joy, interesting and entertaining. Mani, our coffee breaks and daily banter kept me going strong. Leona, thanks for making me laugh and baking delicious treats. Jonathan, a great mentee and reminder of what I enjoy most about science…mentoring! Thanks for your dedication to all things exciting and mundane. Brandon, conference partner in crime, writing buddy and mentor. Thanks.

Familia- Through your many sacrifices I have achieved success. Thank you. Your everlasting support and unconditional love from near and far have inspired me to prosper. Grammy y Grampy te extraño y espero que estan orgullosos. Uncle Jerry your influence, support and perseverance continue to guide me. Yes, Dad, I'm finally done! Your tough love helped me to see this through. Seems I couldn't sprint this last lap fast enough…as usual! I wish you were here. You are all beautiful reminders that this is only the first of many great things you dreamed I would accomplish. Not a moment to waste.

My closest confidants- Thank you for seeing me through the darkest of times. I am forever here for you. Brandon: No hay palabras…. Has sido el mejor de mejores amigos. Gracías por tu constante apoyo y aliento. Trajiste el diversión, la risa, el enfoque y la felicidad cuando lo necesitábamos más. Gracías por siempre escuchando y dando abrazos fenomenales…los extrañaré muchísimo! Chuck: Gym partner and friend. Thanks for welcoming me to NST, helping me de-stress at the gym and making me laugh over coffee with your witty music references. Cyndi, Krissett and Priscilla: Thanks for always answering the phone all these years and making me laugh from afar. Jon, Allison and David: Thank you for bringing me back to life and showing me how to have fun again. The happy hours, rock climbing and shenanigans have helped me to finish this last stretch with a smidge of sanity and wonderful memories. I will miss you tons! Steve: colleague, best friend and stellar co-habitant. Your humor, candor and willingness to go on adventures in Albany and beyond have brought me smiles when I needed them most. Vince: Even when I felt most discouraged about my science you always saw the positive. I aspire to be a fraction of the great scientist and thinker you are. Thank you for believing in me when I didn't. Beta Lounge: My refuge for liquid courage. Nothing will ever compare.

IMSD and SACNAS- John, Corey, fellows and SACNISTAS: You have been a family away from home. Your support, sage advice, warmth and kindness have given me confidence as a scientist, educator and latina. Gracías!

CHAPTER I

INTRODUCTION

History of Trichloroethylene

Trichloroethylene (TCE) is a chlorinated organic solvent, environmental contaminant and human carcinogen (1,2). Introduced in the 1920's as a replacement for chloroform and ether, TCE was utilized for medical anesthesia, dry cleaning processes, and as an industrial metal degreaser (1,3). By 1990, metal cleaning use accounted for between 80 and 95% of the trichloroethylene produced in the United States and Western Europe (4). Amid health concerns, the use of TCE declined at the start of the 21st century, but continues to be used mostly as a degreaser in industrial processes (4). This reduction in use has resulted in decreased occupational exposure, but TCE remains an environmental health hazard due to improper disposal and leaching from storage tanks into the surrounding soil, air and water (2,5). TCE is the most common water contaminant with an estimated 9-34% of drinking water sources contaminated with TCE and is the 3rd most prevalent contaminant at Superfund waste sites (2,5). Additionally, chronic indoor air exposure via TCE vapor plumes has become increasingly more common and relevant for the general population, though TCE blood levels remain low (6,7).

Role of Metabolism in TCE Toxicity

TCE is an electrophilic molecule that undergoes complex metabolism via two pathways, cytochrome P450 (CYP)-dependent oxidation and glutathione (GSH) conjugation (**Fig. 1.1**) (8). The preferrential pathway, oxidative metabolism, occurs mainly in the liver in both rodents and humans but has been observed in the lungs, testses, and kidney to lesser extents (4). Oxidative mtabolsim is mediated mainly by CYP2E1, but additional CYP enzymes such as CYP1A1/2, CYP3A4, and CYP2A6 have also been implicated in various steps of TCE metabolism (8,9). The chemistry of TCE and metabolism by CYP2E1 suggests a TCE-O-CYP intermediate followed by the formation of a highly reactive TCE epoxide intermediate, though these predicted metabolites have not been observed or measured in any cellular system (10). The initial CYP reaction yields a chloral hydrate metabolite, which is reduced to trichloroethanol (TCOH) by alcohol dehydrogenase (ADH) or oxidized by aldehyde dehydrogenase (ALDH) to form trichloroacetic acid (TCA). Trichloroethanol can undergo glucuronidation, forming a TCOH-glucuronide that has been measured as the major metabolite in urine (11). The glutathione conjugation pathway is a common detoxification pathway for electrophilic xenobiotics, but has been shown to yield bioactive metabolites that are more toxic than the parent compound for a variety of organic halogens (12,13). Mass spectrometry measurements in rodents with CYP-mediated metabolism saturated by TCE showed glutathione conjugation metabolites are formed less than oxidative metabolites by a whole order of magnitude indicating that glutathione conjugation serves as a secondary mechanism (14). While oxidative metabolism occurs primarily in the liver, GSH conjugation of TCE is concentrated to the kidney due to higher levels of gamma glutamyl transpeptidase (GGT), cysteine conjugate dipeptidases (CGDP) and beta-lyase levels in the kidney compared to the liver. TCE is conjugated with glutathione by glutathione S-transferase (GST) to form the dichlorovinyl glutathione conjugate. Upon distribution via the hepatic portal vein to the kidney for excretion, DCVG is metabolized by GGT and CGDPs to form the

penultimate reactive metabolite DCVC (8,15,16). In the kidney, DCVC is metabolized by cysteine conjugate beta-lyases to form a potent and highly reactive dichlorovinyl thiolate (DCVT) intermediate that can tautomerize to form a reactive thioketene capable of damaging DNA (12,13).

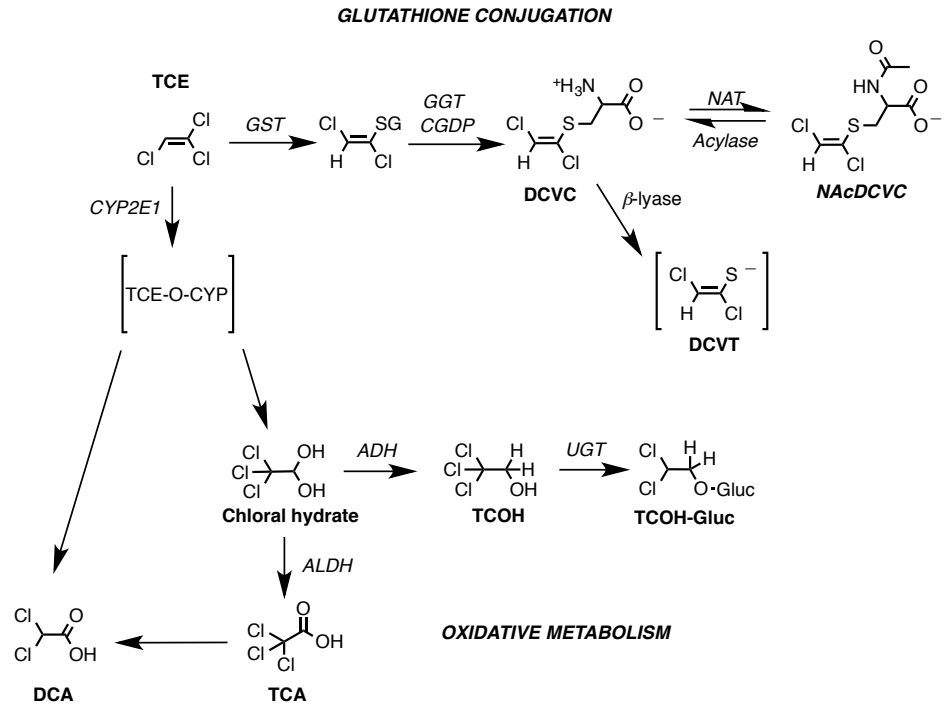

Figure 1.1. Overview of TCE metabolism and the chemical structures of important metabolites associated predominately with toxicity and carcinogenesis

Numerous studies over the last 25 years have established the role of metabolism in mediating TCE toxicity (8,9,15-17). Oxidative metabolites are associated with liver toxicity and cancer, whereas the glutathione conjugates are implicated in renal toxicity and cancer (15,18,19). Of particular interest are the conjugate metabolites DCVG and DCVC. Both are nephrotoxic, but DCVC is considered the penultimate toxic metabolite causing changes in kidney morphology, renal function and cytotoxicity *in vitro* and *in vivo* (20-25). Recent work by Vermeulen *et al.* reported an increase in the nephrotoxicity biomarker KIM-1 in TCE exposed workers, suggesting that chronic, low level exposures can also cause renal damage in humans (26). Trichloroethylene alone is not considered genotoxic, but DCVG and DCVC have shown mutagenicity in the Ames test, increased unscheduled DNA synthesis, double strand breaks, and chromosomal aberrations, suggesting a mutagenic mode of action (19,21,27-29). Chemical inhibition of glutathione conjugation enzymes *in vitro* and *in vivo* results in decreased nephrotoxicity and mutagenicity, confirming the significant role of metabolism-dependent bioactivation in mediating renal toxicity (8,25,30-32). However, the argument against a mutagenic mode of action is the minute level (less than 0.1% of the total metabolite formation) of DCVC produced and the instability of the reactive thiolate and thioketene intermediates are insufficient to elicit DNA damage and repair (33).

Trichloroethylene and Cancer

The Environmental Protection Agency (EPA) and the International Agency for Research on Cancer (IARC) classify TCE as a human carcinogen by all routes of exposure (5). There is strong evidence from rodent and epidemiological studies supporting the link between TCE exposure and renal cancer (4). The rarity of renal tumors in rodent and human populations makes the findings rather significant. To a lesser extent, evidence supporting associations with TCE exposure and leukemia, liver, and testicular cancers have also been reported (4). The epidemiological evidence regarding kidney cancer and occupational exposure to TCE was first reported in initial cohort studies by Brauch *et al.* (4,34-36). This was followed by a series of small international case control and cohort studies reporting mixed results on the association between kidney cancer and TCE exposure (4). A more recent meta analysis of all existing studies by Karami *et al* determined a relative risk ratio of 1.3 to 1.4, supporting an association between TCE and kidney cancer (37). Meta-analysis adjusting for the highest level of TCE exposure increased relative risk to 1.6, suggesting a dose response relationship (37). Occurrence of renal cell carcinoma is associated with mutations in the von Hippel Lindau (VHL) tumor suppressor gene. In the majority of cases, there is a propensity of small base changes, such as insertions, point mutations and deletions that result in loss of VHL function, protein truncation or altered expression (38). Brauch *et al.* analyzed renal cancer cell tissues for mutations of the *VHL* gene in TCE exposed workers and reported an increased occurrence of mutations in patients exposed to high concentrations (34,36). A hot spot mutation of cytosine to thymine at nucleotide 454 (C454T) in exon 1 was found in 39% of samples that had a *VHL* mutation and was not found in renal cell cancers from non-exposed patients. This mutation results in a single amino acid change from proline to serine at codon 81 of the VHL protein (P81S) and causes deregulation of HIF factors *in vitro* and suppression of apoptosis in tumors (34,39). These initial results suggested a unique genetic signature for TCE exposure and a mechanism for the development of renal cell carcinoma, yet proceeding studies were unable to observe any significant increase in *VHL* mutations and concluded the high frequency of mutations was irrespective of TCE exposure (35,38). While such findings would provide a link between TCE and renal cancer, inconcistencies in sample size, analysis, risk factors and exposure history render these results inconclusive. There remains a need for molecular evidence supporting a mutagenic mode of action in mediating TCE renal cancer. With the advancement in next generation sequencing and the availbility of genome-wide functional profiling platforms, these tools can be utilized in conjunction with human studies to better assess genotoxicity and mutagenic potential as well as identify exposure signatures (40,41).

Functional Genomics: A tool for assessing genotoxicity

Trichloroethylene has been subjected to a battery of traditional genotoxicity tests over the last 25 years, yielding inconsistent results, but suggesting a mutagenic mode of action in mediating renal toxicity and cancer even without adequate mechanistic evidence. This long-lasting approach for identifying and characterizing genotoxicants has relied heavily on a combination of traditional analyses (**see Table 1.1**), but these tests suffer from high false positive/negative rates and do not offer mechanistic insight on genotoxicity. The Ames test is a bacterial reverse mutation test that detects mutations using strains of *Salmonella typhimurium* (42). Potential mutagens revert mutations present in the strain and restore the functional capability of the bacteria to synthesize

an essential amino acid. While rapid and inexpensive, this system does not accurately portray metabolism, requiring the addition of a metabolically active extract and exhibits poor sensitivity (43,44). Similar forward mutation assays in yeast and mammalian systems include the canavanine resistance (CanR), thymidine kinase (TK) and hypoxanthine-guanine phosphoribosyl transferase (HPRT) tests with mutations measured at the respective loci. The advantage of the thymidine kinase (TK) assay is the autosomal location of the TK locus, which allows for the detection of genetic events such as large deletions and recombination that cannot be detected with the HPRT assay due to it's location on the X chromosome. These tests are more sensitive than the Ames test and have the advantage of metabolism, but suffer from a lack of specificity resulting in false positives (43,44).

Table 1.1 Examples of traditional tests used to determine genotoxicity of chemicals

Assay	Model System	Endpoint
Ames test	bacteria	mutations
HPRT	mammalian	mutations
Thymidine Kinase (TK)	mammalian	mutations
Micronucleus	mammalian	chromosomal damage
Comet	mammalian	DNA damage
Chromosome aberrration test	mammalian	chromosomal damage
Sister Chromatid Exchange (SCE)	yeast, mammalian	DNA damage
Canavanine	yeast	mutations
FOA	yeast	mutations
PIG-O	DT40	mutations

HPRT, hypoxanthine-guanine phosphoribosyl transferase; FOA, 5-Fluoroorotic Acid Monohydrate; PIG-O, phosphatidylinositol glycan complementation group O

In addition to these mutation assays, a suite of chromosomal damage tests has been used both *in vitro* and *in vivo* to determine genotoxicity. The chromosomal aberration (CA) and micronucleus (MN) tests measure structural chromosome aberrations as well as chromosome polyploidy and duplication events. Many compounds that are positive in the CA test are mammalian carcinogens; however, there is not a correlation between this test and carcinogenicity. The sister chromatid exchange (SCE) assay detects reciprocal exchanges of DNA between two sister chromatids of a duplicating chromosome by differentially labeling sister chromatids. The comet assay is a highly sensitive method for measuring DNA strand breaks in individual cells. Again, these assays possess improved sensitivity, but lack specificity, are time consuming and are not amenable to high-throughput testing (43). The persistence of low specificity highlights the need for understanding the mechanisms that mediate genotoxicity in an effort to improve testing.

A functional toxicogenomics approach is amenable to (i) Identifying and characterizing genotoxicants (ii) Providing insight on the molecular pathways involved in mediating genotoxicity and carcinogenicity of toxicants (iii) Identifying novel endpoints to improve genotoxicity testing. With the advancement of gene technologies, functional profiling platforms are available in a variety of model systems, including *S.cerevisiae*, avian cell lines, human cell lines and C. *elegans* that can be utilized in the context of assessing genotoxicity (40). Discussed below are the models of focus for this dissertation.

Yeast

S. cerevisiae has long been a model organism in molecular biology research due to the myriad of resources available to the yeast community. The *S. cerevisiae* genome is extensively annotated and the majority of the metabolic, signaling, and stress response pathways are conserved in higher eukaryotes. Classical genetic studies in yeast have played a central role in elucidating the highly conserved mechanisms of mammalian DNA repair and genome maintenance (45). With the development of the yeast non-essential diploid deletion collection, genome-wide profiling in yeast has emerged as a tool to enhance our understanding of genotoxicants and DNA repair mechanisms (**Table 1.2)**. The deletion library consists of ~4,600 strains with each strain missing a single non-essential gene and each is uniquely identified by DNA ”barcodes” that are flanked by common primer sites (**Fig. 1.2**) (46). This approach allows for the simultaneous analysis of the entire deletion library, termed parallel deletion analysis (PDA). This approach has proven successful in previous studies investigating toxicity mechanisms across a wide range of toxicant classes including heavy metals, pesticides, and organic solvents (47-51). Several studies have examined a spectrum of chemicals, including novel therapeutics such as platinum acridines and imidazo compounds to determine genotoxicity and construct structure-activity relationships to reduce DNA damage and decrease resistance that is usually asssociated with chemotherapeutics (**Table 1.2**).

DT40 Avian cells

The DT40 avian cell line is a leucosis virus transformed B-lymphocyte cell line that undergoes high rates of efficient gene targeting via homologous recombination (52,53). This capability has allowed for the construction of isogenic DT40 cell lines with stable deletions of various DNA repair, cell cycle and signaling genes. Unlike RNAi experiments in mammalian cell culture, DT40 deletion cell lines are more amenable to experimental manipulation and offer full loss of gene function without off-target effects(53). Since their introduction, Takeda *et al*. have and continue to develop sensitive assays to study mechanisms of DNA repair and genotoxicity, including high-throughput viability and mutation assays (53-55). DT40 studies have provided insight on the human DNA damage resposne for a diverse panel of DNA lesions including interstrand crosslinks, base modifications, abasic sites, bulky adducts, single and double strand breaks caused by a variety of alkylating agents, ROS, crosslinking agents, ionizing radiation, and UV rays (54-58). These features make the DT40 system ideal for studying mechanisms of DNA repair and identifying and characterizing unknown genotoxicants.

The availability of functional profiling platforms in these models and others provides a collection of tools well suited for identifying potential genotoxicants, characterizing genotoxicity of chemicals and identifying genetic fingerprints for classes of genotoxicants. This dissertation aims to utlize this approach to identify potential genotoxic mechansisms that mediate the carcinogenesis of the common and often controversial environmental contaminant, trichloroethylene (TCE).

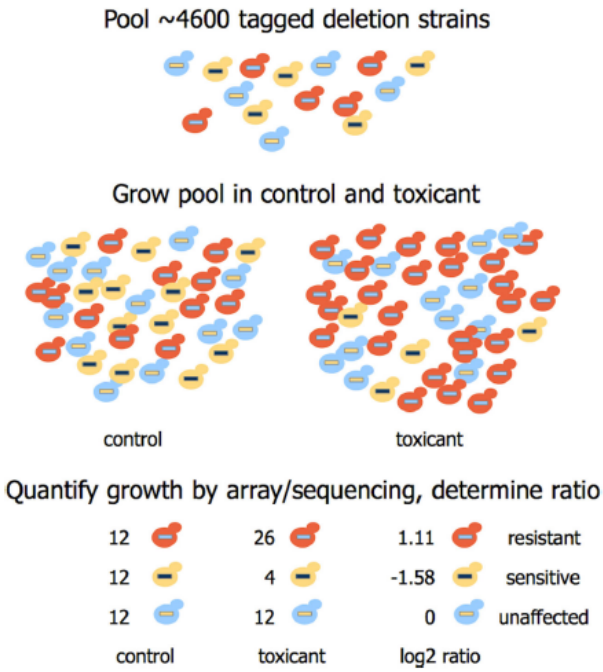

Figure 1.2 Genome-wide screens in yeast can be conducted in parallel to identify genes required in response to toxicant. ~4600 deletion strains uniquely identified by DNA sequences (barcodes) are pooled and exposed to a toxicant at multiple doses and generation times. Barcodes are amplified from purified genomic DNA by PCR and quantified by hybridization to a microarray or high-throughput sequencing methods. Adapted from (40).

Table 1.2 Summary of functional screens in yeast and avian models to assess genotoxicity of chemicals.

Organism	Chemical(s)	Method	Reference
Yeast			
	Interstrand crosslinking agents	deletion library	(59)
	MMS	deletion library	(60)
	Various agents	deletion library	(61)
	Platinum acrinides	deletion library	(62)
	Benzo[a]pyrene	deletion library	(63)
	DMSO	deletion library	(49)
	Imidazo-pyridines and -pyrimidines	deletion library	(64)
	Benzene	deletion library	(51)
Avian DT40			
	MMS, cisplatin	deletion mutants	(54)
	γ-rays, UV, sodium metaarsenite ($NaAsO_2$)	deletion mutants	(55)
	MMS, UV, NQO	deletion mutants	(57)
	MMS, UV, cisplatin	deletion mutants	(56)
	Interstrand crosslinking agents	deletion mutants	(58)

References

1. Guha N, Loomis D, Grosse Y, Lauby-Secretan B, Ghissassi El F, Bouvard V, et al. Carcinogenicity of trichloroethylene, tetrachloroethylene, some other chlorinated solvents, and their metabolites. Lancet Oncol. 2012;:1192–3.

2. Chiu WA, Jinot J, Scott CS, Makris SL, Cooper GS, Dzubow RC, et al. Human health effects of trichloroethylene: key findings and scientific issues. Environ Health Persp. 2013;121:303–11.

3. Bakke B, Stewart PA, Waters MA. Uses of and exposure to trichloroethylene in US industry: A systematic literature review. J Occup Environ Hyg. 2007;4:375–90.

4. Rusyn I, Chiu WA, Lash LH, Kromhout H, Hansen J, Guyton KZ. Trichloroethylene: Mechanistic, epidemiologic and other supporting evidence of carcinogenic hazard. Pharmacol Therapeut. 2013.

5. US EPA OIRISD. TOXICOLOGICAL REVIEW OF TRICHLOROETHYLENE. 2011;:1–1200.

6. Wu C, Schaum J. Exposure assessment of trichloroethylene. Environ Health Persp. 2000;108 Suppl 2:359–63.

7. Jia C, Yu X, Masiak W. Blood/air distribution of volatile organic compounds (VOCs) in a nationally representative sample. Sci Total Environ. 2012;419:225–32.

8. Lash L, Fisher J, Lipscomb J, Parker J. Metabolism of trichloroethylene. Environ Health Persp. 2000;108:177–200.

9. Chiu WA, Caldwell JC, Keshava N, Scott CS. Key scientific issues in the health risk assessment of trichloroethylene. Environ Health Persp. 2006;114:1445–9.

10. Miller R, Guengerich F. Metabolism of Trichloroethylene in isolated hepatocytes, microsomes and reconstituted enzyme systems containing cytochrome P-450. Cancer Res. 1983;43:1145–52.

11. Kim S, Kim D, Pollack GM, Collins LB, Rusyn I. Pharmacokinetic analysis of trichloroethylene metabolism in male B6C3F1 mice: Formation and disposition of trichloroacetic acid, dichloroacetic acid, S-(1,2-dichlorovinyl)glutathione and S-(1,2-dichlorovinyl)-L-cysteine. Toxicol Appl Pharm. 2009;238:90–9.

12. Anders MW. Chemical toxicology of reactive intermediates formed by the glutathione-dependent bioactivation of halogen-containing compounds. Chem Res Toxicol. 2008;21:145–59.

13. Anders M. Glutathione-dependent bioactivation of haloalkanes and haloalkenes. Drug Metab Rev. 2004;36:583–94.

14. Kim S, Collins LB, Boysen G, Swenberg JA, Gold A, Ball LM, et al. Liquid chromatography electrospray ionization tandem mass spectrometry analysis method for simultaneous detection of trichloroacetic acid, dichloroacetic acid, S-(1,2-dichlorovinyl)glutathione and S-(1,2-dichlorovinyl)-L-cysteine. Toxicology. 2009;262:230–8.

15. Goeptar A, Commandeur J, Vanommen B, Vanbladeren P, Vermueulen N. Metabolism and kinetics of trichloroethylene in relation to toxicity and carcinogenicity- relevance of the mercapturic acid pathway. Chem Res Toxicol. 1995;8:3–21.

16. Lash LH, Putt DA, Huang P, Hueni SE, Parker JC. Modulation of hepatic and renal metabolism and toxicity of trichloroethylene and perchloroethylene by alterations in status of cytochrome P450 and glutathione. Toxicology. 2007;235:11–26.

17. Caldwell JC, Keshava N, Evans MV. Difficulty of mode of action determination for trichloroethylene: An example of complex interactions of metabolites and other chemical exposures. Environ Mol Mutagen. 2008;49:142–54.

18. Lash L, Parker J, Scott C. Modes of action of trichloroethylene for kidney tumorigenesis. Environ Health Persp. 2000;108:225–40.

19. Moore M, Harrington-Brock K. Mutagenicity of trichloroethylene and its metabolites: Implications for the risk assessment of trichloroethylene. Environ Health Persp. 2000;108:215–23.

20. Green T, Dow J, Ellis M, Foster J, Odum J. The role of glutathione conjugation in the development of kidney tumours in rats exposed to trichloroethylene. Chem-Biol Interact. 1997;105:99–117.

21. Bruning T, Bolt H. Renal toxicity and carcinogenicity of trichloroethylene: Key results, mechanisms, and controversies. Crit Rev Toxicol. 2000;30:253–85.

22. Cummings B, Zangar R, Novak R, Lash L. Cytotoxicity of trichloroethylene and S-(1,2-dichlorovinyl)-L-cysteine in primary cultures of rat renal proximal tubular and distal tubular cells. Toxicology. 2000;150:83–98.

23. Cummings B, Lash L. Metabolism and toxicity of trichloroethylene and S-(1,2-dichlorovinyl)-L-cysteine in freshly isolated human proximal tubular cells. Toxicol Sci. 2000;53:458–66.

24. Khan S, Priyamvada S, Khan SA, Khan W, Farooq N, Khan F, et al. Effect of trichloroethylene (TCE) toxicity on the enzymes of carbohydrate metabolism, brush border membrane and oxidative stress in kidney and other rat tissues. Food Chem Toxicol. 2009;47:1562–8.

25. Lash L, Sausen P, Duescher R, Cooley A, Elfarra A. Roles of cysteine conjugate beta-lyase and S-oxidase in nephrotoxicity- Studies with S-(1,2-dichlorovinyl)-L-cysteine and S-(1,2-dichlorovinyl)-L-cysteine sulfoxide. J Pharmacol Exp Ther. 1994;269:374–83.

26. Vermeulen R, Zhang L, Spierenburg A, Tang X, Bonventre JV, Reiss B, et al. Elevated urinary levels of kidney injury molecule-1 among Chinese factory workers exposed to trichloroethylene. Carcinogenesis. 2012;33:1538–41.

27. Bhattacharya R, Schultze M. Properties of DNA treated with S-(1,2-dichlorovinyl)-L-cysteine and a lyase. Arch Biochem Biophys. 1972;153:105–&.

28. Clay P. Assessment of the genotoxicity of trichloroethylene and its metabolite, S-(1,2-dichlorovinyl)-L-cysteine (DCVC), in the comet assay in rat kidney. Mutagenesis. 2008;23:27–33.

29. Irving RM, Elfarra AA. Mutagenicity of the cysteine S-conjugate sulfoxides of trichloroethylene and tetrachloroethylene in the Ames test. Toxicology. 2013;306:157–61.

30. McGoldrick T, Lock E, Rodilla V, Hawksworth G. Renal cysteine conjugate C-S lyase mediated toxicity of halogenated alkenes in primary cultures of human and rat proximal tubular cells. Arch Toxicol. 2003;77:365–70.

31. Chen JC, Stevens JL, Trifillis AL, Jones TW. Renal cysteine conjugate beta-lyase-mediated toxicity studied with primary cultures of human proximal tubular cells. Toxicol Appl Pharm. 1990;103:463–73.

32. Chen Q, Jones T, Stevens J. Early cellular events couple covalent binding of reactive metabolites to cell-killing by nephrotoxic cysteine conjugates. J Cell Physiol. 1994;161:293–302.

33. Mally A, Walker CL, Everitt JI, Dekant W, Vamvakas S. Analysis of renal cell transformation following exposure to trichloroethene in vivo and its metabolite S-(dichlorovinyl)-L-cysteine in vitro. Toxicology. 2006;224:108–18.

34. Brauch H, Weirich G, Hornauer M, Storkel S, Wohl T, Bruning T. Trichloroethylene exposure and specific somatic mutations in patients with renal cell carcinoma. J Natl Cancer I. 1999;91:854–61.

35. Charbotel B, Gad S, Caïola D, Béroud C, Fevotte J, Bergeret A, et al. Trichloroethylene exposure and somatic mutations of the VHL gene in patients with Renal Cell Carcinoma. J Occup Med Toxicol. 2007;2:13.

36. Brauch H, Weirich G, Klein B, Rabstein S, Bolt H, Bruning T. VHL mutations in renal cell cancer: does occupational exposure to trichloroethylene make a difference? Toxicol Lett. 2004;151:301–10.

37. Karami S, Lan Q, Rothman N, Stewart PA, Lee K-M, Vermeulen R, et al. Occupational trichloroethylene exposure and kidney cancer risk: a meta-analysis. Occup Environ Med. 2012;69:858–67.

38. Shiao Y-H. Genetic Signature for Human Risk Assessment: Lessons From Trichloroethylene. Environ Mol Mutagen. 2009;50:68–77.

39. Desimone MC, Rathmell WK, Threadgill DW. Pleiotropic effects of the trichloroethylene-associated P81S VHL mutation on metabolism, apoptosis, and ATM-mediated DNA damage response. J Natl Cancer I. 2013;105:1355–64.

40. Gaytán BD, Vulpe CD. Functional toxicology: tools to advance the future of toxicity testing. Front Genet. 2014;5:110.

41. Schmitt MW, Kennedy SR, Salk JJ, Fox EJ, Hiatt JB, Loeb LA. Detection of ultra-rare mutations by next-generation sequencing. P Natl Acad Sci Usa. 2012;109:14508–13.

42. McCann J, Ames BN. Detection of carcinogens as mutagens in the Salmonella/microsome test: assay of 300 chemicals: discussion. P Natl Acad Sci Usa. 1976;73:950–4.

43. Walmsley RM, Billinton N. How accurate is in vitro prediction of carcinogenicity? Br J Pharmacol. 2011;162:1250–8.

44. Kirkland D, Aardema M, Henderson L, Müller L. Evaluation of the ability of a battery of three in vitro genotoxicity tests to discriminate rodent carcinogens and non-carcinogens I. Sensitivity, specificity and relative predictivity. Mutat Res. 2005;584:1–256.

45. Boiteux S, Jinks-Robertson S. DNA repair mechanisms and the bypass of DNA damage in Saccharomyces cerevisiae. Genetics. 2013;193:1025–64.

46. Giaever G, Chu A, Ni L, Connelly C, Riles L, Veronneau S, et al. Functional profiling of the Saccharomyces cerevisiae genome. Nature. 2002;418:387–91.

47. Jo WJ, Loguinov A, Chang M, Wintz H, Nislow C, Arkin AP, et al. Identification of genes involved in the toxic response of Saccharomyces cerevisiae against iron and copper overload by parallel analysis of deletion mutants. Toxicol Sci. 2008;101:140–51.

48. Jo WJ, Loguinov A, Wintz H, Chang M, Smith AH, Kalman D, et al. Comparative Functional Genomic Analysis Identifies Distinct and Overlapping Sets of Genes Required for Resistance to Monomethylarsonous Acid (MMA(III)) and Arsenite (As-III) in Yeast. Toxicol Sci. 2009;111:424–36.

49. Gaytán BD, Loguinov AV, La Rosa De VY, Lerot J-M, Vulpe CD. Functional genomics indicates yeast requires Golgi/ER transport, chromatin remodeling, and DNA repair for low dose DMSO tolerance. Front Genet. 2013;4:154.

50. Gaytán BD, Loguinov AV, Lantz SR, Lerot J-M, Denslow ND, Vulpe CD. Functional profiling discovers the dieldrin organochlorinated pesticide affects leucine availability in yeast. Toxicol Sci. 2013;132:347–58.

51. North M, Tandon VJ, Thomas R, Loguinov A, Gerlovina I, Hubbard AE, et al. Genome-wide functional profiling reveals genes required for tolerance to benzene metabolites in yeast. Plos One. 2011;6:e24205.

52. Buerstedde J, Takeda S. Increased ration of targeted to random integration after transfection of chicken B-cell lines. Cell. 1991;67:179–88.

53. Yamazoe M, Sonoda E, Hochegger H, Takeda S. Reverse genetic studies of the DNA damage response in the chicken B lymphocyte line DT40. Dna Repair. 2004;3:1175–85.

54. Ridpath JR, Takeda S, Swenberg JA, Nakamura J. Convenient, multi-well plate-based DNA damage response analysis using DT40 mutants is applicable to a high-throughput genotoxicity assay with characterization of modes of action. Environ Mol Mutagen. 2011;52:153–60.

55. Ji K, Kogame T, Choi K, Wang X, Lee J, Taniguchi Y, et al. A Novel Approach Using DNA-Repair-Deficient Chicken DT40 Cell Lines for Screening and Characterizing the Genotoxicity of Environmental Contaminants. Environ Health Persp. 2009;117:1737–44.

56. Simpson LJ, Ross A-L, Szüts D, Alviani CA, Oestergaard VH, Patel KJ, et al. RAD18-independent ubiquitination of proliferating-cell nuclear antigen in the avian cell line DT40. EMBO Rep. 2006;7:927–32.

57. Edmunds CE, Simpson LJ, Sale JE. PCNA ubiquitination and REV1 define temporally distinct mechanisms for controlling translesion synthesis in the avian cell line DT40. Mol Cell. 2008;30:519–29.

58. Nojima K, Hochegger H, Saberi A, Fukushima T, Kikuchi K, Yoshimura M, et al. Multiple repair pathways mediate tolerance to chemotherapeutic cross-linking agents in vertebrate cells. Cancer Res. 2005;65:11704–11.

59. Smith AM, Ammar R, Nislow C, Giaever G. A survey of yeast genomic assays for drug and target discovery. Pharmacol Therapeut. 2010;127:156–64.

60. Huang D, Piening BD, Paulovich AG. The preference for error-free or error-prone postreplication repair in Saccharomyces cerevisiae exposed to low-dose methyl methanesulfonate is cell cycle dependent. Mol Cell Biol. 2013;33:1515–27.

61. Svensson JP, Quirós Pesudo L, McRee SK, Adeleye Y, Carmichael P, Samson LD. Genomic phenotyping by barcode sequencing broadly distinguishes between alkylating agents, oxidizing agents, and non-genotoxic agents, and reveals a role for aromatic amino acids in cellular recovery after quinone exposure. Plos One. 2013;8:e73736.

62. Cheung-Ong K, Song KT, Ma Z, Shabtai D, Lee AY, Gallo D, et al. Comparative chemogenomics to examine the mechanism of action of dna-targeted platinum-acridine anticancer agents. ACS Chem Biol. 2012;7:1892–901.

63. O'Connor STF, Lan J, North M, Loguinov A, Zhang L, Smith MT, et al. Genome-Wide Functional and Stress Response Profiling Reveals Toxic Mechanism and Genes Required for Tolerance to Benzo[a]pyrene in S. cerevisiae. Front Genet. 2012;3:316.

64. Yu L, Lopez A, Anaflous A, Bali El B, Hamal A, Ericson E, et al. Chemical-genetic

profiling of imidazo[1,2-a]pyridines and -pyrimidines reveals target pathways conserved between yeast and human cells. Plos Genet. 2008;4:e1000284.

CHAPTER II

Functional Profiling of the Heavy Metals Cadmium, Lead, and Zinc in Yeast

ABSTRACT

The metals cadmium (Cd), lead (Pb) and zinc (Zn) are common environmental contaminants. A yeast homozygous deletion library of over 4,700 mutant strains, each with a single gene deletion, were assayed in parallel to identify susceptibility genes to metal toxicity. By using this approach, we determined how the unique genotype of each strain in the pool impacts growth in the presence of these toxicants. The genetic requirements for yeast resistance to Cd, Pb and Zn include genes associated with highly conserved intracellular transport pathways, protein ubiquitination, protein catabolism and metal homeostasis. Common yeast resistance pathways included intracellular trafficking pathways and the vacuole despite the different mechanisms of toxicity proposed for these metals. Based on the mutant sensitivity profile, oxidative stress did not appear to be a major mechanism of Cd toxicity in yeast.

INTRODUCTION

Heavy metals cadmium (Cd), lead (Pb) and zinc (Zn) are widely distributed environmental contaminants associated with a range of adverse health effects, including neurological disease, development and cancer [1]. The International Agency for Research on Cancer (IARC) has classified Cd as a Group 1 human carcinogen and inorganic Pb as a Group 2B possible human carcinogen [1]. The prevalence and carcinogenicity of these heavy metals is a long-standing and continued public health concern.

Cadmium is a persistent and bioaccumulative contaminant used mainly in the manufacture of batteries and pigments. General population exposure is via contaminated foods and cigarette smoke. A potent nephrotoxicant, cadmium is associated with an increased risk of kidney cancer as well as prostate and lung cancers [2, 3]. Several mechanisms of Cd toxicity have been proposed, including disruption of Zn-containing enzymes and inhibition of DNA mismatch repair [4], alteration of essential metal homeostasis such as calcium, iron and zinc [5], and generation of reactive oxygen species (ROS) [32, 33, 34, 40].

Although lead use was banned in household paint and gasoline additives, occupational exposure and consumption of contaminated food and water remains a serious health issue. Lead reduces hemoglobin, heme, and vitamin D synthesis resulting in decreased production of many neural and metabolic enzymes, and can also produce ROS and oxidative stress through lipid peroxidation and accumulation of aminolevulinic acid [35, 36, 38, 40] resulting in neuro-, hemopoietic system, and kidney toxicities [6]. Lead is associated with neurotoxicity in children, and hemopoietic system and kidney toxicity [6].

In contrast to cadmium and lead, zinc is an essential trace nutrient serving as a cofactor for the function of numerous enzymes and proteins. Zn toxicity is rare and the most common adverse

health effects (stunted growth, diarrhea, and impaired immunity) are associated with Zn deficiency [37,39]. The applications for Zn are primarily in industrial processes where it is used to galvanize steel and iron and to make alloys. Occupational Zn exposure occurs by inhalation of zinc fumes, causing fever and discomfort in industrial workers [7, 8].

The baker's yeast *Saccharomyces cerevisiae* shares many fundamental cellular processes with humans [9]. Oxidative stress response, DNA replication and repair, protein synthesis, intracellular trafficking, and metal homeostatic mechanisms, all of which are reported to be targets of Cd, Pb and Zn toxicity, are highly conserved in yeast. The involvement of a gene of interest in response to a toxicant has been traditionally assessed in yeast by generating a knock out strain and evaluating the phenotype in the presence of the toxicant, usually by growth assays. Homozygous yeast deletion mutants for non-essential genes can be analyzed simultaneously to interrogate their growth phenotype and functionally profile the yeast genome under selective conditions of interest [10, 11]. We used this parallel, competitive growth approach, to gain insight into the mechanisms of toxicity of Cd, Pb and Zn. We evaluated pools of mutants grown for 5 and 15 generations exposed to different concentrations of each of these toxicants in order to identify the genes that modulate yeast toxicity response.

RESULTS AND DISCUSSION

Functional Profiling of the Yeast Genome in the Presence of Cd, Pb and Zn

The genetic requirements for yeast growth (fitness) in the presence of metals were compared at equitoxic concentrations that resulted in 20% growth inhibition (IC_{20}) of the diploid wild type (Wt) strain BY4743, as well as 50% and 25% of the IC_{20}. The calculated IC_{20} values for Cd, Pb and Zn were 4, 1000 and 2500 μM, respectively. Fitness was evaluated at 5 generations (5G) and 15 generations (15G) of growth. Homozygous deletion mutant pools were therefore exposed to 3 metal concentrations for 5G and 15G, totaling 6 treatments per metal, with 3 biological replicates each (**Table 2.1**).

The number of identified strains (genes) increased with increased dose and number of generations of growth, ranging from a few genes after 5G to several hundred after 15G (**Fig. 2.1, Appendix 1-3**). Genes consistently identified as sensitive in at least 4 of the 6 treatments (**Tables 2.2, 2.3 and 2.4**), were mostly associated with intracellular transport and were metal-specific. Of the total 89 genes, Cd and Pb only shared 4 genes; Cd and Zn shared 6 genes; while Pb and Zn did not have any genes in common. Further, the sensitive or resistant phenotype increased with treatment concentration and number of generations of exposure.

Enrichment Analysis

Most of the identified genes were associated with vacuole biogenesis and transport processes and were required against all three metals, as identified by gene ontology scoring (**Table. 2.5**). In contrast, protein ubiquitination, (a post-translational modification that identifies proteins for degradation) and catabolism genes were predominant only against Cd and Pb toxicity. Previously genes individually associated with metal detoxification were also identified. One of these genes was *ZSP1*, which has been shown to be essential for growth at high Zn concentrations, although its function is unknown. The *zsp1Δ* strain was very sensitive to Zn at the IC_{20} but not at the lower concentrations tested, i.e. 0.625 and 1.25 mM, both after 5G and 15G.

In other cases, known genes involved in detoxification were not identified. In the case of Cd, requirement of metallothionein genes or glutathione biosynthesis could not be verified. These discrepancies may be due to the shorter exposure, lower doses (more than 100-fold lower than previously reported [26]) and/or functional redundancy, as is the case for the metallothionein genes.

Pathway enrichment, hierarchical clustering and network clustering analyses reveal shared tolerance requirements

We performed two pathway analyses of the microarray data (described in Methods). First, we identified significantly enriched KEGG (Kyoto Encyclopedia of Genes and Genomes) pathways required for tolerance to treatment for each metal. 43 KEGG pathways were represented in the data sets. These 43 were then clustered to determine shared tolerance pathways in a compound- and generational-dependent context (**Figure 2.6**). Additionally, data for all metals was mapped to the STRING database of *S. cerevisiae* protein-protein interactions and clusters (sub-networks) enriched for targets of any metal were identified (**Figure 2.7**). 6 sub-networks were identified at 5G, and 16 at 15G. Overrepresentation of Gene Ontology (GO) biological process categories were identified for each sub-network. These analyses identified common pathways required in response to all three metals and complement DSSA and network analyses conducted for each metal individually.

Intracellular Transport and Vacuolar Function

Several genes encoding subunits of the endosomal sorting complex required for transport (ESCRT) I, II and III, as well as genes associated with vacuole biogenesis and function, were essential for growth in the presence of all three metals (**Fig. 2.3, 2.4 and 2.5**). Another complex associated with intracellular trafficking and important in Cd resistance was the retromer complex, involved in endosome-to-Golgi retrograde protein transport; deletion of the Pep8p, Vps17p, and Vps35p subunits resulted in Cd sensitivity. There was high similarity in the requirements of genes associated with vacuolar/lysosomal transport and protein targeting, sorting, and translocation for growth in Cd and Zn. This finding indicated common metabolic and/or detoxification pathways. Among the overlapping high-confidence genes were *VPS3*, *VPS24*, *VPS9*, *PEP12* and *VPS21*. However, Cd was >600-fold more toxic than Zn based on yeast growth IC_{20} values; thus, Cd toxicity appears to be mediated through mechanisms not common to Zn.

The vacuole participates in Cd and Zn detoxification by functioning as a storage location. Cadmium is sequestered into this organelle by Ycf1p [12], whereas Zn by the vacuolar zinc transporter Zrc1p [13]. The latter was essential for growth and the deletion mutant exhibited a very sensitive phenotype in the presence of Zn. However, *ycf1Δ* was not identified in the screen as sensitive and this could be due to experimental variability or to the existence of an alternative detoxification pathway that operates at the Cd concentrations tested. The mechanisms of Pb detoxification in yeast are not known. However, the similarity of the intracellular trafficking mutant profiles with Cd and Zn suggests that the vacuole also plays an important role in Pb detoxification.

Identification of vacuolar H^+-ATPase genes provided additional evidence of the importance of the vacuole in Zn detoxification (**Fig. 2.5**), as acidification is necessary for proper function of

this organelle. Considering the number of genes identified, vacuolar acidification appeared to be more important for resistance to Zn than to Cd and Pb at the concentrations tested. Essential genes included ones encoding the vacuolar H^+-ATPase subunits (*VMA5*, *VMA8* and *YCL007C*) or elements involved in its assembly (*VPH2*, *VMA22*, *RAV1*, *RAV2*). Interestingly, *YCL007C* and the V-ATPase-associated genes *VMA5*, *VMA8* and *VMA22* were sensitive to Zn at all concentrations tested at 5G but not at 15G.

Two yeast dubious open reading frames, *BRP1* and *YCL007C*, were identified as essential for growth in Cd and Zn, respectively. In growth assays, *brp1Δ* was sensitive to Cd and high Zn concentrations but not Pb (**Fig. 2.2**). The requirement of *BRP1* could be related to its proximity to *PMA1*, which encodes a plasma membrane H+-ATPase that regulates cytoplasmic pH and plasma membrane potential. Similarly, *YCL007C* overlaps with *VMA9*, a subunit of the V-ATPase V0 subcomplex of the H^+ ATPase involved in vacuolar acidification. Deletion of PMA1 and VMA9 results in a nonviable phenotype so they were not evaluated in the screen.

Protein synthesis and catabolism

Several genes identified as essential for Cd resistance are involved in protein ubiquitination and catabolism processes (*STP22*, *VPS25*, *VPS24*, *SNF7*, *SRN2,* and *VPS28*). Cadmium has been shown to alter proteasome activity and to induce accumulation of high-molecular weight polyubiquitinated proteins in rat primordial germ cells and Sertoli cell co-cultures, and ubiquitination of mixed-disulfide proteins in mouse neuronal cells [14, 15]. Pb identified protein catabolism as a significantly enriched biological process although only two genes (*SNF7* and *VPS36*) were present. In contrast, this category was not essential for growth in Zn. Further, ribosomal (*MRPL11*, *YDR186C*, *RSM18*, *MRPL9*, *RPL2B*, *RSM25*, *MRPL31,* and *MRPS17*) and mitochondrial ribosomal genes (*RSM18*, *RSM25*, *MRPS17*, *MRPL9*, *MRPL11,* and *MRPL31*) were consistently identified as detrimental in Pb and indicated that Pb effects protein synthesis.

Metal homeostasis

Biological processes associated with metal metabolism and homeostasis were not significant in the gene ontology scoring. However, several important genes involved in these processes that are markers of metal homeostasis disruption were identified. The toxic effects of Cd, Pb and Zn on the metabolism of essential metals have been reported extensively in the literature. Cadmium can gain access into cells by mimicking calcium, iron and Zn and disrupt cellular processes in which these essential metals participate [5]. Excess Zn resulted in decreased intracellular iron levels [16]. The iron metabolic pathways are highly conserved among species and have been extensively studied in yeast. The transcription factor *AFT1*, the iron transporter *FTR1*, the low affinity transporter *FET4* and the iron ferroxidase *FET3* are involved in iron uptake under iron deficiency conditions. The Cd, Pb and/or Zn sensitivity of mutants with deletions of these genes suggests an effect on iron metabolism. An exception was *FET3*, which deletion resulted in resistance to Pb but sensitivity to Cd and Zn. The *fet3Δ* mutant was found to be sensitive to copper, Zn, cobalt and manganese due to competition of these metals with iron for uptake by Fet4p [17]. The reason for *fet3Δ* resistance to Pb is unknown. *AFT1* was essential for growth in all metals in at least one concentration at 5G. *AFT1* encodes a transcription factor that is upregulated and induces the expression of iron uptake transporters in iron deficiency conditions [18]. Thus, these results suggest that Cd, Pb, and Zn toxicity alter iron metabolism. In the case of Cd, all three concentrations tested in the screen resulted in a significant decrease in growth of

aft1Δ. There were a total of 66 genes identified in the Cd treatments that were common to the ones that we previously identified in iron deficiency conditions [22]. These genes mainly encoded components of the endosome and ESCRT I, II and III complexes and are mainly involved in intracellular transport. Consistent with iron deficiency conditions, genes associated with iron metabolism *FTR1*, *FET3,* and *FRE1* were essential in Cd. Increased Cd accumulation in tissues has been shown in mice with induced iron deficiency [23, 24]. Therefore, these results indicate that Cd alters iron metabolism. In the presence of Pb and Zn, components of the iron and copper metabolic pathways were essential for optimal growth. In addition to *AFT1*, the transcription factor gene *MAC1* involved in regulation of copper metabolism and activated under copper deficiency conditions was identified [19]. In support of an iron deficiency state in lead-exposed cells, *FET4* was also essential.

Based on the requirement of marker genes, one common mechanism of Cd, Pb and Zn appears to be their ability to affect iron metabolism. Thus, some of the cytotoxic effects associated with these metals could result from disruption of metal homeostasis. Because copper is required for high affinity iron uptake and MAC1 was essential in Pb and Zn, iron deficiency may be a secondary effect of copper deficiency. Cadmium downregulates copper intake through Mac1p, which in turn decreases Fet3p activity and iron uptake resulting in iron and copper deficiency [20]. These findings are consistent with the genetic requirements observed in this study for Pb and Zn. However, it is unclear why *MAC1* was not identified in the Cd treatments.

The yeast transcription factor Zap1p responds to intracellular Zn levels by inducing the expression of target genes. Interestingly, *zap1Δ* was resistant to both Cd and Zn, indicating that *ZAP1* confers a growth disadvantage when these metals are in excess. Zap1p regulates the high affinity Zn transporter Zrt1p, which is constitutively expressed by virtue of Zap1p. Thus, Zap1p may be detrimental by inducing expression of metal transporters which in turn permit access of toxic metals into the cell. In contrast, the presence of *ZAP1* adversely affected fitness as the deletion mutant grew better in Zn overload conditions. Zap1p induces the expression of the zinc transporter *ZRT1* under low zinc conditions [21]. Thus, deletion of *ZAP1* may be beneficial at toxic Zn concentrations by eliminating basal expression of Zrt1p leading to Zn entry into the cell.

Oxidative stress

One of the mechanisms by which Cd is thought to be toxic is through the induction of reactive oxygen species (ROS). Based on the mutant sensitivity profile, oxidative stress did not appear to be a major contributor to Cd toxicity in yeast. Only few oxidative response genes, gamma glutamylcysteine synthetase, *GSH1*, and glutaredoxin, *GRX3*, became essential after 15G of exposure and were confirmed by individual strain growth assays (**Fig. 2.2**). Thus, Cd-induced oxidative stress did not induce a marked phenotypic effect until after several generations of exposure or may be a result of chronic exposure. Similarly, oxidative stress may only play a significant role in chronic exposure to Pb based on moderate sensitivity in *GRX3* mutants and the identification of glutathione metabolism (KEGG pathway map00480) only after 15G (Fig. 2.6). In contrast, *GSH1* and the glutathione reductase gene *GLR1* are highly essential for fitness after 5G and 15G exposure to monomethylarsonous acid (a methylated arsenic form) [22]. Further, genes required for yeast resistance against Cd and oxidative stress agents such as hydrogen peroxide were mainly distinct and suggest that Cd generates a different ROS type [25]. These results suggest differences in the mechanisms and type of oxidative stress between methylated

arsenic and Cd.

CONCLUSIONS

Functional profiling of the yeast genome at toxic concentrations of Cd, Pb and Zn revealed that deletions associated with intracellular trafficking pathways, vacuolar function and protein catabolism resulted in sensitivity to these metals. Intracellular trafficking pathways and the vacuole appear to play an important role and are consistent with the vacuole's prominence in metal detoxification. Known genes involved in iron, copper and Zn metabolism were also identified, providing evidence of the disruption of metal homeostasis. Although Cd, Pb and Zn produce a variety of adverse human health effects probably through different mechanisms, the pathways of yeast resistance were similar.

MATERIALS AND METHODS

Yeast strains and chemical exposures

All yeast strains used in this study were of the BY4743 background (*MATa*/*MATα his3Δ1*/*his3Δ1, ura3Δ0*/*ura3Δ0, leu2Δ0*/*leu2Δ0, lys2Δ0*/+, *met15Δ0*/+). Pool growth was conducted in either liquid rich (1% yeast extract-2% peptone-2% dextrose, YPD) media, at 30˚C with shaking at 200 rpm. Stock solutions of Cd, Pb and Zn chloride (Sigma-Aldrich, Saint Louis, MO) were freshly prepared in sterile MilliQ-water and added to the sterile media to the desired final concentrations.

Parallel Analysis of Yeast Deletion Mutants

Pool growth, genomic DNA extraction, barcode amplification and hybridization were performed as previously described [27], with minor modifications. Briefly, homozygous diploid deletion mutants (n = 4612) were grown in YPD at different metal concentrations for 5G and 15G. Mutant strains that failed the original PCR quality control [11], were not included in the pools. Cells were collected and genomic DNA was extracted using the YDER kit (Pierce Biotechnology). The strain-specific barcodes in the yeast DNA were amplified by PCR using a set of biotinylated primers, and reactions hybridized to TAG4 arrays (Affymetrix Inc., Santa Clara, CA). Arrays were incubated overnight and then stained and scanned at an emission wavelength of 560 nm using a GeneChip scanner (Affymetrix Inc.).

Differential Strain Sensitivity Analysis

Raw TAG4 array data were $\log_2$-transformed, corrected for signal saturation as previously described [27], and corrected for mean chip background using robust location and scale estimators for $\log_2$-transformed intensities of null features (total of 18,000 equally distributed on the array). To account for variability in strain growth, data from each treatment array were paired to data from twelve controls (5G or 15G) for analysis. Treatment-control pairs were normalized with LOWESS (global normalization), and the differentially growing strains identified using an *alpha*-outlier approach [28, 29]. Data from three biological replicates were combined, resulting in 36 treatment-control data pairs per treatment group. Residual variances (with a robust scale estimator) of $\log_2$ (treatment/control) for each 36 pairs were inspected using box plots, and pairs with relatively high variance or suspected serial correlation (regular patterns in the box plots) were removed from the analysis. These "effective pairs" were therefore based on 36 treatment-control pairs excluding ones with abnormally high residual variance based on a robust scale

estimator or suspected to serial correlation in variability. Significant genes (strains) were then statistically inferred using an exact binomial test, assuming that the outcomes for each gene in all effective treatment-control pairs, were independent binary variables with the same probability of success ($p = 0.5$) for all trials (Bernoulli trials). For a particular gene n, outcomes were considered as "successful" if they were significant in the outlier analysis with q-values ≤ 0.05 in each of all effective pairs with $\log_2$ ratios of the same sign, simultaneously. The corresponding raw p-values based on the exact binomial test were then corrected for multiplicity of comparisons using q-value approach and only the genes with q-value ≤ 0.05 were considered for further analysis. This approach does not apply a scale estimator and, as a result, it does not require between-chip pair normalization for the statistical inference.

Growth Curve Assays

Yeast strains were pre grown to mid-log phase, diluted to an optical density at 595 nm (OD_{595}) of 0.0165, and dispensed into different wells of a 48-well plate. Metal stock solutions were added to the desired final concentrations with at least three replicates per dose. Plates were incubated in a Tecan Genios spectrophotometer set to 30°C with intermittent shaking. OD_{595} measurements were taken at 15-minute intervals for a period of 24 hours. Raw absorbance data were averaged for all replicates, background corrected and plotted as a function of time. The area under the curve (AUC) was calculated with Prism version 5.01 (GraphPad Software), as a measure of growth, and expressed as a percentage of the untreated control.

Gene Ontology Scoring

Data sets were verified for enrichment of any particular biological attribute by identifying significantly enriched Gene Ontology (GO) categories by a hypergeometric distribution using the Functional Specification resource, FunSpec (http://funspec.med.utoronto.ca/), with a P-value cutoff of 0.01. Yeast fitness data was mapped onto the extended Wi-Phi yeast interactome [30], consisting of more than 10,000 protein-protein interactions, and onto the regulatory network (www.yeastract.com) [31] (accessed July 2007) using Cytoscape versions 2.4.1 and 2.5.1 (www.cytoscape.org).

Pathway Enrichment and Hierarchical Clustering

Data sets were analyzed as outlined in North *et al* [41]. Briefly, the normalized data for each metal was used in a pathway enrichment method called Structurally Enhanced Pathway Enrichment Analysis (SEPEA). The biochemical pathways chosen were from the *S. cerevisiae* KEGG pathway database. This resulted in 43 pathways whose associated p-values were negative log10 transformed and hierarchically clustered using Spearman rank correlation as a measure of distance and average linkage for forming clustering.

Network Clustering

As described in [41], an overall system-wide interaction network was utilized as a basis for the analyses. In this analysis, the protein interaction network from the STRING database is used. For the analysis across the metals, deletion strains sensitive to at least one of the metals were selected and data for the different generation points (5 g and 15 g) were considered independently. The metal specific data sets were mapped onto the system-wide interaction network with the goal of finding sub-networks in this system-wide network that are enriched with targets of different combinations of the heavy metals. The significance of different clusters is based on the overall

neighborhood characteristics of the nodes of the interaction network. Clusters were analyzed for enrichment of Gene Ontology (GO) Biological Processes within each sub-network. The edges between the clusters represent the interactions between the clusters. Cluster 0 represents the hub of proteins connecting all other sub-networks.

Table 2.1. Metal treatments used in the functional profiling experiments. IC_{20} = concentration resulting in 20% growth inhibition of the wild type strain. Each metal treatment was performed in triplicate for a total of 18 pools of homozygous mutants and compared to 12 control cultures grown in rich media in order to identify the strains that exhibit a significant change in growth.

Growth inhibitory concentration	**Cadmium chloride (Cd^{2+})**	**Lead chloride (Pb^{2+})**	**Zinc chloride (Zn^{2+})**
25% IC_{20}	1 µM	0.25 mM	0.625 mM
50% IC_{20}	2 µM	0.5 mM	1.25 mM
IC_{20}	4 µM	1 mM	2.5 mM

Table 2.2. Fitness scores of significant genes identified in at least four of the six Cd treatments. A total of 36 of the identified genes were important for fitness in at least 4 of the 6 Cd treatments. See Appendix 1 for the list of all identified genes.

Gene Name	5 generations			15 generations		
	25% IC_{20}	50% IC_{20}	IC_{20}	25% IC_{20}	50% IC_{20}	IC_{20}
	1 μM	2 μM	4 μM	1 μM	2 μM	4 μM
VPS8	-0.80	-1.80	-2.50	-3.60	-5.10	-3.70
VPS24	-1.00	-1.15	-1.50	-2.05	-3.80	-4.15
VPS27	-1.15	-1.30	-1.80	-2.80	-4.45	-4.05
VPS4	-1.00	-1.10	-1.55	-2.50	-4.00	-3.90
BST1	0.60	1.35	1.30	ns	1.70	5.50
VPS45	-1.60	-1.60	-2.10	-2.80	-3.10	Ns
SRN2	ns	-0.70	-1.30	-1.60	-4.10	-5.10
YNR005C	ns	-0.70	-1.15	-0.70	-3.30	-4.70
PEP12	-1.40	-1.50	-2.40	-2.70	-3.10	ns
VPS21	ns	-1.30	-1.50	-3.25	-3.75	-4.70
VPS28	ns	-0.90	-1.35	-2.10	-3.25	-2.90
BRO1	ns	-1.70	-2.10	-1.80	-3.80	-3.80
STP22	ns	-1.00	-1.60	-2.30	-2.70	ns
PEP7	-1.20	-1.50	-1.70	-2.10	ns	ns
NHX1	ns	-0.80	-1.60	1.80	-1.70	ns
VPS3	-1.30	-1.35	-2.05	ns	-1.90	ns
BRP1	ns	-1.10	Ns	-1.30	-2.05	-3.20
YGR272C	0.80	1.00	1.20	ns	ns	4.70
GGA2	ns	ns	-1.00	-1.00	-2.75	-2.65
RPL34B	ns	0.90	1.20	ns	1.75	3.80
IMP2'	ns	0.90	0.90	ns	1.45	3.20
PEP8	ns	-0.85	-1.40	ns	-3.35	-3.80
ZAP1	1.10	1.55	1.30	ns	ns	6.40
VPS35	ns	-1.40	-1.90	ns	-3.80	-3.25
VPS25	ns	ns	-1.40	-2.05	-2.85	-3.20
OPI8	ns	-1.30	-1.70	-1.30	-2.45	ns
SNF7	ns	ns	-0.80	-2.85	-3.40	-2.75
VPS38	ns	-1.10	-2.05	ns	-3.15	-4.00
VPS9	ns	-2.40	-2.20	-3.70	-3.20	ns
VAN1	ns	1.00	ns	1.05	3.00	4.45
BUL1	ns	-1.20	-2.10	-1.50	-4.50	ns
VAM10	ns	-1.00	-1.15	ns	-2.00	-2.40
LDB19	ns	ns	-0.90	-2.10	-3.55	-3.45
SUR1	ns	-1.00	ns	-2.15	-4.70	-4.75
VPS30	ns	-1.10	-1.50	ns	-4.10	-5.60
ROX1	ns	-1.15	ns	-1.85	-4.05	-4.30

Fitness score = $\log_2$ treatment - $\log_2$ control; ns = not significant

Table 2.3. Fitness scores of significant genes identified in at least four of the six Pb treatments A total of 42 of the identified genes were important for fitness in at least 4 of the 6 Pb^{2+} treatments. See Appendix 2 for the list of all identified genes.

Gene Name	5 generations			15 generations		
	25% IC_{20}	50% IC_{20}	IC_{20}	25% IC_{20}	50% IC_{20}	IC_{20}
	0.25 mM	0.5 mM	1 mM	0.25 mM	0.5 mM	1 mM
YCR050C	ns	-1.00	-1.65	-3.00	-3.50	-2.75
GCS1	ns	-1.10	-1.60	-4.90	-3.90	-4.50
YDR186C	ns	-0.70	-1.45	-3.10	-2.60	-2.90
RCY1	ns	-1.10	-1.45	-4.50	-5.90	-4.00
SEL1	ns	-1.00	-1.10	-5.00	-4.00	-3.60
CBC2	ns	-1.50	-1.10	-4.20	-3.10	-3.90
YCR049C	ns	ns	-1.00	-2.00	-2.35	-3.20
ATG15	ns	ns	-0.80	-2.60	-2.15	-3.25
SOL2	ns	-1.40	ns	2.50	3.20	3.30
ARF1	ns	ns	-1.40	-3.40	-2.30	-3.80
MRPL11	ns	ns	1.20	2.40	2.60	4.55
HBT1	ns	-1.20	ns	2.10	2.15	3.00
SWF1	ns	ns	-1.60	-3.00	-2.90	-2.60
ENT5	ns	-1.60	ns	3.60	4.00	4.20
ERD1	ns	ns	1.30	4.00	3.55	4.25
YDR455C	ns	ns	-1.25	-2.30	-2.05	-3.55
RSM18	ns	ns	0.90	3.00	3.00	4.65
IES5	ns	ns	0.80	1.40	1.90	2.40
ERG4	-1.20	-1.20	-1.70	-3.90	ns	ns
ARO2	ns	ns	-0.90	-4.90	-3.75	-3.00
MRPL9	ns	ns	0.70	1.90	1.80	2.75
RPL2B	ns	ns	0.85	2.60	2.10	4.30
RSM25	ns	ns	1.10	2.15	2.35	3.65
PEP8	ns	ns	-1.50	-2.70	-2.70	-3.10
VPS35	ns	ns	-1.50	-2.95	-2.45	-2.65
MRPL31	ns	ns	1.20	2.20	2.20	3.60
MMM1	ns	ns	1.30	1.70	2.95	4.60
SNF7	-0.70	ns	-0.70	-2.30	-2.45	ns
SSQ1	ns	ns	0.80	1.20	2.10	2.55
VPS36	-0.90	-0.80	-1.35	-1.70	ns	ns
FET3	ns	ns	1.00	1.60	1.90	1.90
MRPS17	ns	ns	0.80	1.35	1.45	2.30
AVT4	ns	-1.70	ns	2.70	2.60	3.10
LEM3	-1.00	-1.00	-1.50	-3.10	ns	ns
TLG2	ns	ns	-1.60	-3.10	-3.40	-3.40
HAL9	ns	ns	-1.65	-4.70	-4.10	-2.10
VAM10	ns	ns	-0.80	-2.40	-2.35	-3.50
LEO1	ns	ns	0.80	1.95	2.05	3.05
VPS17	ns	ns	-0.90	-1.80	-1.60	-2.40
EFT1	ns	-1.2	ns	2.30	3.70	3.50
YOR246C	ns	ns	-1.05	-2.20	-2.55	-2.65
AEP3	ns	ns	1.20	2.90	2.60	4.45

Fitness score = $\log_2$ treatment - $\log_2$ control; ns = not significant

Table 2.4. Fitness scores of genes identified in at least four of the six Zn treatments.
A total of 11 of the identified genes were important for fitness in at least 4 of the 6 Zn treatments. See Appendix 3 for the list of all identified genes.

Gene Name	5 generations			15 generations		
	25% IC_{20} 0.625 mM	50% IC_{20} 1.25 mM	IC_{20} 2.5 mM	25% IC_{20} 0.625 mM	50% IC_{20} 1.25 mM	IC_{20} 2.5 mM
ZAP1	1.55	1.80	1.40	5.10	4.90	4.60
VPS9	-2.30	-2.75	-2.40	-2.80	-2.15	-3.30
PER1	ns	1.80	1.40	3.40	3.90	4.85
FLC2	ns	-1.60	-2.80	ns	-1.70	-4.50
MRPL16	ns	ns	1.20	1.35	2.15	4.40
VPS3	-2.15	-2.35	-1.65	-2.00	ns	ns
VPS24	-1.10	ns	-2.80	ns	-1.35	-4.80
DFG5	ns	-2.65	-2.50	ns	-1.75	-4.25
PEP12	-2.70	-2.50	ns	-2.40	-2.60	ns
VPS21	ns	-2.00	-1.80	ns	-2.50	-3.65
VPH1	-2.90	-2.90	-3.80	ns	-1.90	ns

Fitness score = $\log_2$ treatment - $\log_2$ control; ns = not significant

Table 2.5. Genes required for growth in the presence of each metal and their associated gene ontology categories.

Biological process[a]	p-value	K[b]	F[c]
Cadmium			
late endosome to vacuole transport [GO:0045324]	2.92e-14	8	20
protein targeting to vacuole [GO:0006623]	3.306e-13	9	41
protein transport [GO:0015031]	9.729e-13	17	379
ubiquitin-dependent protein catabolic process via the multivesicular body sorting pathway [GO:0043162]	6.837e-11	6	15
vacuole inheritance [GO:0000011]	2.507e-10	6	18
transport [GO:0006810]	2.153e-08	18	815
protein retention in Golgi apparatus [GO:0045053]	2.127e-07	4	11
intralumenal vesicle formation [GO:0070676]	1.355e-06	3	5
Lead			
protein transport [GO:0015031]	1.641e-05	11	379
protein retention in Golgi apparatus [GO:0045053]	3.812e-05	3	11
retrograde transport, endosome to Golgi [GO:0042147]	0.0001828	3	18
mitochondrial translation [GO:0032543]	0.0002163	5	88
transport [GO:0006810]	0.000321	14	815
early endosome to Golgi transport [GO:0034498]	0.002095	2	11
ubiquitin-dependent protein catabolic process via the multivesicular body sorting pathway [GO:0043162]	0.003936	2	15
multivesicular body membrane disassembly [GO:0034496]	0.006361	1	1
cell surface receptor linked signaling pathway [GO:0007166]	0.006361	1	1
membrane disassembly [GO:0030397]	0.006361	1	1
Zinc			
vacuole inheritance [GO:0000011]	1.261e-08	4	18
protein targeting to vacuole [GO:0006623]	3.543e-05	3	41
fungal-type cell wall biogenesis [GO:0009272]	0.0001377	2	11
vacuolar acidification [GO:0007035]	0.0008024	2	26
carbohydrate catabolic process [GO:0016052]	0.003329	1	2
FAD transport [GO:0015883]	0.006649	1	4
intralumenal vesicle formation [GO:0070676]	0.008304	1	5

[a]A list of strains exhibiting sensitivity in 4 of the 6 Cd treatments was entered into the FunSpec tool and analyzed for overrepresented biological attributes (see Materials and Methods section).
[b] Number of genes from the input cluster in given category.
[c] Number of genes total in given category.

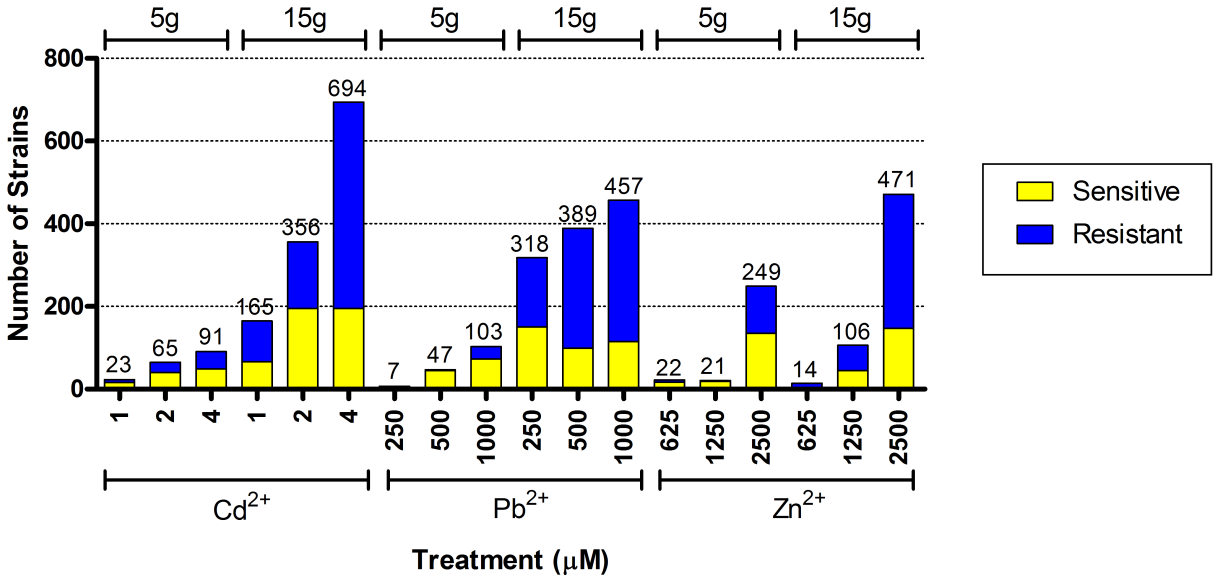

Figure 2.1. The number of identified strains (genes) increased with concentration and number of generations of exposure to Cd, Pb, or Zn and ranged from only a few genes after 5G to several hundred after 15G.

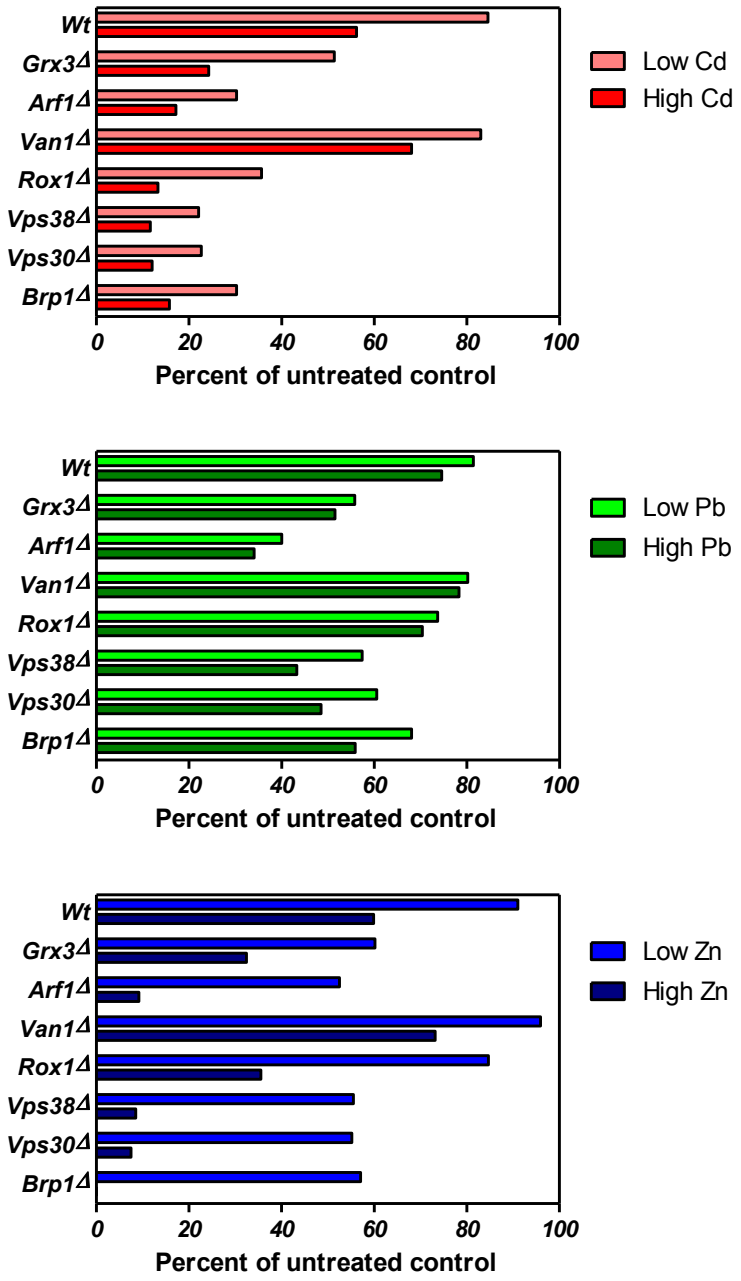

Figure 2.2. Confirmatory growth curve assays for selected deletion mutants. Treatment concentrations used were IC_{20} and twice this concentration, $2*IC_{20}$. For each strain tested, growth was calculated as the area under the OD_{595}-time curve (AUC) for a period of 24 hours and expressed as a percentage of the metal treatment relative to the untreated control. Cadmium and Zn treatments inhibited growth in a dose dependent manner. Lead was poorly soluble and inhibited growth similarly at the two concentrations tested.

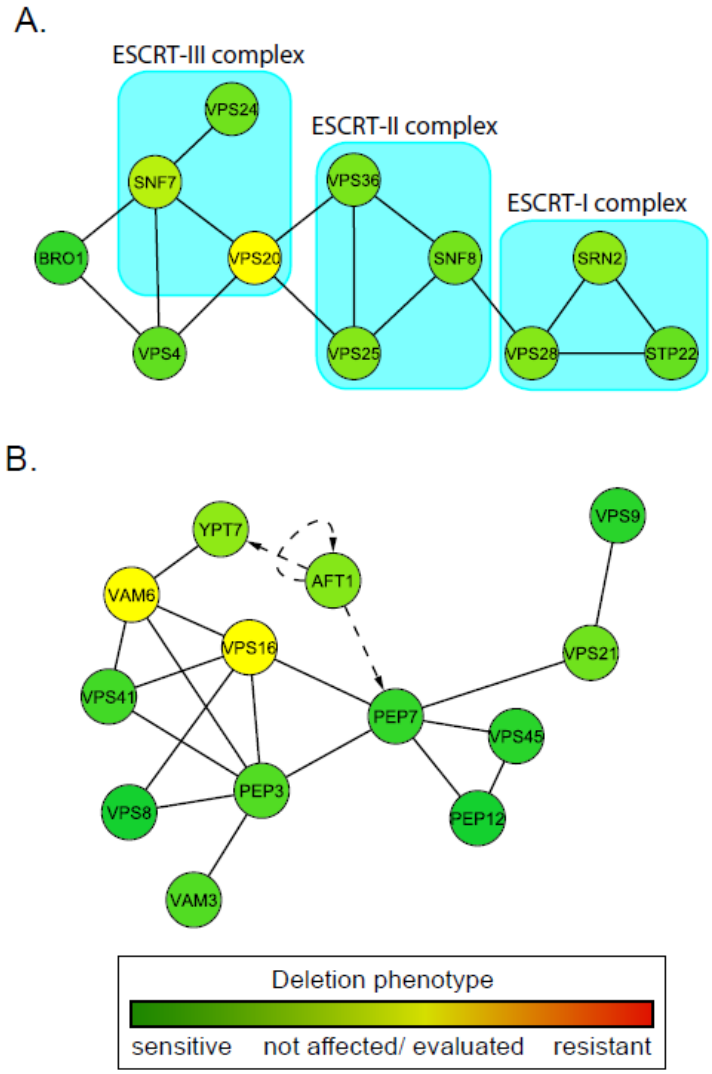

Figure 2.3. Cd resistance genes following exposure to 4 μM $CdCl_2$ for 5G. **A.** The ESCRT complexes I, II and III mediate resistance to cadmium. **B.** Cadmium resistance is associated with intracellular trafficking through endosomal intermediates that target the vacuole. The transcription factor Aft1p regulates iron homeostasis and its presence suggests that some of the genes identified in the network such as Ypt7p and Pep7p may be required to regulate iron levels in the presence of cadmium. Only subunits that were identified by network analysis are shown. Solid lines connecting nodes indicate protein-protein interactions while broken lines protein-DNA interactions.

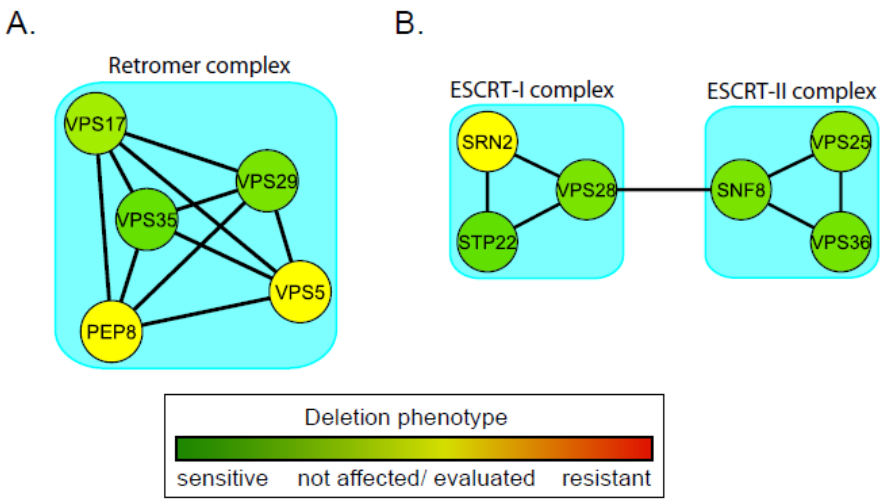

Figure 2.4. Pb resistance genes following exposure to 1000 µM $PbCl_2$ for 5G. **A.** The retromer complex functions in Pb resistance. This complex is involved in endosome-to-Golgi retrograde protein transport. **B.** The ESCRT complexes are essential for growth in Pb. Deletion of SNF7, component of the ESCRT-III, resulted in sensitivity to Cd. SNF7 is not shown in the network. Solid lines connecting nodes indicate protein-protein interactions.

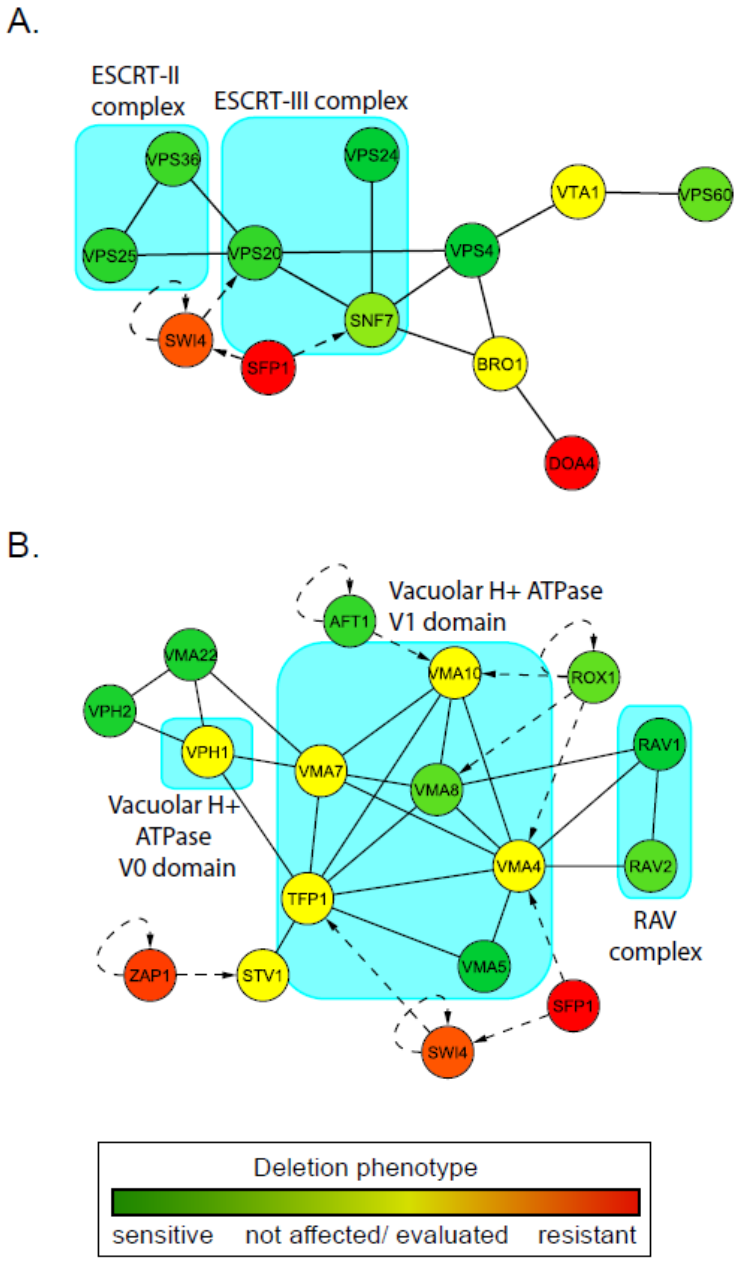

Figure 2.5. Zn resistance genes following exposure to 2500 µM $ZnCl_2$ for 5G. **A.** The ESCRT complexes are involved in yeast resistance to Zn. **B.** The vacuolar H+-ATPase is necessary for yeast resistance to Zn. The H+-ATPase is involved in vacuolar acidification, supporting the fact that vacuoles play an important role in zinc detoxification. Solid lines connecting nodes indicate protein-protein interactions while broken lines protein-DNA interactions.

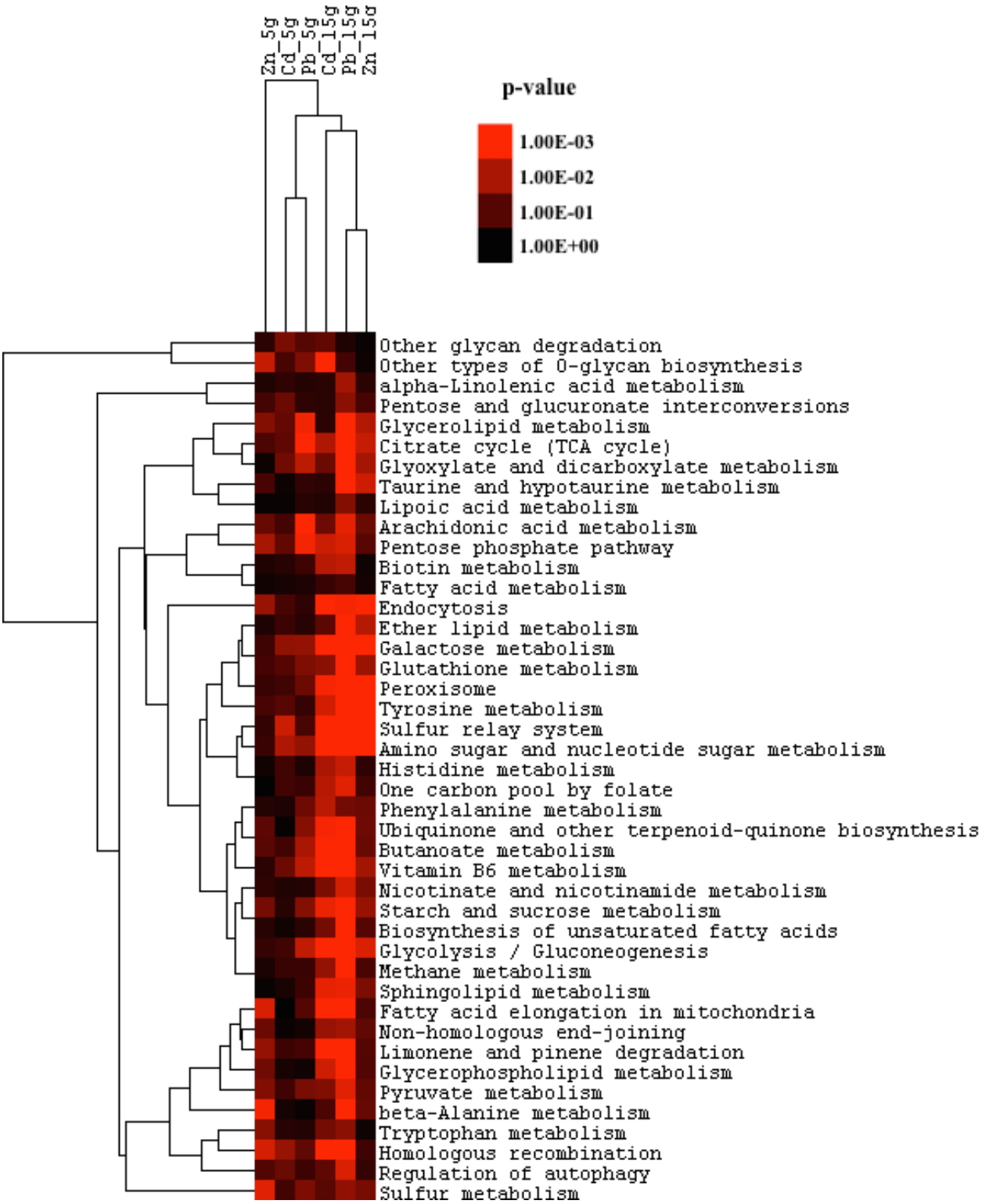

Figure 2.6. Clustergram of KEGG pathways significantly affected by heavy metal treatment.

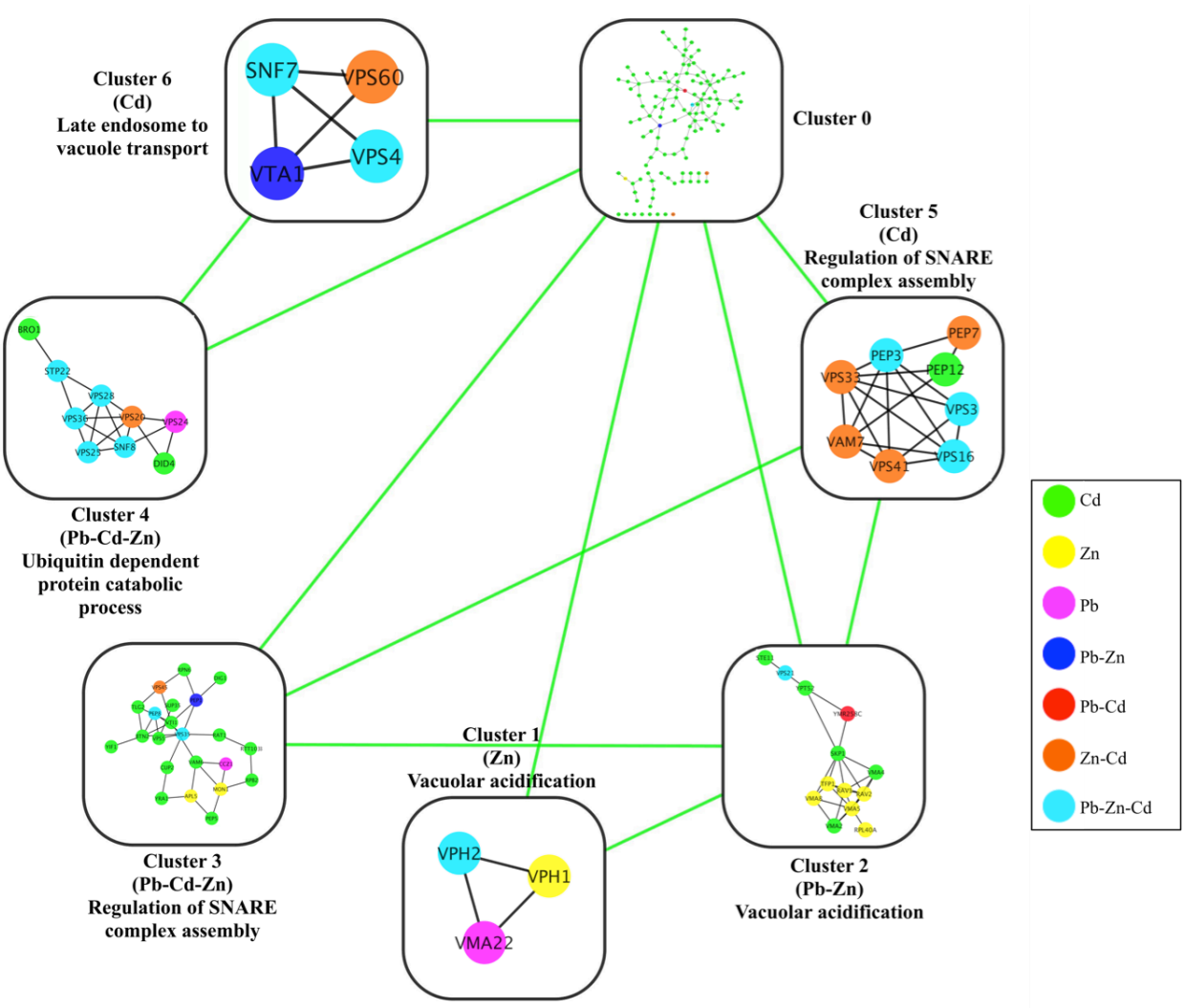

Figure 2.7. Clusters (sub-networks) of proteins enriched for targets of Zn, Cd, and Pb that are identified by mapping fitness data to the STRING yeast interaction data set using the statistical approach detailed in [41]. The nodes of the sub-networks represent yeast proteins and are colored according to whether the corresponding protein is a target of a particular combination of Zn, Pb, and Cd.

References

1. International Agency for Research on Cancer website

2. Nawrot T, Plusquin M, Hogervorst J, Roels HA, Celis H, Thijs L, Vangronsveld J, Van Hecke E, Staessen JA: Environmental exposure to cadmium and risk of cancer: a prospective population-based study. *Lancet Oncol* 2006, 7(2):119-126.

3. Goyer RA, Liu J, Waalkes MP: Cadmium and cancer of prostate and testis. *Biometals* 2004, 17(5):555-558.

4. McMurray CT, Tainer JA: Cancer, cadmium and genome integrity. *Nature genetics* 2003, 34(3):239-241.

5. Martelli A, Rousselet E, Dycke C, Bouron A, Moulis JM: Cadmium toxicity in animal cells by interference with essential metals. *Biochimie* 2006, 88(11):1807-1814.

6. White LD, Cory-Slechta DA, Gilbert ME, Tiffany-Castiglioni E, Zawia NH, Virgolini M, Rossi-George A, Lasley SM, Qian YC, Basha MR: New and evolving concepts in the neurotoxicology of lead. *Toxicology and applied pharmacology* 2007, 225(1):1-27.

7. Goyer RA, Clarkson TW: Toxic effects of metals. In Cassarett & Doull's Toxicology, Sixth edn: McGraw-Hill; 2001.

8. ATSDR: Toxicological Profile for Zinc: Agency for Toxic Substances and Disease Registry; 2005.

9. Hughes TR: Yeast and drug discovery. *Functional & integrative genomics* 2002, 2(4-5):199-211.

10. Winzeler EA, Shoemaker DD, Astromoff A, Liang H, Anderson K, Andre B, Bangham R, Benito R, Boeke JD, Bussey H *et al*: Functional characterization of the S. cerevisiae genome by gene deletion and parallel analysis. *Science (New York, NY* 1999, 285(5429):901-906.

11. Giaever G, Chu AM, Ni L, Connelly C, Riles L, Veronneau S, Dow S, Lucau-Danila A, Anderson K, Andre B *et al*: Functional profiling of the Saccharomyces cerevisiae genome. *Nature* 2002, 418(6896):387-391.

12. Li ZS, Lu YP, Zhen RG, Szczypka M, Thiele DJ, Rea PA: A new pathway for vacuolar cadmium sequestration in Saccharomyces cerevisiae: YCF1-catalyzed transport of bis(glutathionato)cadmium. *Proceedings of the National Academy of Sciences of the United States of America* 1997, 94(1):42-47.

13. Kamizono A, Nishizawa M, Teranishi Y, Murata K, Kimura A: Identification of a gene conferring resistance to zinc and cadmium ions in the yeast Saccharomyces cerevisiae. *Mol Gen Genet* 1989, 219(1-2):161-167.

14. Yu X, Hong S, Faustman EM: Cadmium-induced activation of stress signaling pathways, disruption of ubiquitin-dependent protein degradation and apoptosis in primary rat Sertoli cell-gonocyte cocultures. *Toxicol Sci* 2008, 104(2):385-396.

15. Figueiredo-Pereira ME, Yakushin S, Cohen G: Disruption of the intracellular sulfhydryl homeostasis by cadmium-induced oxidative stress leads to protein thiolation and ubiquitination in neuronal cells. *J Biol Chem* 1998, 273(21):12703-12709.

16. Pagani MA, Casamayor A, Serrano R, Atrian S, Arino J: Disruption of iron homeostasis in Saccharomyces cerevisiae by high zinc levels: a genome-wide study. *Molecular microbiology* 2007, 65(2):521-537.

17. Li L, Kaplan J: Defects in the yeast high affinity iron transport system result in increased metal sensitivity because of the increased expression of transporters with a broad transition metal specificity. *The Journal of biological chemistry* 1998, 273(35):22181-22187.

18. Yamaguchi-Iwai Y, Dancis A, Klausner RD: AFT1: a mediator of iron regulated transcriptional control in Saccharomyces cerevisiae. *The EMBO journal* 1995, 14(6):1231-1239.

19. Yonkovich J, McKenndry R, Shi X, Zhu Z: Copper ion-sensing transcription factor Mac1p post-translationally controls the degradation of its target gene product Ctr1p. *The Journal of biological chemistry* 2002, 277(27):23981-23984.

20. Heo DH, Baek IJ, Kang HJ, Kim JH, Chang M, Jeong MY, Kim TH, Choi ID, Yun CW: Cadmium regulates copper homoeostasis by inhibiting the activity of Mac1, a transcriptional activator of the copper regulon, in Saccharomyces cerevisiae. *Biochem J* 2010, 431(2):257-265.

21. Zhao H, Eide DJ: Zap1p, a metalloregulatory protein involved in zinc-responsive transcriptional regulation in Saccharomyces cerevisiae. *Molecular and cellular biology* 1997, 17(9):5044-5052.

22. Jo WJ, Kim JH, Oh E, Jaramillo D, Holman P, Loguinov AV, Arkin AP, Nislow C, Giaever G, Vulpe CD: Novel insights into iron metabolism by integrating deletome and transcriptome analysis in an iron deficiency model of the yeast Saccharomyces cerevisiae. *BMC genomics* 2009, 10:130.

23. Min KS, Iwata N, Tetsutikawahara N, Onosaka S, Tanaka K: Effect of hemolytic and iron-deficiency anemia on intestinal absorption and tissue accumulation of cadmium. *Toxicology letters* 2008, 179(1):48-52.

24. Min KS, Ueda H, Kihara T, Tanaka K: Increased hepatic accumulation of ingested Cd is associated with upregulation of several intestinal transporters in mice fed diets deficient in essential metals. *Toxicol Sci* 2008, 106(1):284-289.

25. Thorsen M, Perrone GG, Kristiansson E, Traini M, Ye T, Dawes IW, Nerman O, Tamas MJ: Genetic basis of arsenite and cadmium tolerance in Saccharomyces cerevisiae. *BMC Genomics* 2009, 10:105.

26. Momose Y, Iwahashi H: Bioassay of cadmium using a DNA microarray: genome-wide expression patterns of Saccharomyces cerevisiae response to cadmium. *Environmental toxicology and chemistry / SETAC* 2001, 20(10):2353-2360.

27. Pierce SE, Fung EL, Jaramillo DF, Chu AM, Davis RW, Nislow C, Giaever G: A unique and universal molecular barcode array. *Nature methods* 2006, 3(8):601-603.

28. Loguinov AV, Mian IS, Vulpe CD: Exploratory differential gene expression analysis in microarray experiments with no or limited replication. *Genome biology* 2004, 5(3):R18.

29. Jo WJ, Loguinov A, Wintz H, Chang M, Smith AH, Kalman D, Zhang L, Smith MT, Vulpe CD: Comparative Functional Genomic Analysis Identifies Distinct and Overlapping Sets of Genes Required for Resistance to Monomethylarsonous Acid (MMAIII) and Arsenite (AsIII) in Yeast. *Toxicol Sci* 2009.

30. Kiemer L, Costa S, Ueffing M, Cesareni G: WI-PHI: a weighted yeast interactome enriched for direct physical interactions. *Proteomics* 2007, 7(6):932-943.

31. Teixeira MC, Monteiro P, Jain P, Tenreiro S, Fernandes AR, Mira NP, Alenquer M, Freitas AT, Oliveira AL, Sa-Correia I: The YEASTRACT database: a tool for the analysis of transcription regulatory associations in Saccharomyces cerevisiae. *Nucleic acids research* 2006, 34(Database issue):D446-451.

32. Matovic, V., Buha, A., Bulat, Z., & Dukic-Cosic, D. Cadmium toxicity revisited: Focus in oxidative stress induction and interactions with zinc and magnesium. *Archives of Industrial Hygiene and Toxicology* 2011, 62 (1), 65-76.

33. Thevenod, F., & Friedmann, J. Cadmium-mediated oxidative stress in kidney proximal tubule cells induces degradation of Na+/K+-ATPase through proteasomal and endo-/lysosomal proteolytic pathways. *Faseb Journal* 1999, *13* (13), 1751-1761.

34. Stohs, S. & Bagchi, D. Oxidative mechansims in the toxicity of metal ions. Free Radical Biology And Medicine 1995, 18 (2), 321-336.

35. Adonaylo, V., & Oteiza, P. Lead intoxication: antioxidant defenses and oxidative damage in rat brain. Toxicology 1999, 135 (2-3), 77-85.

36. Adonaylo, V., & Oteiza, P. Pb2+ promotes lipid oxidation and alterations in membrane physical properties. Toxicology 1999, 132 (1), 19-32.

37. Hambidge, M. Human zinc deficiency. *Journal Of Nutrition* 2000*,130* (5), 1344S-1349S.

38. Farant, J., & Wigfield. Biomonitoring lead esposure with delta aminolevulinate dehydratase (ALDA-D) activity ratios. *International Archives Of Occupational And Environmental Health* 1982*,* 51 (1), 15-24.

39. Wapnir, R.. Zinc deficiency, malnutrition and the gastrointestinal tract. *Journal Of Nutrition* 2000*,* 130 (5), 1388S-1392S.

40. Jomova, K., & Valko, M. Advances in metal-induced oxidative stress and human disease. *Toxicology* 2011*,* 283 (2-3), 65-87.

41. North M, Tandon VJ, Thomas R, Loguinov A, Gerlovina I, Hubbard AE, et al. Genome-wide functional profiling reveals genes required for tolerance to benzene metabolites in yeast. *Plos One* 2011, 6 (8), e24205.

Chapter III

Functional profiling in yeast identifies DNA repair pathways required in response to the TCE metabolite dichlorovinyl cysteine (DCVC)

ABSTRACT

Trichloroethylene (TCE) is a common environmental contaminant, particularly at Superfund waste sites. Considered a human carcinogen, there remains a need for molecular evidence linking TCE and renal cancer. Studies have identified the metabolite dichlorovinyl cysteine (DCVC) as the penultimate mediator of TCE renal toxicity and ultimately, renal cancer. Using a functional genomics approach in yeast we aim to identify cellular processes that mediate the renal toxicity of DCVC. Genome profiling revealed genotoxicity as an important contributor in DCVC toxicity and implicates DCVC as a DNA cross-linking agent. Specifically, mutagenic translesion synthesis (TLS), nucleotide excision repair (NER) and homologous recombination pathways were required for tolerance to DCVC. Furthermore, we find that DCVC damage elicits repair predominately by the low fidelity (error-prone) polymerase *Rev3* (Polζ). These findings are the first to provide molecular and genetic evidence supporting DCVC genotoxicity as a contributor to TCE toxicity.

INTRODUCTION

The Superfund contaminant trichloroethylene (TCE) is a common environmental contaminant introduced at the beginning of the 20th century as a replacement for chloroform and ether in many industries (1). TCE is a common contaminant at abandoned military sites, spacecraft/aircraft sites and Superfund sites throughout the US. Consumption of drinking water sources contaminated with leached TCE is the main route of exposure for the general population (1). It is estimated between 9-34% of drinking water sources are contaminated with TCE (1).

TCE undergoes a complex metabolism resulting in bioactive intermediates via the glutathione conjugation pathway (**Fig. 3.1**) (2). The glutathione conjugation pathway is a common mechanism for eliminating electrophilic molecules, but can yield toxic metabolites (3,4). In the case of TCE, glutathione conjugation results in the formation of dichlorovinyl cysteine (DCVC), which has been shown to cause renal toxicity in rodents (5-7). In several studies DCVC caused single and double strand breaks in DNA and tested positive as a mutagen (8,9). Moreover, epidemiological studies revealed an increased incidence of kidney and blood cancers in TCE exposed workers(1). Genetic analysis showed exposed workers had unique mutations in the von Hippel Lindau (VHL) gene, a tumor suppressor gene commonly associated with renal cell carcinomas (10-13) This data suggests a mutagenic mode of action for TCE induced renal cancer, mediated predominately by the metabolite DCVC. The majority of studies have focused on the use of animal models for mechanistic insight, but have led to controversial and inconsistent results (14). This is attributed to several factors including, complex metabolism, species susceptibility, and sex differences.

S. cerevisiae has long been a model organism in molecular biology and a useful model for

mechanistic toxicity studies. Advantages of yeast include elimination of compounding factors, as mentioned above, associated with whole animal models, ease of genetic manipulation, the availability of bioinformatics resources and most importantly the high degree of conservation of cellular pathways from yeast to humans. The introduction of the homozygous deletion library allows for functional profiling studies to characterize mechanisms of toxicity and identify toxicant susceptibility genes. Genome wide profiling in yeast has proven successful for investigating toxicity mechanisms for numerous toxicant classes, including heavy metals, pesticides, organic solvents and genotoxicants (15-19). Futhermore, results from yeast studies have informed *in vitro* and epidemiological studies (20). The identification of toxicant susceptibility genes from profiling studies highlights the robustness of this approach and its utility for toxicity and environmental health studies (20).

In this chapter, a genome-wide screen in yeast was utilized to identify cellular processes that mediate the toxicity of the TCE metabolite, dichlorovinyl cysteine (DCVC) and the role these processes may play in mediating TCE renal cancer. The results from profiling studies revealed genotoxicity plays a central role in DCVC toxicity and implicated the metabolite causes damage similar to a DNA cross-linking agent. Additionally, the requirement for mutagenic translesion synthesis repair of DCVC lesions supports a mutagenic mode of action for TCE. This study provides exciting mechanistic evidence for further investigation and new insight on the molecular events that mediate TCE renal toxicity.

RESULTS and DISCUSSION

A genome-wide screen identifies mutants with altered growth in the presence of DCVG and DCVC metabolites

Growth curve assays were performed to determine the toxicity of DCVG and DCVC to yeast. From the growth curves, the IC_{20}, a concentration determined as appropriate for use in the functional screen, was calculated as 18μM for DCVC and 6.7 μM for DCVG (**Fig. 3.2a).** Pools of yeast homozygous diploid deletion mutants (n = 4607) were grown for 5 generations at the IC_{20} (18μM and 6.7 μM), 50% IC_{20} (9μM and 3 μM), and 25% IC_{20} (4.5μM and 1.5μM). A differential strain sensitivity analysis (DSSA) identified 114 mutants as sensitive and 103 mutants as resistant to at least one dose of DCVG for a total of 217 genes identified. For DCVC, 56 mutants were identified as sensitive and 155 mutants as resistant to at least one dose for a total of 211 genes identified (**Appendix 4**). The top thirty sensitive strains at the IC_{20} of DCVC are shown in **Table 2.1**. Strains sensitive to DCVC were the focus of this study as it has been shown to be penultimate metabolite responsible for toxicity.

Enrichment analysis identifies attributes necessary for DCVC tolerance

A list of mutant strains displaying sensitivity to DCVC treatments (n = 56) was analyzed using FunSpec and the Yeastmine programs to identify significantly overrepresented biological processes. GO categories were enriched for response to DNA damage stimulus, error-free translesion synthesis, and nucleotide excision repair processes. Based on the results from enrichment analyses we focused further experiments on DNA damage and repair (**Table 3.2**).

Loss of putative beta-lyase proteins do not confer resistance to DCVC toxicity

Metabolic activation by the glutathione conjugation pathway plays a central role in TCE renal toxicity (14,15,17). Renal toxicity is dependent on the formation of the cysteine conjugate and

reactive thiolate intermediate, mediated by gamma-glutamyl transpeptidase (GGT) and beta lyase enzyme, respectively. Conservation of metabolic activation of TCE metabolites in yeast was assayed in mutants deficient in the gamma-glutamyl transpeptidase, *ecm38*Δ and the putative beta lyases *irc7*Δ and *bna3*Δ for resistance to metabolite toxicity. *Ecm38*Δ mutants were significantly resistant to DCVG toxicity compared to wild-type, likely due to the decrease in cysteine conjugate production (DCVC) (**Fig. 3.1b**). This observation is consistent with *in vitro* studies using chemical GGT inhibitors and further supports DCVC as the penultimate metabolite responsible for toxicity (21,22). In contrast, the *irc7*Δ and *bna3*Δ mutants did not confer any resistance to DCVC and had similar toxicity to wild-type (**Fig. 3.1c**). This finding could be due to the redundancy of several proteins present in yeast with beta-lyase activity. Nevertheless, these results coincide with *in vitro* and *in vivo* studies attributing TCE renal toxicity to the cysteine conjugate, DCVC (21-23).

Mutants defective in DNA repair are sensitive to TCE metabolite DCVC

Enrichment analysis implicated two distinct repair pathways, translesion synthesis and nucleotide excision repair, as important processes for DCVC tolerance (**Table. 3.2**). During replication, post-translational modification of the replication factor PCNA (proliferating cell nuclear antigen) in eukaryotes initiates the error-prone translesion synthesis repair (TLS) pathway or the error-free, template-switching (TS) pathway (24). These repair mechanisms prevent replication stalling and fork collapse when a DNA lesion is encountered (25). Monoubiquitination of PCNA at the Lys164 residue by the *Rad6-Rad18* complex initiates the error prone translesion pathway, recruiting special TLS polymerases such as *Rev3, Rad30,* and *Rev1* to sites of damage (**Fig. 3.3**) (25,26). We used competitive growth assays to examine mutants deficient in these pathways (**Fig. 3.3**). Both DSSA and flow cytometry identified *rad18*Δ, which lacks a gene encoding for an E3 ubiquitin ligase important for the initiation and stabilization of translesion synthesis repair, as one of the strains most sensitive to DCVC (**Fig. 3.4a**). Additional translesion synthesis genes were confirmed to be required for DCVC tolerance, including *Rev1*, a deoxycytidyl transferase that preferentially incorporates a cytosine across abasic sites or damaged bases, *Rev3*, the catalytic subunit of the error prone DNA polymerase zeta, and *Rad5* a DNA helicase proposed to promote replication fork regression and error-free repair (**Fig. 3.4a**). *Rad30,* another translesion polymerase involved in the repair of UV induced damage was not identified by DSSA and was not sensitive to DCVC (**Fig. 3.4a**), supporting the specificity and sensitivity of PDA to characterize genotoxicity.

Specific components of nucleotide excision repair were identified as necessary in response to DCVC (**Fig. 3.4b**). The nucleases *PSO2* is required for the repair of DNA single and double-strand breaks and acts at a post-incision step in repair of breaks that result from interstrand crosslinks. *RAD1,* and *RAD10* form a single-strand DNA endonuclease that binds DNA and then nicks the damaged DNA strand on the 5' side of the lesion during nucleotide excision repair (**Fig. 3.3**). Individual growth curve analysis with these TLS, NER and HR mutants were conducted concurrently and showed a dose response supporting flow cytometry results (data not shown). The hypersensitivity of TLS and NER mutants to DCVC suggests DCVC causes direct DNA damage and provides genetic evidence supporting DCVC genotoxicity. As both of these DNA repair pathways are highly conserved in humans (**Table 3.3**), genotoxicity is a likely mechanism for DCVC renal toxicity in humans (24,27).

REV3 polymerase plays a central role in mediating DNA repair and genotoxicity of DCVC

After demonstrating a requirement for translesion synthesis (TLS) repair in DCVC tolerance (**Fig. 3.4A**), we examined the roles of error-prone TLS polymerases such as *Rad30* (*Polη*), *Rev1* and *Rev3* (*Polζ)* or the error-free pathway of *Rad5* in rescuing the DCVC sensitivity of ***rev3Δ*** mutants (**Fig 3.5**). As expected, the ***rev3Δ*** mutant complemented with *REV3*p showed increased resistance to DCVC similar to wild-type levels at both 18μM and 30μM DCVC. Overexpression of the TLS polymerases *RAD30*p or *REV1*p did not rescue sensitivity of the ***rev3Δ*** mutant nor did overexpression of the helicase *RAD5*p, which initiates error-free template switching (a form of recombination repair). These results suggest *Rev3* is the main polymerase in repairing DCVC DNA damage and is a key factor in moderating DCVC genotoxicity. *Rev3* is a B family polymerase and lacks 3'-5' proofreading exonuclease activity, has low processivity and decreased fidelity (25,28). These attributes allow for *Rev3* to bypass a variety of lesions, including interstrand crosslinks, bulky adducts and UV damage, in an effort to prevent stalled forks and double strand breaks at the cost of increasing mutagenesis (24,29-31). The extent of mutagenesis is dependent on a combination of the TLS polymerase, characteristics of the lesion, and the surrounding sequence environment (25,28). The specific requirement for *Rev3* suggests DCVC lesions are preferentially repaired by TLS and has the potenial to increase mutagenesis.

DSSA and flow cytometry experiments identified the DNA helicase, *Rad5,* as required for tolerance to DCVC (**Fig. 3.4a**). *Rad5* is involved in the error-free branch of DNA damage tolerance (DDT) pathway. It is proposed to promote replication fork regression during post-replication repair by template switching (TS), but the intricacies of this pathway remain poorly understood (25). *Rad5* is required for *Rev3* dependent translesion synthesis and mediates translesion synthesis and mutagenesis through structural interactions with *Rev1* and *Rev3* (32,33). The hypersensitivity of ***Rad5Δ*,** mutants further supports that DCVC genotoxicity is mediated by mutagenic *Rev3* TLS repair.

Sensitivity profile of DCVC is similar to known interstrand crosslinking (ICL) agents

In a study by Lee et al, a panel of DNA damaging agents were analyzed using parallel deletion analysis in yeast to determine the genetic requirements for the repair of interstrand crosslinks (34). Their findings revealed translesion synthesis, nucleotide excision repair and homologous recombination genes were required for resistance to various crosslinking agents in yeast. We compared the gene sensitivity profile of DCVC to the profiles of the 12 agents in the Lee *et al* study and found almost matching genetic profiles with established interstrand crosslinking agents. Characteristics of these agents include bifunctionality (cisplatin and nitrogen mustards) or two chemically active leaving groups that can react with DNA bases on each strand, usually at the N7 position of guanine or the exocyclic amino groups (35). Interstrand crosslinks are particularly detrimental to the cell as these lesions disrupt replication and transcription by preventing separation of DNA strands, resulting in fork collapse and ultimately double strand breaks (36). While levels of ICLs are low, it has been shown that even a nominal number of ICLs, 1-2 in yeast and 20-40 in mammalian cells can be deterimental and repair of these lesions is critical to genomic viability (35). Similar to DCVC, TLS mutants such as ***rev3Δ*** have exhibited hypersensitivity to cross linking agents such as cisplatin, nitrogen mustards and mitomycin C (MMC) (37-40).

CONCLUSIONS

Functional profiling of the metabolite DCVC identified a specific subset of cellular processes that modulate toxicity. We hypothesize genotoxicity plays a central role in mediating DCVC toxicity. Our results suggest DCVC genotoxicity is consistent with other interstrand crosslinking agents and requires mutagenic DNA repair. These studies provide new and exciting genetic evidence supporting genotoxicity as a mechanism for DCVC renal toxicity. Data generated by this study can direct additional experimentation to determine the implications of DCVC genotoxicity in genome instability and carcinogenesis. Furthermore, we show that a functional genomics approach in yeast is a viable method for examining toxicity mechanisms and more specifically its utility in characterizing genotoxicity mechanisms.

MATERIALS AND METHODS

Chemical Reagents

Dichlorovinyl glutathione (DCVG) and Dichlorovinyl cysteine (DCVC) conjugates were generous gifts from Professor A. Elfarra at the University of Wisconsin, Madison. Stock solutions were prepared in sterile Milli-Q water (Millipore, Billerica, MA) and stored at -20°C until use. All yeast reagents were purchased from commercial suppliers.

Yeast strains, culture, and plasmids

The diploid yeast deletion strains used for functional profiling and confirmation analyses were of the BY4743 background (*MATa/MATα his3Δ1/his3Δ1 leu2Δ0/leu2Δ0 lys2Δ0/LYS2 MET15/met15Δ0 ura3Δ0/ura3Δ0,* Invitrogen). For deletion pool growth, cells were grown in liquid rich media (1% yeast extract, 2% peptone, 2% dextrose, YPD). All assays were performed in liquid rich media at 30°C with shaking at 200 rpm, except overexpression experiments, which used liquid rich media containing 2% galactose and 2% raffinose (YPGal+Raf). For overexpression analyses, FlexGene expression vectors were transformed into strains of the BY4743 background. Rad5 strains were on the EMY74.7 background (*MATa his3D-1 leu2-3,-112 trp1D ura3-52*). Rad5 strains with wild type or its mutant derivatives were carried on a YCplac133-based plasmid, which contains the ARS1 origin of replication, the centromeric CEN4 region, and the LEU2 gene. The plasmid, pR28, expresses the wild-type Rad5 protein (RAD5). Plasmid pR30 carries the mutations D681, E682 in RAD5, which inactivate the ATPase and DNA helicase activities of Rad5 (Rad5 helicase mutant), and plasmid pR19 carries the mutations C914, C917 in the C3HC4 ring-finger motif that abolishes ubiquitin ligase function (Rad5 Ub ligase mutant).

Dose-finding and growth curve assays

Briefly, cells were grown to mid-log phase, diluted to an optical density at 600nm (OD600) of 0.0165, and dispensed into nontreated polystyrene plates. Dichlorovinyl glutathione (DCVG) and dichlorovinyl cysteine (DCVC) stock solutions were prepared in water and added to the desired final concentrations with at least two technical replicates per dose. Plates were incubated in Tecan microplate readers set to 30°C with shaking and OD595 measurements were taken every 15min for 24h. The raw absorbance data were averaged, background corrected, and plotted as a

function of time. The area under the curve was calculated and expressed as a percentage of the untreated control.

Functional profiling of the yeast genome

Growth of the deletion pools, genomic DNA extraction, barcode amplification, Affymetrix TAG4 array hybridization, and differential strain sensitivity analysis (DSSA) were performed as described (Jo *et al.*, 2009b). Briefly, pools of homozygous diploid deletion mutants (n = 4607) were grown in YPD at various DCVC concentrations for 5 generations and genomic DNA was extracted using the YPER kit (Pierce Biotechnology). The DNA sequences unique to each strain (barcodes) were amplified by PCR and hybridized to TAG4 arrays (Affymetrix), which were incubated overnight, stained, and then scanned at an emission wavelength of 560nm with a GeneChip Scanner (Affymetrix). Data files are available at the Gene Expression Omnibus database.

Overenrichment analysis

Significantly overrepresented Gene Ontology (GO) categories within the DSSA data were identified by a hypergeometric distribution using the Functional Specification resource, FunSpec (funspec.med.utoronto.ca) and the YeastMine database (http://yeastmine.yeastgenome.org/) with a p value cutoff of 0.001.

Confirmatory Growth Analysis

Yeast strains were pre-grown to mid-log phase, diluted to an optical density at 600 nm (OD600) of 0.0165, and dispensed into a 96-well plate (non-treated polystyrene, Grenier Bio-One, Monroe, NC). TCE metabolite stock solutions were added to the desired final concentrations with at least two replicates per dose. Plates were incubated in a microplate reader (Tecan, Durham, NC) set to 30°C with intermittent shaking. OD600measurements were taken at 15-minute intervals for 24 hrs. Raw absorbance data were averaged for all replicates, background corrected, and plotted as a function of time. The area under the curve (AUC) was calculated as a measure of growth, and expressed as a percentage of the control. AUCs were compared by two-way ANOVA followed by Bonferroni post-tests. Data for each strain is derived from at least 3 independent cultures.

Analysis of relative strain growth by flow cytometry

Briefly, green fluorescent protein (GFP)-tagged wild-type and untagged mutant strains were grown overnight in YPD, diluted to 0.5 OD600, and mixed in approximately equal numbers. Cells were inoculated into YPD at 0.00375 OD600 in microplate format, treated with DCVC, and grown for 24hrs at 30°C with shaking at 200 rpm. Approximately 20,000 cells per culture were analyzed at 0 and 24hrs using a FACSCalibur flow cytometer. GFP-expressing wild-type cells were distinguishable from untagged mutant cells. The percentages of wild-type GFP and untagged mutant cells present in the cultures were used to calculate a ratio of growth for untagged cells in treated versus untreated samples. Statistically significant differences between the means of three independent DCVC treated cultures were determined using t-test. Raw p values were corrected for multiplicity of comparisons using Benjamini-Hochberg correction.

Complementation Overexpression Assays

Yeast overexpression strains were pre-grown overnight to stationary phase in SC-ura 2% dextrose, then diluted 1:100 in SC-ura 2% raffinose and grown overnight again to alleviate glucose repression. Cells were then diluted in YPGal+Raf to induce protein overexpression, and grown for 5 hours to mid-log phase. Cells were subsequently diluted to an optical density at 600 nm (OD600) of 0.0165 in YPGal+Raf, and dispensed into a 96-well plate. DCVC treatment, plate measurement and data processing were all carried out in the same manner as the deletion strain growth curve assays.

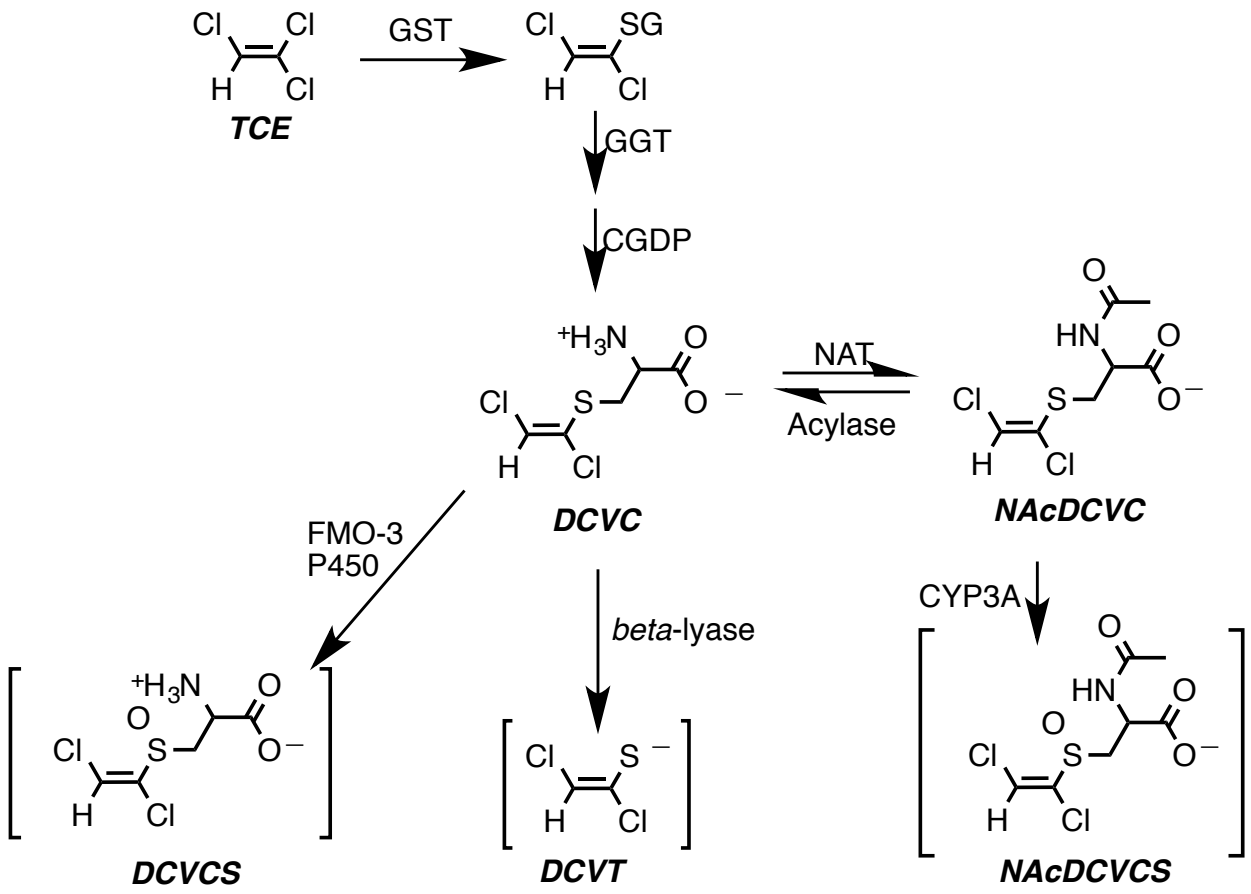

Figure 3.1. Overview of glutathione conjugation metabolism of TCE and the chemical structure of the DCVG and DCVC metabolites associated predominately with kidney toxicity. TCE is conjugated with glutathione in the liver and forms a cysteine conjugate in the kidney (DCVC). DCVC is further metabolized to highly reactive intermediates such as the thiolate DCVT. NAcDCVC is the major urinary metabolite formed.

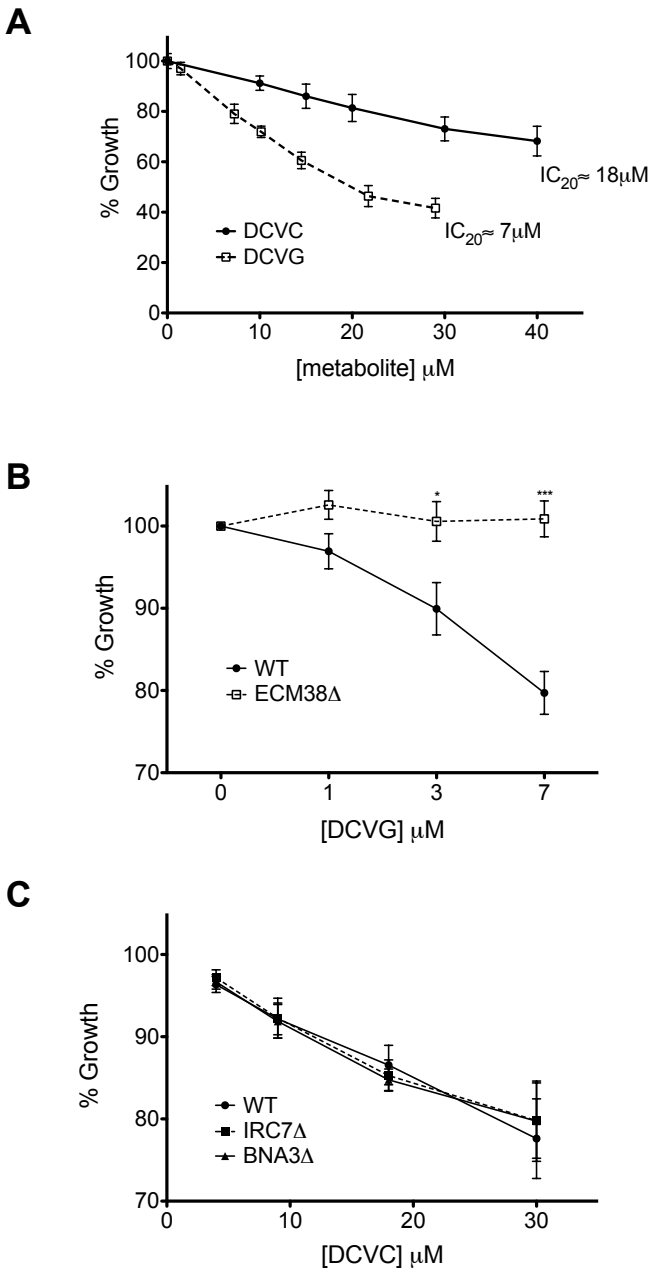

Figure 3.2. (A) Dose response of the metabolites DCVG and DCVC and calculated IC_{20} concentrations for functional profiling. (B) Mutants lacking gamma-glutamyl transpeptidase (*ECM38*) are resistant to DCVG likely due to a decrease in DCVC formation (C) Mutants lacking proteins with known cysteine beta-lyase function do not confer resistance to DCVC. Values are mean ± SEM; $n \geq 3$ for each measurement. Significance values were calculated by two way ANOVA ***$p < 0.001$, **$p < 0.01$, *$p < 0.05$ for DCVC-treated wild-type versus mutants.

Table 3.1. Fitness Scores for the Top 30 Mutants Identified as Significantly Sensitive to the DCVC IC_{20} (18**µ**M) After 5 Generations of Growth

IC_{20} Log_2 value[a]	Yeast Gene	Description
-4	*SUC2*	Invertase; sucrose hydrolyzing enzyme
-3.05	*CDC26*	Subunit of the Anaphase-Promoting Complex/Cyclosome
-2.95	*IRC2*	Dubious open reading frame; partially overlaps verified gene Alt2
-2.7	*RAD5*	DNA helicase/Ubiquitin ligase; involved in DNA damage tolerance (DDT) pathway
-2.4	*RAD18*	E3 ubiquitin ligase; required for postreplication repair
-2.4	*SEC66*	Subunit of Sec63 complex; involved in protein targeting and import into the ER
-2.3	*VPS8*	Involved in endosome to vacuole protein targeting pathway
-2.2	*VPS9*	Guanine nucleotide exchange factor; involved in vesicle-mediated vacuolar transport
-2	*PXA1*	Subunit of a heterodimeric peroxisomal ABC transport complex
-1.95	*VPS21*	Endosomal Rab family GTPase
-1.8	*LYS5*	Phosphopantetheinyl transferase involved in lysine biosynthesis
-1.8	*RAD10*	ssDNA endonuclease; involved in NER and double-strand break repair
-1.75	*PSO2*	Nuclease required for DNA single- and double-strand break repair
-1.7	*YRB30*	RanGTP-binding protein
-1.7	*LTE1*	Protein similar to GDP/GTP exchange factors
-1.7	*VHS1*	Cytoplasmic serine/threonine protein kinase
-1.7	*RAD51*	Strand exchange protein; involved in recombination repair of double-strand breaks
-1.65	*RAD1*	ssDNA endonuclease involved in NER and double-strand break repair
-1.6	*RAD4*	Protein that recognizes and binds damaged DNA during NER
-1.5	*PET10*	Protein of unknown function; expression pattern suggests a role in respiratory growth
-1.5	*BCH1*	Mediates export of specific cargo proteins from the Golgi to the plasma membrane
-1.4	*CUP2*	Copper-binding transcription factor; activates transcription of metallothionein genes
-1.4	*PXA1*	Subunit of peroxisomal ABC transport complex;
-1.4	*ECM37*	Mitochondrial outer membrane protein required to initiate mitophagy
-1.4	*MRP49*	Mitochondrial ribosomal protein of the large subunit
-1.4	*HXK2*	Hexokinase isoenzyme 2; catalyzes phosphorylation of glucose in the cytosol
-1.3	*PEX1*	AAA-peroxin
-1.3	*REV1*	Deoxycytidyl transferase; involved in Dna repair via translesion synthesis pathway (TLS)
-1.3	*CLB4*	B-type cyclin involved in cell cycle progression
-1.3	*PET127*	Protein with a role in 5'-end processing of mitochondrial RNAs
-1.3	*ERP5*	Member of the p24 family involved in ER to Golgi transport

[a]Fitness scores quantify the requirement of a gene for growth and are defined as the normalized log2 ratio of the deletion strain's growth in the presence versus absence of DCVC. A total of 56 genes were important for fitness in at least one DCVC treatment. Supplementary table 1 contains a list of all genes identified as significant by DSSA.

Table 3.2. Genes required for growth in the presence of DCVC and their associated gene ontology categories

GO Biological Process[a]	p-value	Genes Identified
Response to DNA damage stimulus	1.27E-05	*RAD18 HAT2 RAD51 RAD4 RAD5 RAD10 PSO2 REV1 RAD1 REV3*
Error-free translesion synthesis	6.30E-05	*RAD18 REV1 REV3*
Nucleotide-excision repair, DNA incision, 5'-to lesion	6.81E-05	*RAD10 RAD1*
DNA repair	0.0001221	*RAD18 HAT2 RAD51 RAD4 RAD5 RAD10 PSO2 REV1 RAD1 REV3*
Fatty acid transport	0.0002033	*PXA2 PXA1*
Eror-prone translesion synthesis	0.0002318	*RAD18 REV1 REV3*
Double-strand break repair via single-strand annealing, removal of nonhomologous ends	0.001393	*RAD10 RAD1*
Removal of nonhomologous ends	0.002362	*RAD10 RAD1*
Meiotic mismatch repair	0.003571	*RAD10 RAD1*
DNA metabolic process	0.00501	*RAD51 RAD1*
Mitotic recombination	0.00501	*RAD10 RAD1*
Positive regulation of cytoplasmic mRNA Processing body assembly	0.00833	*CAF20*
Regulation of transcription by glucose	0.00833	*HXK2*

GO Biological Process[a]	p-value	Genes Identified
Response to DNA damage stimulus	3.875E-04	*RAD18 RAD5 RAD10 REV1 RAD1 REV3*
Error-prone translesion synthesis	.007438	*RAD18 REV1 RAD5 REV3*

[a]A list of strains exhibiting sensitivity to DCVC was entered into the FunSpec or Yeastmine tools and analyzed for overrepresented biological attributes (see Materials and Methods section).

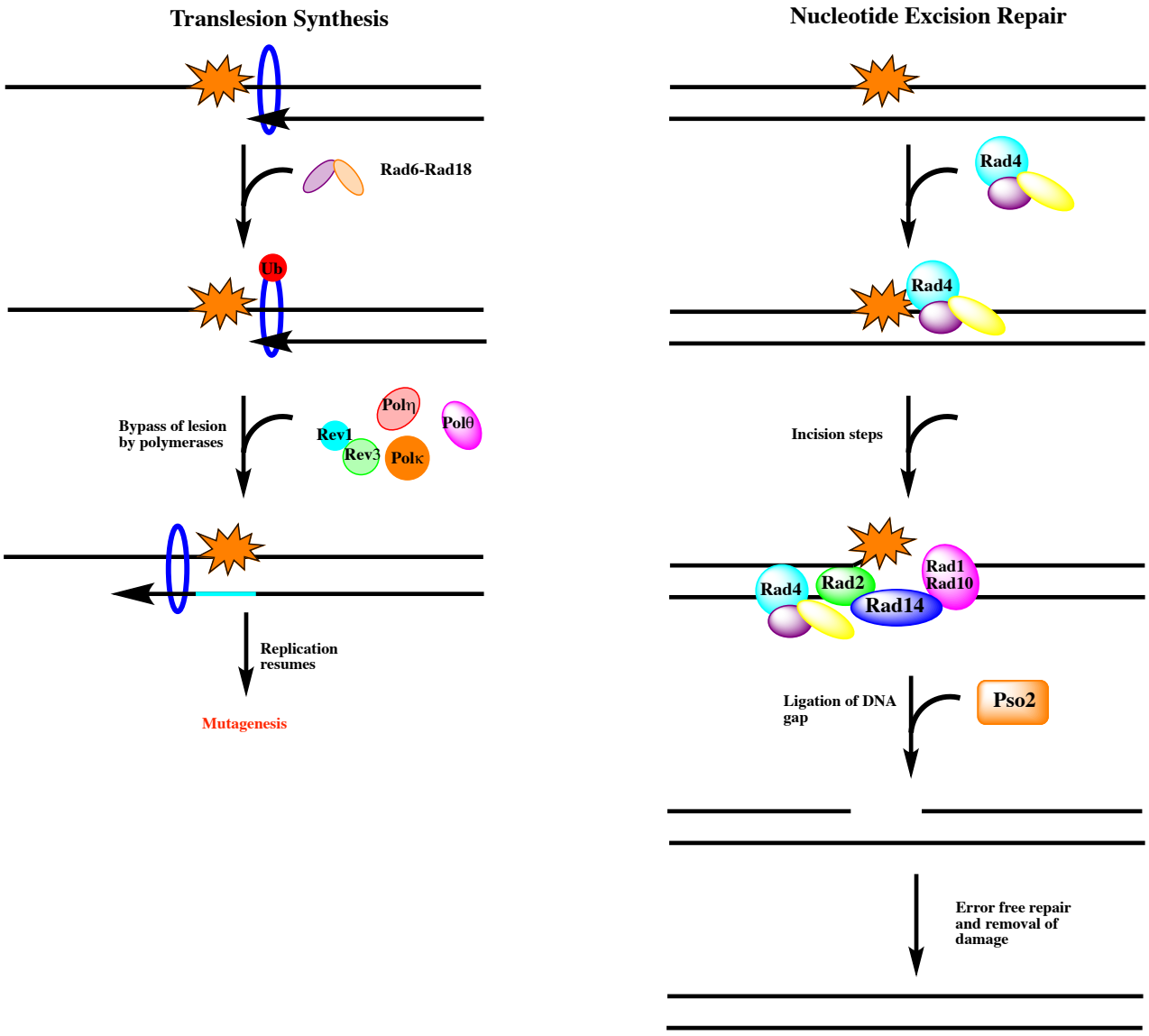

Figure 3.3 Overview of DNA repair pathways identified by functional profiling of DCVC in yeast. Translesion synthesis (TLS) is a DNA damage tolerance pathway that bypasses lesions during replication to prevent stalling and fork collapse. Bypass is mediated by low fidelity polymerases that are error-prone and results in mutagenesis. Nucleotide excision repair (NER) is an error-free repair mechanism that recognizes helix-distorting lesions. Upon lesion detection, a DNA fragment containing the damage is excised followed by and error-free gap filling.

Table 3.3. Selected yeast genes required for DCVC tolerance and their human homologs

Yeast Gene	Description	Human Homolog
RAD5	DNA helicase/Ubiquitin ligase; involved in DNA damage tolerance (DDT) pathway	SHPRH; HLTF
RAD18	E3 ubiquitin ligase; required for postreplication repair	RAD18
RAD10	ssDNA endonuclease; involved in NER and double-strand break repair	ERCC1
PSO2	Nuclease required for DNA single- and double-strand break repair	SNM1B
RAD51	Strand exchange protein; involved in recombination repair of double-strand breaks	RAD51
RAD1	ssDNA endonuclease involved in NER and double-strand break repair	ERCC4
RAD4	Protein that recognizes and binds damaged DNA during NER	XPC
REV1	Deoxycytidyl transferase; involved in DNA repair via translesion synthesis pathway (TLS)	REV1
REV3	Catalytic subunit of DNA polymerase zeta; involved in translesion synthesis during post-replication repair	REV3

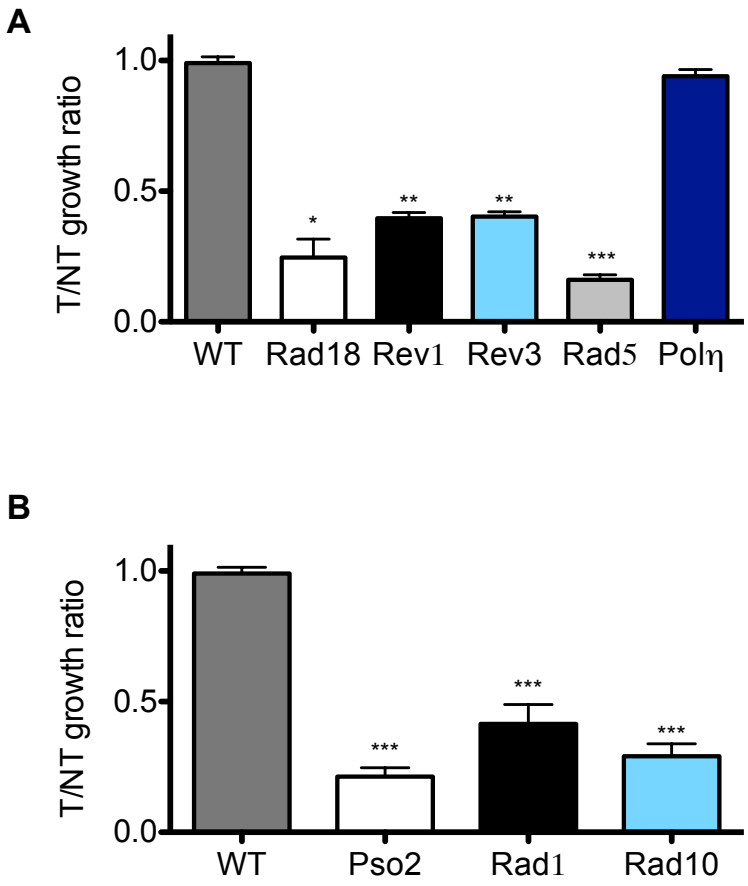

Figure 3.4 Sensitivity of yeast mutants deficient in DNA repair assessed by competitive growth assays. (A) Translesion synthesis repair mutants exposed to DCVC for 24hrs (B) Nucleotide excision repair mutants. Deletion mutants were tested for sensitivity to DCVC (18μM) by flow cytometry. Relative growth of each mutant was compared with a wild-type GFP strain after 24 h. Values of the growth ratios (treatment vs. control—T/NT) to wild-type GFP shown in (A,B) are mean ± SEM; $n \geq 3$ for each measurement. Significance values were calculated by Student's t-test, where ***$p < 0.001$, **$p < 0.01$, *$p < 0.05$ for DCVC-treated wild-type versus mutant.

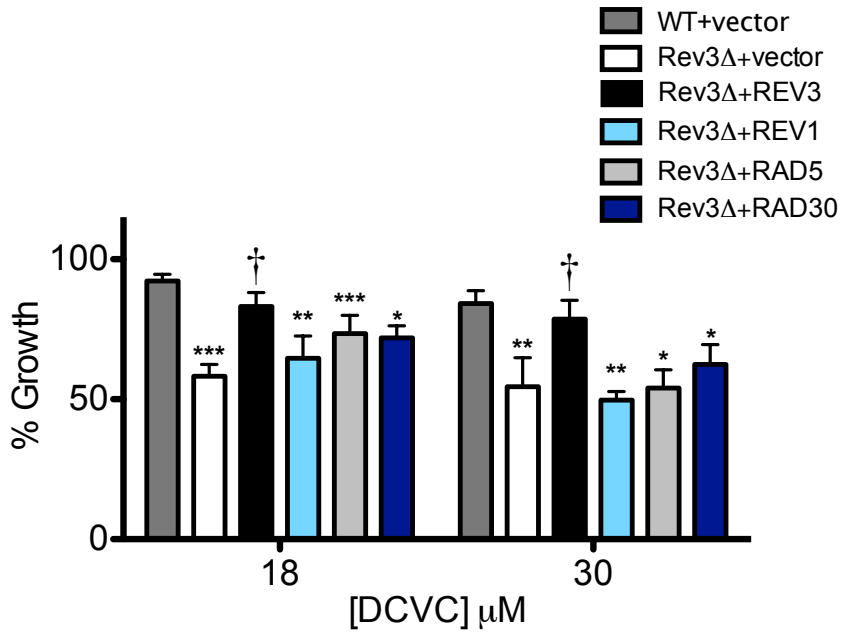

Figure 3.5 Complementation studies with overexpression of TLS proteins. Values are mean ± SEM; n ≥ 3 for each measurement. Significance values were calculated by two way ANOVA ***p < 0.001, **p < 0.01, *p < 0.05 for DCVC-treated wild-type versus mutants; †††p < 0.001, ††p < 0.01, †p < 0.05 for DCVC treated Rev3Δ versus complementation mutants.

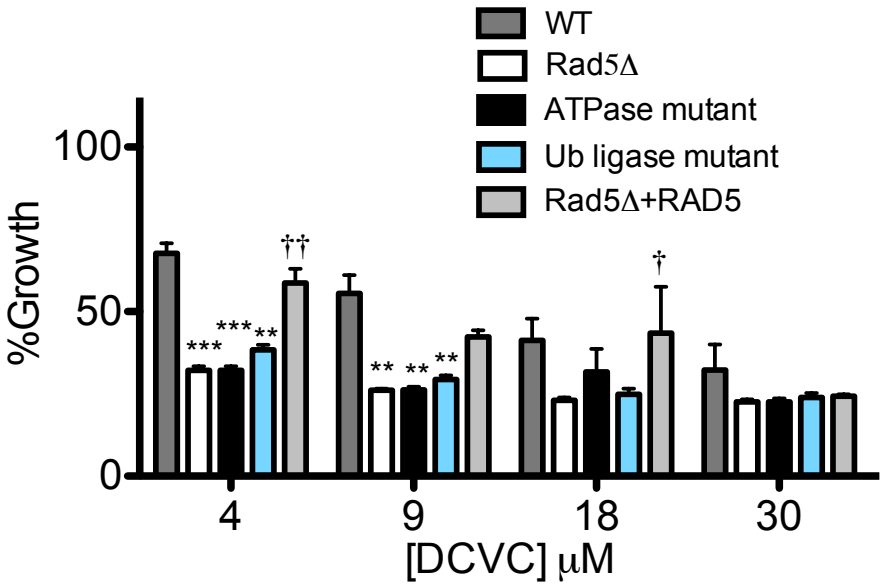

Figure 3.6 Studies with Rad5 mutants support its structural role in mediating DCVC induced repair**.** Values are mean ± SEM; n ≥ 3 for each measurement. Significance values were calculated by two way ANOVA ***p < 0.001, **p < 0.01, *p < 0.05 for DCVC-treated wild-type versus mutants; †††p < 0.001, ††p < 0.01, †p < 0.05 for DCVC treated Rad5Δ versus mutants.

References

1. Rusyn I, Chiu WA, Lash LH, Kromhout H, Hansen J, Guyton KZ. Trichloroethylene: Mechanistic, epidemiologic and other supporting evidence of carcinogenic hazard. Pharmacol Therapeut. 2013.

2. Lash L, Fisher J, Lipscomb J, Parker J. Metabolism of trichloroethylene. Environ Health Persp. 2000;108:177–200.

3. ANDERS M. Glutathione-dependent bioactivation of haloalkanes and haloalkenes. Drug Metab Rev. 2004;36:583–94.

4. Anders MW. Chemical toxicology of reactive intermediates formed by the glutathione-dependent bioactivation of halogen-containing compounds. Chem Res Toxicol. 2008;21:145–59.

5. Goeptar A, Commandeur J, Vanommen B, Vanbladeren P, Vermueulen N. Metabolism and kinetics of trichloroethylene in relation to toxicity and carcinogenicity- relevance of the mercapturic acid pathway. Chem Res Toxicol. 1995;8:3–21.

6. Lash L, Parker J, Scott C. Modes of action of trichloroethylene for kidney tumorigenesis. Environ Health Persp. 2000;108:225–40.

7. Lash LH, Putt DA, Huang P, Hueni SE, Parker JC. Modulation of hepatic and renal metabolism and toxicity of trichloroethylene and perchloroethylene by alterations in status of cytochrome P450 and glutathione. Toxicology. 2007;235:11–26.

8. Bhattacharya R, Schultze M. Properties of DNA treated with S-(1,2-dichlorovinyl)-L-cysteine and a lyase. Arch Biochem Biophys. 1972;153:105.

9. Clay P. Assessment of the genotoxicity of trichloroethylene and its metabolite, S-(1,2-dichlorovinyl)-L-cysteine (DCVC), in the comet assay in rat kidney. Mutagenesis. 2008;23:27–33.

10. Brauch H, Weirich G, Hornauer M, Storkel S, Wohl T, Bruning T. Trichloroethylene exposure and specific somatic mutations in patients with renal cell carcinoma. J Natl Cancer I. 1999;91:854–61.

11. Brauch H, Weirich G, Klein B, Rabstein S, Bolt H, Bruning T. VHL mutations in renal cell cancer: does occupational exposure to trichloroethylene make a difference? Toxicol Lett. 2004;151:301–10.

12. Charbotel B, Gad S, Caïola D, Béroud C, Fevotte J, Bergeret A, et al. Trichloroethylene exposure and somatic mutations of the VHL gene in patients with Renal Cell Carcinoma. J Occup Med Toxicol. 2007;2:13.

13. Shiao Y-H. Genetic Signature for Human Risk Assessment: Lessons From

Trichloroethylene. Environ Mol Mutagen. 2009;50:68–77.

14. Bruning T, Bolt H. Renal toxicity and carcinogenicity of trichloroethylene: Key results, mechanisms, and controversies. Crit Rev Toxicol. 2000;30:253–85.

15. Jo WJ, Loguinov A, Chang M, Wintz H, Nislow C, Arkin AP, et al. Identification of genes involved in the toxic response of Saccharomyces cerevisiae against iron and copper overload by parallel analysis of deletion mutants. Toxicol Sci. 2008;101:140–51.

16. Jo WJ, Loguinov A, Wintz H, Chang M, Smith AH, Kalman D, et al. Comparative Functional Genomic Analysis Identifies Distinct and Overlapping Sets of Genes Required for Resistance to Monomethylarsonous Acid (MMA(III)) and Arsenite (As-III) in Yeast. Toxicol Sci. 2009;111:424–36.

17. Gaytán BD, Loguinov AV, La Rosa De VY, Lerot J-M, Vulpe CD. Functional genomics indicates yeast requires Golgi/ER transport, chromatin remodeling, and DNA repair for low dose DMSO tolerance. Front Genet. 2013;4:154.

18. Gaytán BD, Loguinov AV, Lantz SR, Lerot J-M, Denslow ND, Vulpe CD. Functional profiling discovers the dieldrin organochlorinated pesticide affects leucine availability in yeast. Toxicol Sci. 2013;132:347–58.

19. North M, Tandon VJ, Thomas R, Loguinov A, Gerlovina I, Hubbard AE, et al. Genome-wide functional profiling reveals genes required for tolerance to benzene metabolites in yeast. Plos One. 2011;6:e24205.

20. Gaytán BD, Vulpe CD. Functional toxicology: tools to advance the future of toxicity testing. Front Genet. 2014;5:110.

21. Vamvakas S, Elfarra A, Dekant W, Henschler D, Anders M. Mutagenicity of Amino-Acid and Glutathione S-Conjugates in the Ames Test. Mutat Res. 1988;206:83–90.

22. McGoldrick T, Lock E, Rodilla V, Hawksworth G. Renal cysteine conjugate C-S lyase mediated toxicity of halogenated alkenes in primary cultures of human and rat proximal tubular cells. Arch Toxicol. 2003;77:365–70.

23. Dekant W, Vamvakas S, Berthold K, Schmidt S, Wild D, HENSCHLER D. Bacterial beta-lyase mediated cleavage and mutagenicity of cysteine conjugates derived from the nephrocarcinogenic alkenes trichloroethylene, tetrachloroethylene and hexachlorobutadiene. Chem-Biol Interact. 1986;60:31–45.

24. Ulrich HD. Conservation of DNA damage tolerance pathways from yeast to humans. Biochem Soc T. 2007;35:1334–7.

25. Andersen PL, Xu F, Xiao W. Eukaryotic DNA damage tolerance and translesion synthesis through covalent modifications of PCNA. Cell Res. 2008;18:162–73.

26. Kakar S, Watson NB, McGregor WG. RAD18 signals DNA polymerase IOTA to stalled

replication forks in cells entering S-phase with DNA damage. Adv Exp Med Biol. 2008;614:137–43.

27. Boiteux S, Jinks-Robertson S. DNA repair mechanisms and the bypass of DNA damage in Saccharomyces cerevisiae. Genetics. 2013;193:1025–64.

28. Andersen PL, Xu F, Ziola B, McGregor WG, Xiao W. Sequential assembly of translesion DNA polymerases at UV-induced DNA damage sites. Mol Biol Cell. 2011;22:2373–83.

29. Choi J-Y, Zang H, Angel KC, Kozekov ID, Goodenough AK, Rizzo CJ, et al. Translesion synthesis across 1,N-2-ethenoguanine by human DNA polymerases. Chem Res Toxicol. 2006;19:879–86.

30. Pollack M, Yang I-Y, Kim H-YH, Blair IA, Moriya M. Translesion DNA synthesis across the heptanone-etheno-2 '-deoxycytidine adduct in cells. Chem Res Toxicol. 2006;19:1074–9.

31. Ho V, Schaerer OD. Translesion DNA Synthesis Polymerases in DNA Interstrand Crosslink Repair. Environ Mol Mutagen. 2010;51:552–66.

32. Pagès V, Bresson A, Acharya N, Prakash S, Fuchs RP, Prakash L. Requirement of Rad5 for DNA polymerase zeta-dependent translesion synthesis in Saccharomyces cerevisiae. Genetics. 2008;180:73–82.

33. Kuang L, Kou H, Xie Z, Zhou Y, Feng X, Wang L, et al. A non-catalytic function of Rev1 in translesion DNA synthesis and mutagenesis is mediated by its stable interaction with Rad5. Dna Repair. 2013;12:27–37.

34. Lee W, St Onge RP, Proctor M, Flaherty P, Jordan MI, Arkin AP, et al. Genome-wide requirements for resistance to functionally distinct DNA-damaging agents. Plos Genet. 2005;1:e24.

35. Huang Y, Li L. DNA crosslinking damage and cancer - a tale of friend and foe. Transl Cancer Res. 2013;2:144–54.

36. Deans AJ, West SC. DNA interstrand crosslink repair and cancer. Nat Rev Cancer. 2011;11:467–80.

37. Grossmann K, Ward A, Matkovic M. ScienceDirect.com - Mutation Research/DNA Repair - S. cerevisiae has three pathways for DNA interstrand crosslink repair. Mutation Research/DNA …. 2001.

38. McHugh PJ, Sones WR, Hartley JA. Repair of intermediate structures produced at DNA interstrand cross-links in Saccharomyces cerevisiae. Mol Cell Biol. 2000;20:3425–33.

39. Wu M, Yan S, Patel DJ, Geacintov NE, Broyde S. Relating repair susceptibility of carcinogen-damaged DNA with structural distortion and thermodynamic stability. Nucleic Acids Res. 2002;30:3422–32.

40. Beljanski V, Marzilli LG, Doetsch PW. DNA damage-processing pathways involved in the eukaryotic cellular response to anticancer DNA cross-linking drugs. Mol Pharmacol. 2004;65:1496–506.

CHAPTER IV

Characterizing Genotoxicity Mechanisms of DCVC in Vertebrate Models

ABSTRACT

Functional profiling studies in yeast (Chapter 3) implicate DCVC as a potential direct DNA damaging agent causing lesions similar to that of interstrand crosslinks. A subset of repair pathways, including translesion synthesis, nucleotide excision and homologous recombinaiton were identified as processes required in resposne to DCVC DNA damage. Genetic studies in avian DT40 cell lines were conducted to confirm our findings in yeast and further characterize the DNA repair response to DCVC. DT40 cells defective in error-prone translesion synthesis repair exhibited a significant decrease in viability upon exposure to DCVC, implicating a role for mutagenesis in mediating DCVC toxicity. This was further supported by an increase in mutation frequency in human lymphoblasts exposed to DCVC. Interestingly, DT40 *FANCD2*$^{-/-}$ mutants and human PD20 cells, both of which are deficient in interstrand crosslink repair, were not sensitive to DCVC, suggesting a mechanism of DNA damage and repair not consistent with known interstrand crosslinking agents. From these studies, we propose that DCVC causes non-distorting DNA lesions that are repaired by mainly by translesion synthesis and to a lesser extent, template switching, a form of error-free recombination. These findings are significant as we provide mechanistic and genetic evidence supporting a mutagenic mode of action mediated by the nephrotoxicant metabolite DCVC in vertebrate systems.

INTRODUCTION

Trichloroethylene (TCE) is a common environmental contaminant and human carcinogen found at Superfund waste sites (1). TCE exposure is associated with increased renal cell carcinoma and genetic analyses have identified unique mutation signatures in the von Hippel Lindau (VHL) gene, a tumor suppressor gene commonly associated with renal cell carcinoma in TCE exposed populations (2-5). These data suggest a mutagenic mode of action for TCE induced renal cancer, but there remains a need for molecular evidence supporting this hypothesis. TCE undergoes a complex metabolism resulting in bioactive intermediates via the glutathione conjugation pathway and studies have identified the metabolite dichlorovinyl cysteine (DCVC) as the penultimate mediator of TCE renal toxicity (6-8). The role of DCVC as a nephrotoxicant implicates it as a likely mediator of renal carcinogenesis. This is supported by yeast profiling studies (Chapter 3), which identified the DCVC metabolite as a genotoxicant. Results in yeast suggest DCVC may cause DNA damage similar to interstrand crosslinking agents, which elicits a mutagenic translesion synthesis (TLS) repair response. Thus, we examined the role of interstrand crosslink (ICL) repair and translesion synthesis in avian DT40 and human cell models to gain further insight into the genotoxicty of DCVC.

The DT40 avian system to study mechanisms of genotoxicity

The availability of isogenic DT40 deletion cell lines with stable deletions allows for functional profiling in a vertebrate system (9). DT40 cells exhibit a shorter doubling time than mammalian cells (11hrs at 39°C) and have a stable phenotype even without a functional *TP53* gene. *TP53*

encodes p53, a G1/S phase cell cycle checkpoint protein that arrests cell growth upon the recognition of DNA damage and activates DNA repair (10). Loss of p53 results in DT40 cells spending 70% of the cell cycle in S phase, allowing for the full extent of DNA damage to be observed due to reduced DNA repair in the G1 phase (10,11). DT40 studies have provided insight on the human DNA damage response for a diverse panel of DNA lesions including interstrand crosslinks, base modifications, abasic sites, bulky adducts, single and double strand breaks caused by a variety of alkylating agents, reactive oxygen species (ROS), crosslinking agents, ionizing radiation and UV rays (12-17). While DNA repair is highly conserved in eukaryotes, the DT40 system allows for the examination of repair genes conserved in humans, but not present in yeast. The genetic advantages and availability of deletion strains deficient in interstrand crosslink repair make the DT40 system an appropriate tool to further characterize the DNA damage response of the TCE metabolite DCVC.

RESULTS & DISCUSSION

Evaluation of DCVC genotoxicity in DT40 cell lines

A panel of isogenic DT40 mutants was examined in response to the TCE metabolite, DCVC (**Table 4.1**). In wild-type cells, a significant decrease in viability was observed and the DCVC IC_{50} was determined to be 3μM. A comparison of IC_{50} values revealed cell lines deficient in translesion synthesis (TLS) exhibited a significant decrease in viability compared to wild-type cells. DCVC was 10X more toxic in TLS mutants, with IC_{50} values between 300nM and 1.6uM. The viability of mutants deficient in nucleotide excision repair (NER), base excision repair (BER), non-homologous end joining (NHEJ) and DNA checkpoints was unchanged by DCVC exposure (**Table 4.2**). In contrast, DCVC caused a significant increase in the viability of homologous recombination (HR) deficient cell lines compared to wild-type cells and was 10X less toxic in these mutants with IC_{50} values between 13uM and 36uM. Compared to the chemotherapeutic crosslinking agent cisplatin, DCVC was 10-100X less genotoxic in all cell lines tested, suggesting dissimilar mechanisms of genotoxicity (**Table 4.2**).

Role of translesion synthesis pathway in the repair of DNA damage induced by DCVC

DT40 mutants deficient in translesion synthesis have shown sensitivity to various genotoxicants, including crosslinking agents (16). Our studies in yeast showed TLS mutants were hypersensitive to DCVC, similar to DNA crosslinking agents. To confirm the role of TLS repair of DCVC damage in vertebrates, we exposed *Rev1*$^{-/-}$, *Rad18*$^{-/-}$ and *PCNAK164R* DT40 cells to DCVC. All exhibited extreme sensitivity to DCVC in a dose dependent manner **(Fig. 4.2a**). During replication, post-translational modifications of the replication factor PCNA (proliferating cell nuclear antigen) in eukaryotes initiates the error-prone translesion synthesis repair (TLS) pathway or the error-free, template-switching (TS) pathway (18). These repair mechanisms prevent replication stalling and fork collapse when a DNA lesion is encountered (19). Monoubiquitination of PCNA at the Lys164 residue by the *Rad6-Rad18* complex initiates the error prone translesion pathway and recruits special TLS polymerases such as *Rev3, Rad30,* and *Rev1* to sites of damage (19,20). *PCNAK164R* cells are defective in PCNA ubiquitination and exhibited the greatest sensitivity to DCVC, along with *Rev1*$^{-/-}$ cells, suggesting both PCNA ubiquitination signaling and *Rev1* play critical roles in the repair and the mutagenicity of DCVC DNA damage (**Fig. 4.2a**). Consistent with our results, previous studies have shown that *PCNAK164R* mutants exhibit sensitivity and altered mutagenesis in response to various DNA

lesions (13,14,21-23). The moderate sensitivity of *Rad18-/-* cells to DCVC could be due to Rad18-independent ubiquitination of PCNA, which has been observed in DT40 cells exposed to DNA damaging agents (13). Furthermore, studies in mouse embryonic fibroblasts show translesion synthesis repair does occur in the absence of *Rad18*, albeit significantly decreased (23,24).

Mutation frequency increased by low levels of DCVC in human lymphoblasts

The role of TLS in the repair of DCVC DNA damage suggests an increase in mutagenesis. To examine this we conducted mutation frequency assays in human lymphoblasts exposed to DCVC. The thymidine kinase assay (TK) is a forward mutation assay capable of detecting DNA major (slow growth) and minor (normal growth) mutagenic events at the TK locus. After exposure to DCVC, we observed an increase in mutation frequency of both normal growth (NG) and slow growth (SG) DNA damage at doses 10X below the IC_{50} dose (**Fig. 4.6**). Mutation frequency increased by 2-fold at 1.875μM and 3.75μM DCVC and did not increase at higher concentrations (**Table 4.3**). The leveling of mutation frequency in doses >5uM may be attributed to the increased cellular toxicity of DCVC, rather than genotoxicity. The frequency of large deletions, translocations and recombination (slow growth) mutations increased by 3-fold compared to controls. This type of damage occurred in greater proportion than normal growth mutations, suggesting mutagenic recombination repair may also play a significant role in response to DCVC damage. It should be noted however, that measurement of slow growth mutations does not exclude small passenger mutations that have accumulated over an extended period of time. Slow growth frequencies are determined as the difference between total mutation frequency and normal growth mutation frequency. Thus, small passenger mutations can accumulate and possibly mediate an increase in these larger mutation events. Sequencing of clones is needed to better understand the contribution of the different types of repair and mutagenesis. Nonetheless, the overall increase in mutation frequency supports the role of mutagenic repair in response to DCVC DNA damage and is consistent with previous studies implicating DCVC as a potential mutagen (25). The increase of large deletions implicates repair mechanisms in addition to TLS may play a role in mediating DCVC damage.

DCVC damage does not require Fanconi Anemia (FA) pathway

Functional profiling studies in yeast (Chapter 3) implicated DCVC as an interstrand crosslinking agent, thus we examined the role of the Fanconi Anemia (FA) pathway in avian DT40 and human cell models. ICL repair in vertabrates consists of a collaboration between several DNA repair pathways, including the Fanconi anemia (FA) complex (**Fig. 4.1**) The involvement of these pathways is highly regulated by cell cycle phase and the type of DNA lesion (26-28). Recombination-dependent ICL repair functions during late S/G2 phases and requires recognition of replication fork stalling by the fanconi anemia complex (FA), "unhooking" of the ICL on one stand by NER endonucleases such as *XPF-ERCC1*, followed by gap filling and bypass of the remaining lesion by TLS polymerases and homologous recombination of the double strand break on the sister chromatid. Recombination-independent repair occurs mainly during the G1 phase and again involves the NER nucleases *XPC-ERCC1* to unhook the ICL on one strand and repair synthesis by TLS polymerases. The involvement of TLS polymerases in the repair of ICLs can reuslt in mutagenesis causing point muations as well as deletions and translocations (26). A disitnct difference in ICL repair between yeast and vertebrate systems is the presence of the Fanconi anemia (FA) complex consisting of 14 genes, 7 of which are know to be critical in ICL

repair (27). The functions of all 14 genes are not known, but mutations in these genes are associated with increased susceptibility to a variety of cancers, highlighting their important role in maintaining genome intergity (26). The FA complex detects ICLs in both recombination dependent and independent repair and signals the recruitment of additional factors such as *FANCD2*, which is critical to the initiation and recruitment of downstream repair factors, such as TLS polymerases.

DT40 *FANCD2*$^{-/-}$ cell were not sensitive to DCVC in contrast to the known crosslink agent, cisplatin (**Fig. 4.2b**). Next, we examined the toxicity of DCVC in human PD20 cells. PD20 is a human lymphoblastoid cell line derived from a Fanconi anemia patient. It is deficient in the FANCD2 protein as a consequence of mutations in the *FANCD2* gene. PD20 cells did not exhibit sensitivity to DCVC after 72hr exposures (**Fig. 4.5**). *FANCD2* is required for the initiation and progression of ICL repair (29). The lack of sensitivity in *FancD2*$^{-/-}$ DT40 and human cell models suggests DCVC damage differs from canonical crosslinking agents or that DCVC ICL damge is repaired in a homologous recombination independent manner. Monoadducts and intrastrand crosslinks (crosslinks with bases on the same DNA strand) are highly prevalent lesions caused by ICL agents, accounting for 90% of damage (26). DCVC damage may consist mostly of monoadducts or intrastrand crosslinks and very low levels of ICL damage, which does not cause measurable changes in cell viability. Alternatively, DCVC may cause helix distoring ICL lesions that are detected and repaired in G1 by a recombiantion-independent mechanism as depicted in **Fig. 4.1**. Prior cell-free and *in vitro* studies have shown that ICL repair in G1 is highly dependent on the degree of helix distortion and that not all ICLs are repaired in G1 (26). The extended S-phase and short G0/G1 phase in DT40 cells may not allow for full repair of DCVC damage, which would elicit translesion synthesis and/or template switching repair (a form of recombination repair) during replication, both of which are not dependent on *FANCD2* (**Fig. 4.7**).

DT40 cells deficient in homologous recombination exhibit hyper-resistance to DCVC exposure

Homologous recombination plays an important role in preventing replication fork collapse and as mentioned above, in the repair of ICL damage during replication (16,26,27). Interestingly, DT40 cells deficient in homologous recombination showed increased resistance in response to DCVC exposure (**Fig. 4.3a**). *Rad51D*$^{-/-}$ cells exhibited the greatest resistance to DCVC, followed by moderate resistance in *Rad54*$^{-/-}$ and *Rad52*$^{-/-}$ cells. The resistance of HR mutants suggests a recombination independent repair mechanism is favored in the repair of DCVC DNA damage. Homologous recombination repair is tighly regulated by a variety of factors, including the RecQ helicases which prevent inappropriate HR that can interfere with post replication repair and the formation of undesired intermediates that can lead to cell death (30-33). *Wrn-/-* cells lack the Werner's Syndrome (WS) gene that encodes for a RecQ helicase involved in the promotion of HR, whereas *BLM-/-* cells lack the Bloom's Syndrome gene, which encodes for a RecQ helicase that promotes and inhibits HR. Both *BLM* and *WRN* are involved in overcoming replication blocks and act to resolve complex DNA structures (31). *WRN* (and *BLM*) play a role in resolving replication blocks by mediating fork regression, followed by template switching repair, a form of error-free recombination (32). We observed mild sensitivity in *Wrn-/-* cells exposed to DCVC, suggesting *WRN* and template switching may contribute a minor role in the repair of DCVC damage encountered during replication. The functional redundancy of *WRN* and *BLM* helicases could explain the mild sensitivty to DCVC observed in our studies and is in agreement with

previous findings showing moderate sensitivity to a variety of DNA damaging agents (30-32,34). Cell cycle studies are needed to better characterize DCVC damage and understand the contribution of the different recombination pathways during replication repair.

The differences in sensitivity profiles between yeast and DT40 can be attributed to the role each repair pathway plays in repair. Homologous recombination is preferred in yeast and functions throughout the cell cycle, whereas in vertebrates, HR repair is only active in S/G2. We speculate that our contrasting responses are due to the larger role HR plays in DNA repair in yeast compared to vertebrate cells and the extended S-phase in the DT40 cell system. As expected, non-homologous end joining (NHEJ) mutants *Ku70*$^{-/-}$, *Lig4*$^{-/-}$ and *DNA-PK*$^{-/-}$ were not sensitive to DCVC or cisplatin, consistent with previous findings showing that NHEJ is not required for ICL repair and suggests DCVC does not directly cause DSB (26).

CONCLUSIONS

DNA repair entails complex processes that are tightly regulated by cell cycle and lesion structure. Functional studies in yeast and model vertebrate systems have played central roles in understanding the molecular mechanisms that mediate repair of DNA damage caused by environmental genotoxicants. Our studies utilized the established DT40 avian system to investigate and characterize the genotoxicity of the nephrotoxicant dichlorovinyl cysteine (DCVC), a metabolite of the environmental contaminant trichloroethylene (TCE). We propose a recombination-independent repair mechanism for DCVC DNA damage that is mediated primarily by mutagenic translesion synthesis. DCVC damage may also form intermediates during replication that elicit undesired recombination repair. While recombination repair is predominately error-free, it may be detrimental to the restart of stalled replication and thus unfavored in the repair of DCVC lesions.

Based on our functional studies in DT40 and human cell lines it remains unclear as to the type of damage DCVC causes, but interstrand crosslinks, monoadducts and intrastrand crosslinks are possible lesions. Additional studies are needed to assess the structure of DCVC damage and determine a sensitive mutational "fingerprint" of DCVC exposure. The role of mutagenic repair and increased mutation frequency observed in our studies provides mechanistic and genetic evidence supporting a mutagenic mode of action for TCE. The genotoxicity of DCVC merits further investigation of mutations in important genes associated with RCC to understand the relationship between TCE exposure, mutagenesis and cancer.

MATERIALS AND METHODS

Cell lines and tissue culture. DT40 wild- type cells and a panel of isogenic DNA repair mutant cells were cultured in RPMI 1640 medium with 10% fetal bovine serum and 1% heat inactivated chicken serum at 39.5°C in a humidified atmosphere of 5% CO_2. PD20 is a human lymphoblastoid cell line derived from a Fanconi anemia patient. It is deficient in the FANCD2 protein as a consequence of mutations in the *FANCD2* gene. The PD20D2 cell line was generated from the PD20 cell line to ectopically express the FANCD2 protein. Both cell lines were cultured in RPMI 1640 and 15% fetal bovine serum and 1% PS under standard culture

conditions. The $TK6^{+/-}$ human lymphoblast cell line is heterozygous at the thymidine kinase (TK) locus and was cultured in RPMI 1640 with 10% FBS under standard culture conditions.

Viability Assays. DT40 viability assays were conducted as outlined previously (17) using wild-type and DT40 knockout strains. $2.5x10^2$ cells were seeded in 96-well plates and treated for 48rs with DCVC or cisplatin prepared in PBS. For PD20 studies, cells were seeded at $1x10^4$ in 96 well plates and treated with DCVC for 3 days. The XTT assay (ATCC) was conducted per kit directions. Viability was measured as a function of absorbance at 450nm and normalized to untreated controls.

Thymidine kinase mutation assay. TK6 human lymphoblastoid cells were seeded at ~2×106 cells/exposure (n = 2 per level) and treated with DCVC diluted in PBS for 24hrs. Following completion of the exposure, cells were plated in 96-well plates at 40,000 cells per well in medium containing trifluorothymidine (TFT) and 2 cells per well in medium without TFT. The plates were incubated at 37 °C with 5% CO2. After 2 weeks, the presence or absence of normal growth (NG) colonies in each well was measured, followed by measurements at the end of 4 weeks for slow growth colonies (SG). Colony growth was measured per the XTT assay. Mutation frequency was calculated as outlined in (35).

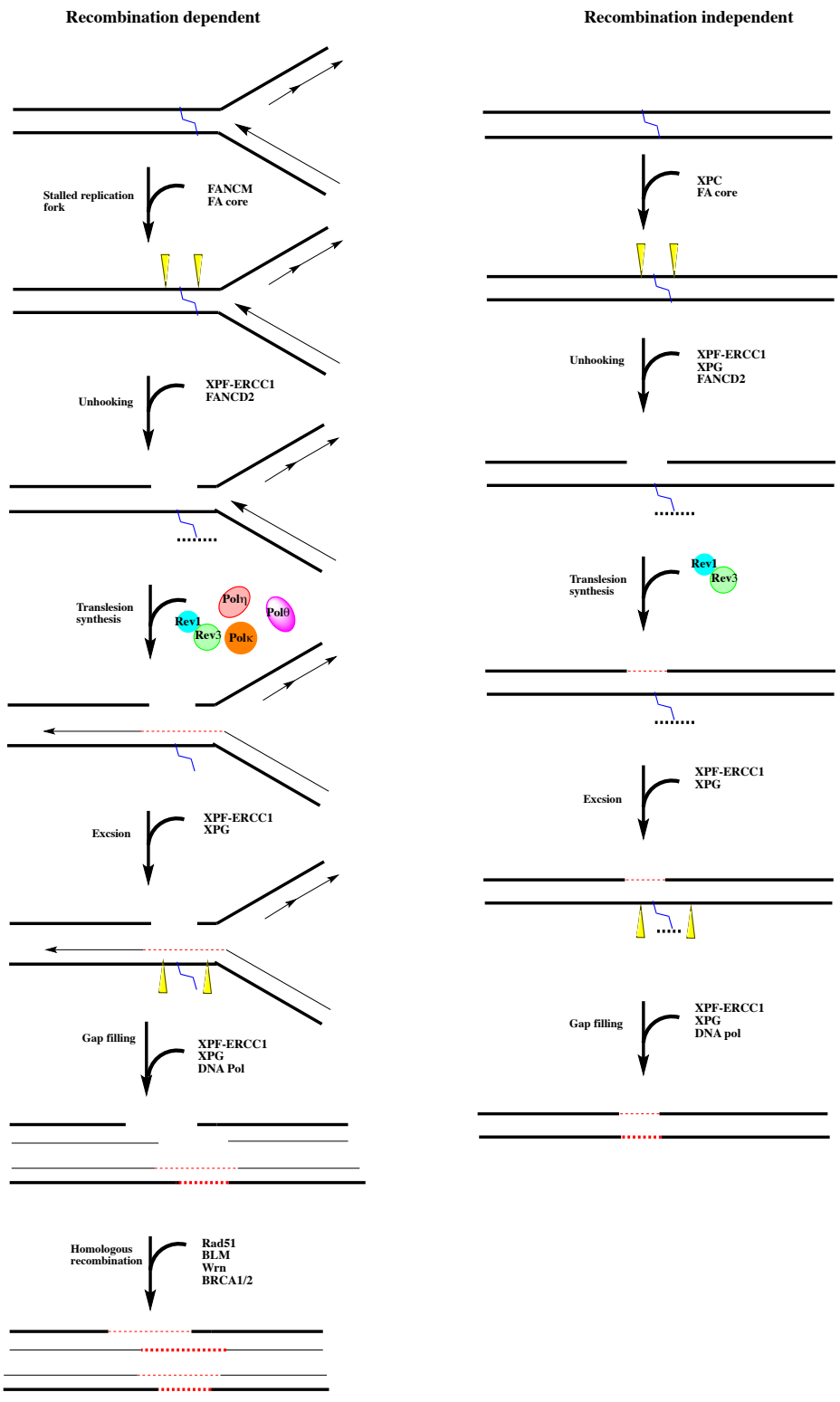

Figure 4.1. Overview of interstrand crosslink (ICL) repair in vertebrates. Recombination dependent ICL repair is replication dependent and occurs during S phase. Recombination independent ICL repair occurs during G0/G1 phases. Both pathways require *FANCD2*, which is responsible for initiation and recruitment of repair factors, such as TLS polymerases.

Table 4.1 DT40 mutant cell lines analyzed in this study and their role in DNA repair

Gene	Function
RAD18	TLS
REV1	TLS
REV3	TLS
PCNAK164R	TLS
POLQ	TLS
XPG	NER
XPA	NER
FEN1	BER
PARP1	BER
POL B	BER
DNA-PK	NHEJ
KU70	NHEJ
LIG4	NHEJ
WRN	helicase
BLM	helicase
RAD52	HR
RAD51D	HR
RAD54	HR
XRCC3	HR
XRCC2	HR
FANCD2	ICL
BRCA1	ICL/HR
BRCA2	ICL/HR
ATM	DNA damage checkpoint
RAD17	DNA damage sensor
RAD9	DNA damage sensor

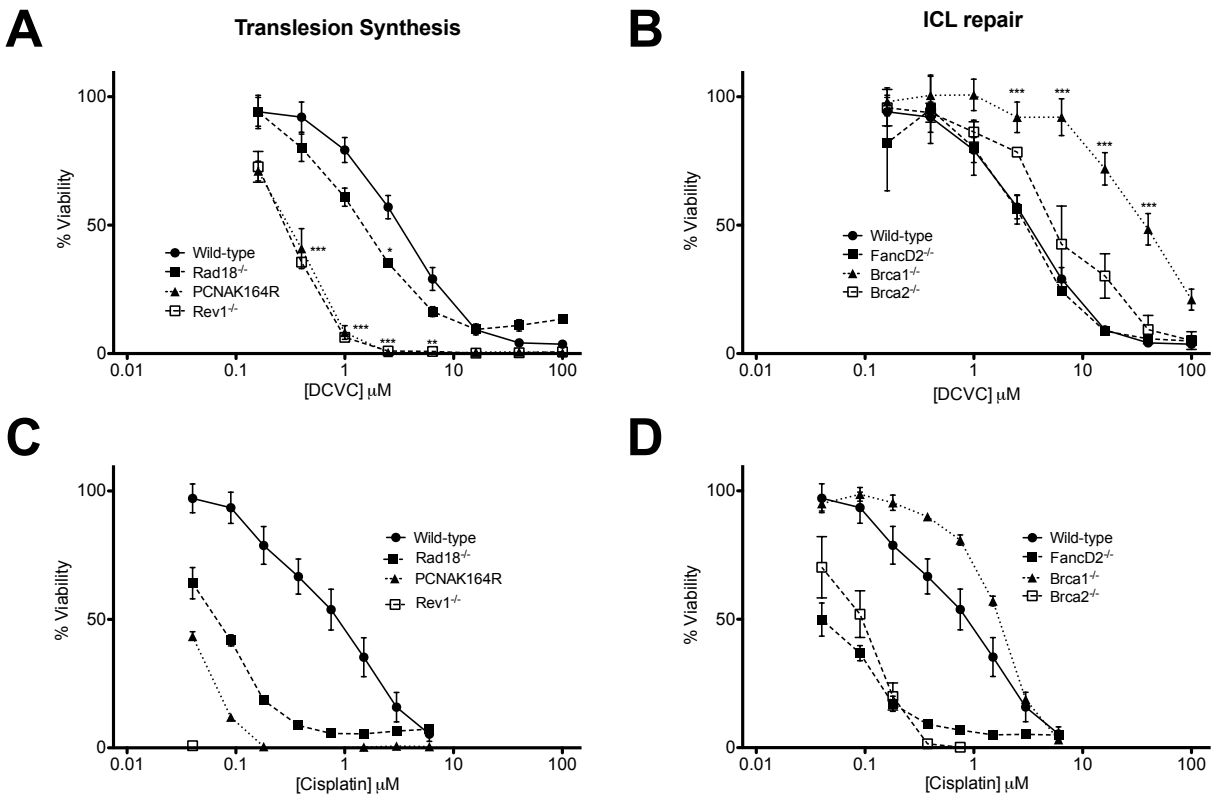

Figure 4.2 Sensitivity of DT40 TLS and ICL repair deficient mutants to DCVC (A,B) and cisplatin (C,D) assessed by XTT. Values are mean ± SEM; n ≥ 3 for each measurement. Significance values were calculated by two-way ANOVA, where ***p < 0.001, **p < 0.01, *p < 0.05

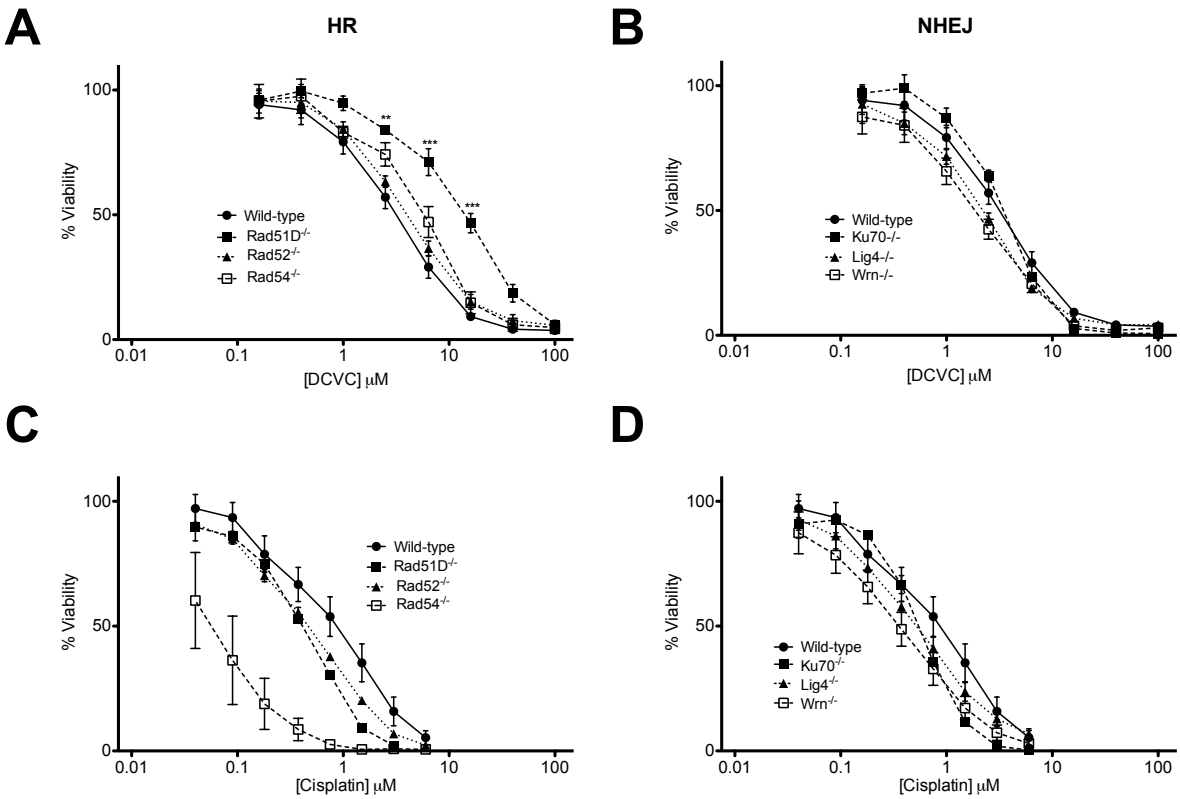

Figure 4.3. Sensitivity of DT40 homologous recombination (HR) and non-homologous end joining (NHEJ) repair deficient mutants to DCVC (A,B) and cisplatin (C,D) assessed by XTT. Values are mean ± SEM; $n \geq 3$ for each measurement. Significance values were calculated by two-way ANOVA, where ***$p < 0.001$, **$p < 0.01$, *$p < 0.05$

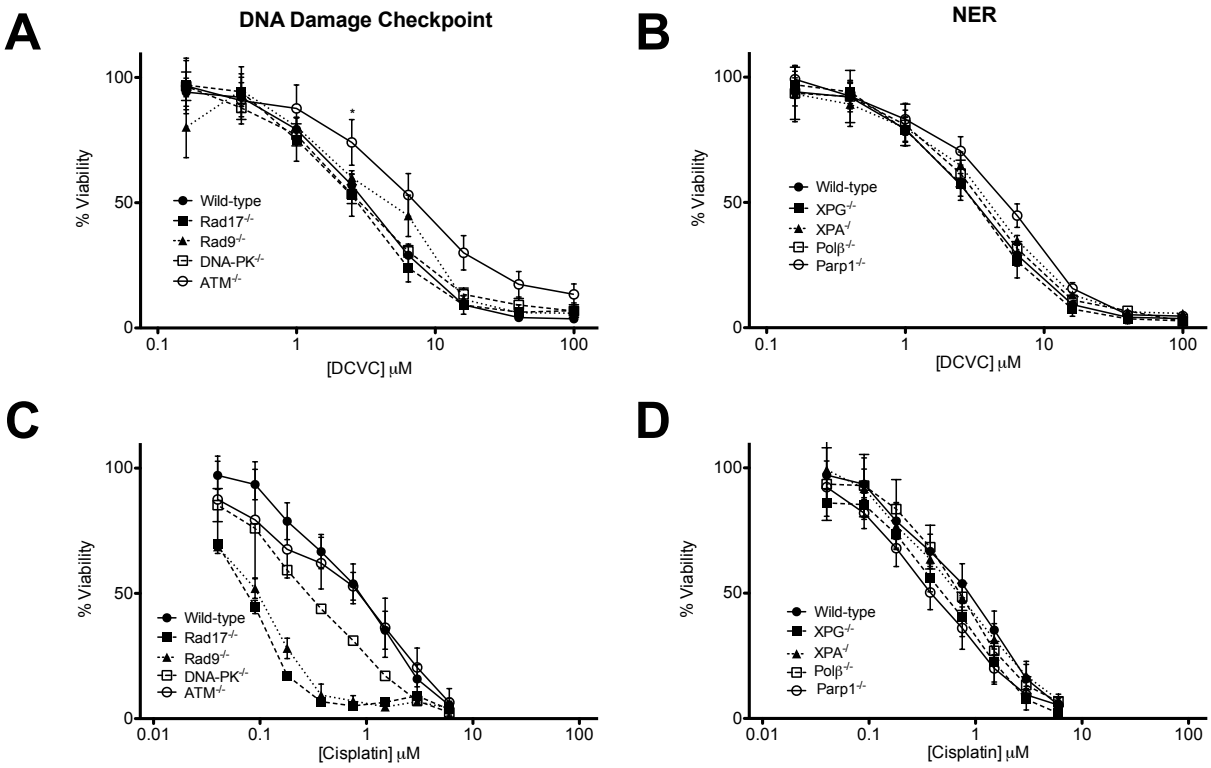

Figure 4.4. Sensitivity of DT40 DNA damage checkpoint and nucleotide excision repair (NER) deficient mutants to DCVC (A,B) and cisplatin (C,D) assessed by XTT. Values are mean ± SEM; $n \geq 3$ for each measurement. Significance values were calculated by two-way ANOVA, where ***$p < 0.001$, **$p < 0.01$, *$p < 0.05$

Table 4.2 Summary of DCVC and Cisplatin IC_{50} values for each DT40 mutant. The ICL agent cisplatin is 10-100X more genotoxic than DCVC.

	IC50 (M)	
Mutant	**DCVC**	**Cisplatin**
Wild-type	3.1E-06	7.7E-07
REV1	2.9E-07	ND
PCNAK164R	3.0E-07	4.2E-08
RAD18	1.6E-06	7.1E-08
MSH2	1.7E-06	ND
WRN	1.8E-06	3.5E-07
LIG4	2.1E-06	5.1E-07
RAD17	2.7E-06	7.9E-08
FANCD2	2.9E-06	4.8E-08
DNA-PK	3.0E-06	2.9E-07
XPG	3.0E-06	4.7E-07
KU70	3.4E-06	5.3E-07
FEN1	3.4E-06	1.1E-06
POLB	3.5E-06	6.9E-07
XRCC3	3.7E-06	1.5E-07
XPA	3.7E-06	6.8E-07
POLQ	3.8E-06	4.2E-07
RAD9	3.9E-06	9.1E-08
BLM	4.0E-06	ND
RAD52	4.1E-06	4.4E-07
XRCC2	4.8E-06	2.8E-07
PARP1	4.9E-06	4.0E-07
RAD54	5.3E-06	6.3E-08
BRCA2	6.2E-06	8.7E-08
ATM	7.4E-06	6.3E-07
RAD51D	1.3E-05	3.9E-07
BRCA1	3.6E-05	1.6E-06

ND, not determined

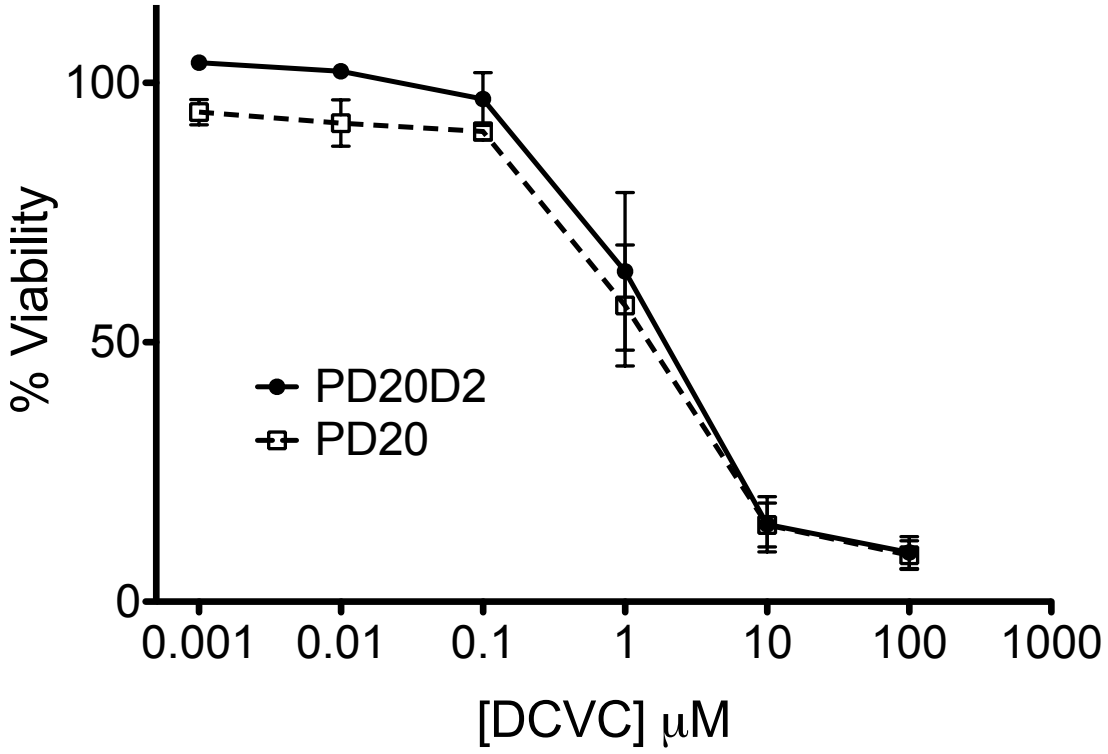

Figure 4.5 Sensitivity of ICL repair deficient lymphoblasts (PD20) and FancD2 complemented (PD20D2) cells to DCVC after 72hrs. Values are mean ± SEM; n ≥ 3 for each measurement.

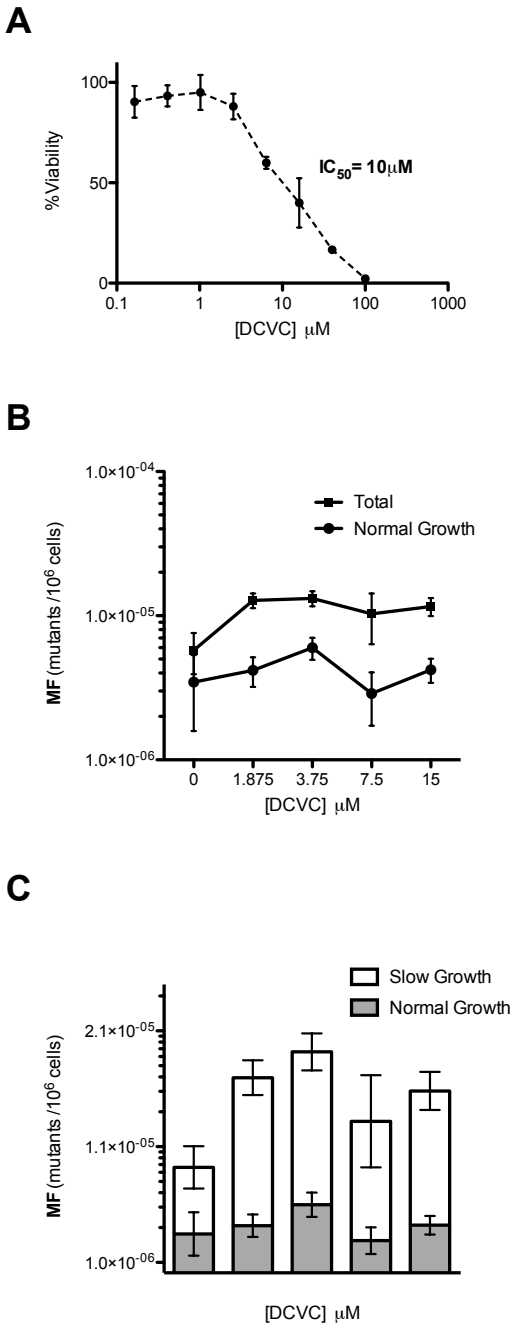

Figure 4.6 Mutation frequency analysis at the TK locus in human lymphoblasts with and without DCVC. (A) Dose response of DCVC showing IC_{50}= 10 uM. (B) Mutation frequency of normal growth (NG) mutations and total mutations. (C) Mutation frequency of NG mutations and slow growth (SG) mutations. Point mutations and small indels are classified as NG mutations. Large deletions, translocations and recombination events are considered SG mutations. SG mutation frequency was calculated as *Total mutation frequency-NG mutation frequency*. Values are mean ± SEM; n = 2 for each measurement in duplicate.

Table 4.3. Mutation frequency (mean ± SEM) in human lymphoblasts exposed to DCVC in human lymphoblasts[a]

DCVC (μM)	MF x 10^{-6} cells	Fold change[b]
0	5.76 ± 1.83	
1.875	1.28 ± 1.50	2.2
3.25	1.32 ± 1.60	2.3
7.5	1.03 ± 3.98	1.8
15	1.16 ± 1.65	2.0

[a] Mutagenesis at the TK locus was measured in human lymphoblasts after exposure to DCVC for 4 weeks. Mutation frequency is the number of mutation events per 1 million cells. Values are mean ± SEM; n = 2 for each measurement.
[b] Fold increase over untreated control

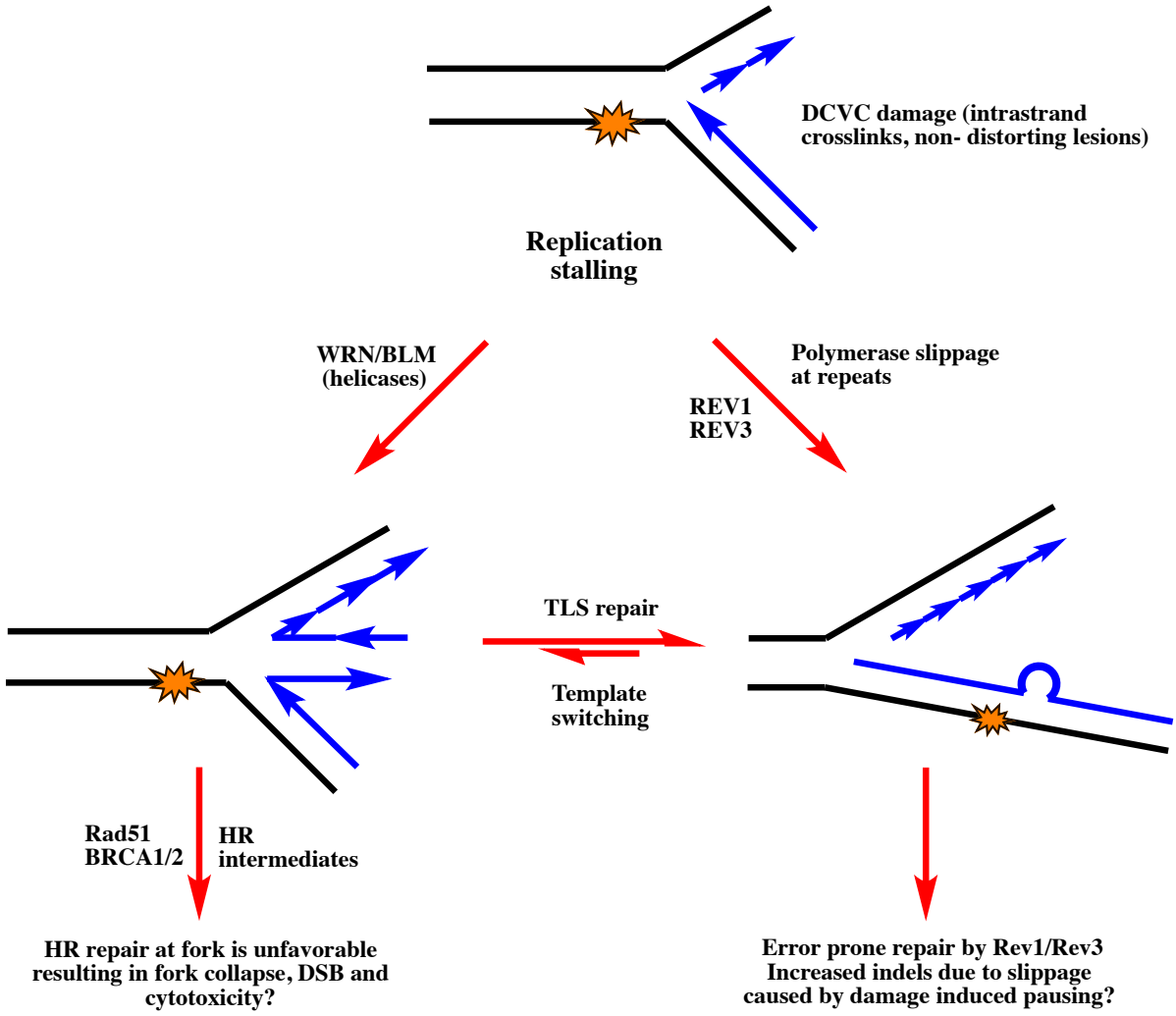

Figure 4.7 Working model for DCVC mutagenic mechanism. DCVC causes DNA damage that does not distort the DNA helix, but stalls the replicative polymerase during DNA replication. Upon stalling, DCVC lesions elicit repair by error-prone translesion synthesis and may also cause replication slippage, resulting in mutagenesis at sites of damage. While TLS repair is favored, DCVC lesions may become substrates for a form of recombination known as template switching repair.

References

1. Rusyn I, Chiu WA, Lash LH, Kromhout H, Hansen J, Guyton KZ. Trichloroethylene: Mechanistic, epidemiologic and other supporting evidence of carcinogenic hazard. Pharmacol Therapeut. 2013.

2. Brauch H, Weirich G, Hornauer M, Storkel S, Wohl T, Bruning T. Trichloroethylene exposure and specific somatic mutations in patients with renal cell carcinoma. J Natl Cancer I. 1999;91:854–61.

3. Brauch H, Weirich G, Klein B, Rabstein S, Bolt H, Bruning T. VHL mutations in renal cell cancer: does occupational exposure to trichloroethylene make a difference? Toxicol Lett. 2004;151:301–10.

4. Karami S, Lan Q, Rothman N, Stewart PA, Lee K-M, Vermeulen R, et al. Occupational trichloroethylene exposure and kidney cancer risk: a meta-analysis. Occup Environ Med. 2012;69:858–67.

5. Charbotel B, Gad S, Caïola D, Béroud C, Fevotte J, Bergeret A, et al. Trichloroethylene exposure and somatic mutations of the VHL gene in patients with Renal Cell Carcinoma. J Occup Med Toxicol. 2007;2:13.

6. Goeptar A, Commandeur J, Vanommen B, Vanbladeren P, Vermueulen N. Metabolism and kinetics of trichloroethylene in relation to toxicity and carcinogenicity- relevance of the mercapturic acid pathway. Chem Res Toxicol. 1995;8:3–21.

7. Caldwell JC, Keshava N, Evans MV. Difficulty of mode of action determination for trichloroethylene: An example of complex interactions of metabolites and other chemical exposures. Environ Mol Mutagen. 2008;49:142–54.

8. Lash LH, Putt DA, Hueni SE, Payton SG, Zwickl J. Interactive toxicity of inorganic mercury and trichloroethylene in rat and human proximal tubules: Effects on apoptosis, necrosis, and glutathione status. Toxicol Appl Pharm. 2007;221:349–62.

9. Yamazoe M, Sonoda E, Hochegger H, Takeda S. Reverse genetic studies of the DNA damage response in the chicken B lymphocyte line DT40. Dna Repair. 2004;3:1175–85.

10. Buerstedde J, Takeda S. Increased ration of targeted to random integration after transfection of chicken B-cell lines. Cell. 1991;67:179–88.

11. Sonoda E, Morrison C, Yamashita Y, Takata M, Takeda S. Reverse genetic studies of homologous DNA recombination using the chicken B-lymphocyte line, DT40. Philos T Roy Soc B. 2001;356:111–7.

12. Ji K, Kogame T, Choi K, Wang X, Lee J, Taniguchi Y, et al. A Novel Approach Using DNA-Repair-Deficient Chicken DT40 Cell Lines for Screening and Characterizing the Genotoxicity of Environmental Contaminants. Environ Health Persp. 2009;117:1737–44.

13. Simpson LJ, Ross A-L, Szüts D, Alviani CA, Oestergaard VH, Patel KJ, et al. RAD18-independent ubiquitination of proliferating-cell nuclear antigen in the avian cell line DT40. EMBO Rep. 2006;7:927–32.

14. Edmunds CE, Simpson LJ, Sale JE. PCNA ubiquitination and REV1 define temporally distinct mechanisms for controlling translesion synthesis in the avian cell line DT40. Mol Cell. 2008;30:519–29.

15. Ridpath JR, Nakamura A, Tano K, Luke AM, Sonoda E, Arakawa H, et al. Cells deficient in the FANC/BRCA pathway are hypersensitive to plasma levels of formaldehyde. Cancer Res. 2007;67:11117–22.

16. Nojima K, Hochegger H, Saberi A, Fukushima T, Kikuchi K, Yoshimura M, et al. Multiple repair pathways mediate tolerance to chemotherapeutic cross-linking agents in vertebrate cells. Cancer Res. 2005;65:11704–11.

17. Ridpath JR, Takeda S, Swenberg JA, Nakamura J. Convenient, multi-well plate-based DNA damage response analysis using DT40 mutants is applicable to a high-throughput genotoxicity assay with characterization of modes of action. Environ Mol Mutagen. 2011;52:153–60.

18. Ulrich HD. Conservation of DNA damage tolerance pathways from yeast to humans. Biochem Soc T. 2007;35:1334–7.

19. Andersen PL, Xu F, Xiao W. Eukaryotic DNA damage tolerance and translesion synthesis through covalent modifications of PCNA. Cell Res. 2008;18:162–73.

20. Kakar S, Watson NB, McGregor WG. RAD18 signals DNA polymerase IOTA to stalled replication forks in cells entering S-phase with DNA damage. Adv Exp Med Biol. 2008;614:137–43.

21. Arakawa H, Moldovan G-L, Saribasak H, Saribasak NN, Jentsch S, Buerstedde J-M. A role for PCNA ubiquitination in immunoglobulin hypermutation. Plos Biol. 2006;4:e366.

22. Okada T, Sonoda E, Yamashita Y, Koyoshi S, Tateishi S, Yamaizumi M, et al. Involvement of vertebrate Pol kappa in Rad18-independent postreplication repair of UV damage. J Biol Chem. 2002;277:48690–5.

23. Hendel A, Krijger PHL, Diamant N, Goren Z, Langerak P, Kim J, et al. PCNA ubiquitination is important, but not essential for translesion DNA synthesis in mammalian cells. Plos Genet. 2011;7:e1002262.

24. Hashimoto K, Cho Y, Yang I-Y, Akagi J-I, Ohashi E, Tateishi S, et al. The vital role of polymerase ζ and REV1 in mutagenic, but not correct, DNA synthesis across benzo[a]pyrene-dG and recruitment of polymerase ζ by REV1 to replication-stalled site. J Biol Chem. 2012;287:9613–22.

25. Irving RM, Elfarra AA. Mutagenicity of the cysteine S-conjugate sulfoxides of

trichloroethylene and tetrachloroethylene in the Ames test. Toxicology. 2013;306:157–61.

26. Deans AJ, West SC. DNA interstrand crosslink repair and cancer. Nat Rev Cancer. 2011;11:467–80.

27. Huang Y, Li L. DNA crosslinking damage and cancer - a tale of friend and foe. Transl Cancer Res. 2013;2:144–54.

28. Lehoczký P, McHugh PJ, Chovanec M. DNA interstrand cross-link repair in Saccharomyces cerevisiae. FEMS Microbiol Rev. 2007;31:109–33.

29. Huang D, Piening BD, Paulovich AG. The preference for error-free or error-prone postreplication repair in Saccharomyces cerevisiae exposed to low-dose methyl methanesulfonate is cell cycle dependent. Mol Cell Biol. 2013;33:1515–27.

30. Mao FJ, Sidorova JM, Lauper JM, Emond MJ, Monnat RJ. The human WRN and BLM RecQ helicases differentially regulate cell proliferation and survival after chemotherapeutic DNA damage. Cancer Res. 2010;70:6548–55.

31. Brosh RM. DNA helicases involved in DNA repair and their roles in cancer. Nat Rev Cancer. 2013;13:542–58.

32. Machwe A, Karale R, Xu X, Liu Y, Orren DK. The Werner and Bloom syndrome proteins help resolve replication blockage by converting (regressed) holliday junctions to functional replication forks. Biochemistry-Us. 2011;50:6774–88.

33. Machwe A, Xiao L, Groden J, Orren DK. The Werner and Bloom syndrome proteins catalyze regression of a model replication fork. Biochemistry-Us. 2006;45:13939–46.

34. Kawabe Y-I, Seki M, Yoshimura A, Nishino K, Hayashi T, Takeuchi T, et al. Analyses of the interaction of WRNIP1 with Werner syndrome protein (WRN) in vitro and in the cell. Dna Repair. 2006;5:816–28.

35. Caspary WJ, Langenbach R, Penman BW, Crespi C, Myhr BC, Mitchell AD. The mutagenic activity of selected compounds at the TK locus: rodent vs. human cells. Mutat Res. 1988;196:61–81.

CHAPTER V

Future Directions: Closing the gap in TCE risk assessment

ABSTRACT

TCE toxicity has been studied considerably, yet TCE risk assessment with regards to cancer remains controversial. The last 20 years have relied heavily on *in vivo* rodent models and *in vitro* genotoxicity testing to understand the carcinogenicity of TCE and other environmental contaminants. As described in Chapter 1, genotoxicity testing can prove to be arduous, insensitive and lacking specificity, while rodent studies are costly and time consuming. Current efforts are also biased toward known endpoints, thus overlooking potential molecular processes that are important for mediating toxicity and cancer associated with TCE exposure. The knowledge generated from decades of studies has painted a blurred portrait of the cellular processes that are perturbed by TCE and how these perturbations mediate carcinogenesis. In an effort to improve TCE risk assessment, rapid, biologically based models evaluating molecular mechanisms are needed. It was the goal of the work presented herein, to address mechanistic gaps identified in the risk assessment of TCE-induced renal carcinogenesis using a functional genomics approach across a variety of models systems. Using this powerful unbiased approach in yeast, we identified genotoxicity mechanisms that may play critical roles in mediating TCE–induced renal cancer. We propose a mutagenic mechanism of action where damage caused by reactive TCE metabolites elicts translesion synthesis and recombination-independent DNA repair.. Our functional studies present much needed mechanistic insight on TCE toxicity, but also provide direction for future studies that are imperative for comprehensive TCE risk assessment- (i) determination of a mutational signature of TCE exposure and (ii) identification of TCE susceptibility genes. Below we describe the utility of next-generation sequencing to fill in these important data gaps.

MUTATIONAL SIGNATURE OF EXPOSURE

Environmental carcinogens can interact with DNA structure both directly and indirectly, with heritable change in DNA sequence constituting mutational effects. The specific type of DNA damage and the DNA repair mechanism elicited by specific chemical exposures results in unique mutational signatures. The study of mutational signatures can provide clues on type of DNA damage, extent of damage and mechanisms of carcinogenesis. Typically, mutational signatures of exposure have been determined from the study of mutations in a single gene or a small subset of specific genes. For example, several studies have revealed unique mutational signatures of exposure in *TP53* for a small handful of environmental carcinogens, including aristolochic acid, cigarette smoke and aflatoxin B1 (1-6). While data from these experiments has been insightful, it does not provide information at the genome-wide level.

Bruning *et al.* and Brauch *et al.* published studies identifying a *VHL* mutational hotspot in exon 1 associated with high occupational exposure to TCE (9-11). Occurrence of renal cell carcinoma is associated with mutations in the von Hippel Lindau (*VHL*) tumor suppressor gene. In the majority of cases, there is a propensity of small base changes, such as insertions, point mutations

and deletions that result in loss of *VHL* function, protein truncation or altered expression (12). These initial results suggested a unique mutational signature for TCE exposure, but a series of follow-up analyses concluded the high frequency of mutations was irrespective of TCE exposure (12,13).

Next generation sequencing (NGS): closing the gap in TCE risk assessment

As described in Chapter 1, current genotoxicity testing relies on a handful of mutagenesis assays that provide a *biased* mutational landscape. Mutagenic potential and mutational profiles are determined by *selection* experiments at a single, specific, loci i.e. *TK* or *HPRT* loci in mammalian tests; canavanine or FOA loci in yeast. Other studies have also used PCR-based approaches to determine exposure signatures by sequencing a handful of gene targets (usually oncogenes) in exposed populations with cancer. The power of these approaches are limited by their inherent design. Both approaches provide spectrums biased for driver mutations and limited insight on potentially carcinogenic passenger mutations. Furthermore, interpretation of this mutational data has relied on simple analyses of somatic base substitutions (C·G→A·T, C·G→G·C, C·G→T·A, T·A→A·T, T·A→C·G and T·A→G·C) to determine low resolution mutation patterns. It is known that sequence context affects mutation rates and should be taken into consideration when defining a mutational signature (8). Therefore, in addition to the 6 classes of base substitutions, there are 16 possible sequence contexts for each mutated base (A, C, G or T at the 5′ end and A, C, G or T at the 3′ end), and thus 96 different mutated trinucleotides are possible.

Aside from the few targeted sequencing studies described above, identifying specific TCE exposure "signatures" at the genome level have not been undertaken. An increase in mutation frequency (Chapter IV) suggests TCE exposure could produce a unique mutational fingerprint of exposure. Efforts to determine mutational signatures of TCE exposure are complicated by (i) poor exposure histories, (ii) lack of *in vitro* models to confirm mutation spectrums and (iii) interpretation of mutational data. Historical studies of TCE-associated kidney cancer have relied primarily on questionnaire data and estimates of occupational exposure based on workplace variables that have been characterized as low, medium or highly exposure. Unfortunately, these assessments often neglect personal information and other risk factors associated with renal cancer such as smoking (7).

With the advancement of NGS technologies, it is becoming more feasible to determine mutation patterns through whole genome, whole exome and whole transcriptome sequencing (See Fig. 5.1) (14). NGS technologies have led to a surge in mutation data available from cancer genomes and the mutational signatures generated can provide important insight on etiology, prevention, and therapy (8,14-21). NGS is a powerful and *unbiased* approach to determine high-resolution, genome-wide mutational signatures of TCE exposure. Hoang *et al* utilized a NGS approach to examine the carcinogen aristolochic acid (AA) (22). Whole exome sequencing of urothelial carcinoma of the upper urinary tract (UTUC) from individuals with documented exposure revealed a distinct mutational signature of A:T>T:A transversions attributable to AA (22,23). Subsequent *in vitro* studies with the Hupki MEF immortalization assay produced an exome-wide mutational signature in concordance with the human tumor mutation profile (24). These results demonstrate the (i) power of NGS to identify unique signatures of exposure and (ii) potential of

the MEF immortalization assay to recapitulate human carcinogen mutation signatures observed from whole-genome analysis of human tumors. Future studies utilizing the Hupki MEF immortalization model could provide much needed information on TCE mutation signatures and facilitate the interpretation of human mutation data.

TCE SUSCEPTIBILLITY GENES

The susceptibility of humans to diseases related to environmental chemical exposure is determined in large part by genetics (25). Given the knowledge of human genetic variants, and the role they play in determining toxicant susceptibility, there have been surprisingly few models allowing for the identification of genes underlying susceptibility. Functional genomic studies in yeast identified a S-adenosylmethionine dependent methyltransferase required for resistance to arsenic toxicity. Follow-up epidemiological studies in Andean women demonstrated that *N6AMT1* (the human homolog) polymorphisms could be used as susceptibility markers for arsenic toxicity (25,26). These studies highlight the utility of genome-wide profiing in yeast for studying TCE susceptibility genes.

Information on TCE genetic susceptibility remains limited. Early studies by Bruning *et al.* and Moore *et al.* reported significant associations between polymorphisms in *GSTM1, GSTT1* and *CCBL1* and renal cell carcinoma susceptibility in workers with long-term high occupational exposure to TCE (27,28). *GSTM1, GSTT1,* and *CCBL1* encode enzymes involved in the metabolism of TCE to nephrotoxic metabolites such as DCVC. These associations further support the role of metabolism in nephrotoxicity and indicate genetic variation in the glutathione conjugation metabolism enzymes could alter cancer susceptibility in TCE exposed populations. The results from studies presented in Chap. III and IV presents a novel list of candidate susceptibility genes for TCE-associated renal cancer (Table 5.1). NGS studies have identified novel hypoxic response and chromatin modifying genes as candidate renal cell carcinoma susceptibility genes, but none have reported DNA repair genes as candidates (20,21,29,30) (reviewed in (8)). We propose that polymorphisms in translesion synthesis and recombination repair genes could increase renal cell carcinoma risk in TCE-exposed populations and merits further investigation. In collaboration with the National Cancer Institute (NCI) and IARC, we have preliminary results suggesting significant associations between TCE exposure, renal cell carcinoma risk, and variants in the DNA repair genes WRN, ERCC1, ERCC4, and SNM1B. Given that there are very few examples of established gene–environment interactions in cancer (31), the discovery of four potential susceptibility genes for TCE and renal cancer is tremendous and would have significant implications for TCE risk assessment. Analyses are on going to determine the phenotype of these variants, which will provide important clues on the TCE mode of action.

On-going studies

Studies presented in Chapters III and IV revealed genetic evidence supporting TCE induced mutagenesis mediated by error-prone translesion synthesis. Furthermore, our results from *selection* experiments in TK-6 human lymphoblasts suggest TCE exposure could result in a mutational signaure of exposure. Studies are on-going to determine a novel mutational signature of TCE exposure *in vitro* and in renal cell carcinoma cases with documented TCE exposure

using an *unbiased* whole exome sequencing approach. These efforts would be the first to identify and validate a mutational signature for the human carcinogen TCE.

MATERIALS AND METHODS

Cell lines and tissue culture. HK-2 (human kidney 2) is a proximal tubular cell (PTC) line derived from normal kidney immortalized by transduction with human papilloma virus 16 (HPV-16) E6/E7 genes (ATCC). Cells were cultured in Keratinocyte Serum Free Medium (K-SFM), supplemented with 0.05 mg/ml bovine pituitary extract (BPE) and 5 ng/ml human recombinant epidermal growth factor (EGF) (GIBCO) under standard culture conditions.

DNA preparation and whole exome sequencing (WES). $1x10^5$ cells were seeded in 24 well plates and treated with 6 different concentrations of DCVC as outlined in Fig. 5.2. Genomic DNA (gDNA) was extracted from cells using DNeasy blood and tissue kit (QIAGEN) and checked for purity, concentration, and integrity by OD260/280 ratio using and agarose gel electrophoresis. Illumina libraries were generated using the Nextera Exome library kit (Illumina), following manufacturer's instructions. The libraries were sequenced in paired-end 100 nucleotide (nt) reads using the Illumina HiSeq 2500 platform according to manufacturer's protocols.

Mutation Identification. Sequencing reads will be analyzed and aligned to human genome hg18 with the Eland algorithm in CASAVA 1.7 software (Illumina). A mismatched base will be determined as a mutation as outlined in (22) . For analyses of mutation signatures, mutations will be classified into 96 types determined by the six possible substitutions (C·G→A·T, C·G→G·C, C·G→T·A, T·A→A·T, T·A→C·G and T·A→G·C) and the 16 combinations of flanking (5' and 3') nucleotides.

THE FUTURE OF FUNCTIONAL TOXICOGENOMICS

The new paradigm in toxicity testing continues to evolve from the traditional, whole organism "kill them and count them" approach, an inefficient model for meeting the demands of toxicological risk assessments. High-throughput, mechanistic based, *in vitro* models are strongly needed in toxicological evaluations to fill data gaps for probable carcinogens and chemicals with unknown cancer risk. The need for new methods was echoed in a recent report from the National Academy of Sciences, which described the need to identify common toxicity pathways and develop high throughput predictive screening assays (32). By identifying the key molecular interactions, steps, or processes that mediate toxicity, cost-effective mode-of-action testing approaches would enable rapid data generation to improveve risk assessment. The work presented herein exhibits the power of an unbiased approach in yeast and avian cells to evaluate the genotoxicity of environmental carcinogens and chemicals with unknown genotoxicity.

In addition to these models, the newly developed CRISPR-Cas9 system allows for large-scale, loss of function screening in mammalian cells. With lentiviral delivery of a CRISPR-Cas9 knockout library, sgRNAs serve as distinct barcodes that can be counted via high-throughput sequencing to perform selection screening in human cells (26). The new availability of the

CRISPR platform will greatly advance toxicity testing and enable the generation of mechanistic toxicity data most relevant to human health and cancer.

The utility of NGS technology in the field of toxicology is two-fold; first, it allows for the determination of unique mutational signatures associated with exposure and second, it provides mechanistic insight. Mutations that usually go undetected in current testing can provide information on cellular processes that play a role in mediating cancer in populations exposed to environmental carcinogens such as TCE and identify chemicals with unknown genotoxicity. An integrated approach using functional profiling, next generation sequencing and bioinformatics tools presents an opportunity to strengthen TCE risk assessment and has the potential to become a new paradigm in the evaluation of chemical risk assessment. Our results highlight the power of a systems approach to (i) identify mechanisms of action; (ii) define more specific toxicological endpoints for further study; and (iii) identify toxicant susceptibility genes (22,26,33,34).

Table 5.1 Candidate TCE susceptibility genes identified by functional profiling studies in yeast.

Yeast candidate gene	Human homolog
Rev1	REV1
Rev3	REV3L
Rad5	HLTF
Rad18	RAD18
Rad51	RAD51
Rad10	ERCC1
Rad1	ERCC4
Pso2	DCLRE1C DCLRE1B
Wrn	WRN

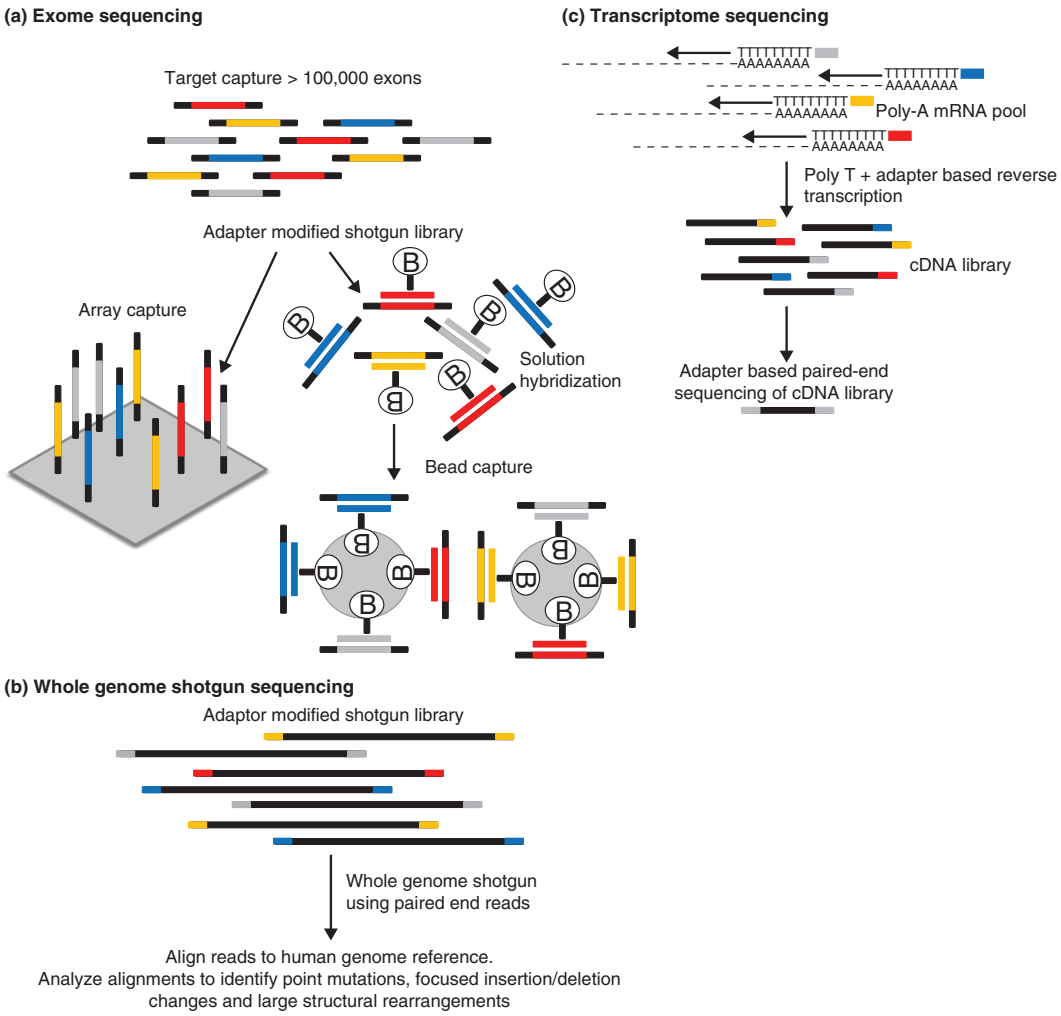

Fig. 5.1 Overview of next generation sequencing approaches that can be used to determine mutational signatures of exposure **(a)** In exome capture, a random library of genomic fragments, each containing platform-specific adapters on each end, is combined with a set of probes that define the human exome. Following hybridization, the probe:genomic library fragment hybrids are captured using magnetic beads and isolated from solution by the application of a magnet, or by solid phase capture. Denaturing conditions are used to elute the captured genomic library fragment population from the hybrids, and prepared for sequencing. **(b)** In whole genome sequencing, the same random fragment library is constructed as in (a), but the resulting fragments are sequenced directly without a capture step. **(c)** In transcriptome sequencing, the RNA is converted to cDNA, the resulting cDNAs are fragmented, and the library adapters are ligated to the resulting fragments, followed by sequencing. Adapted from (14).

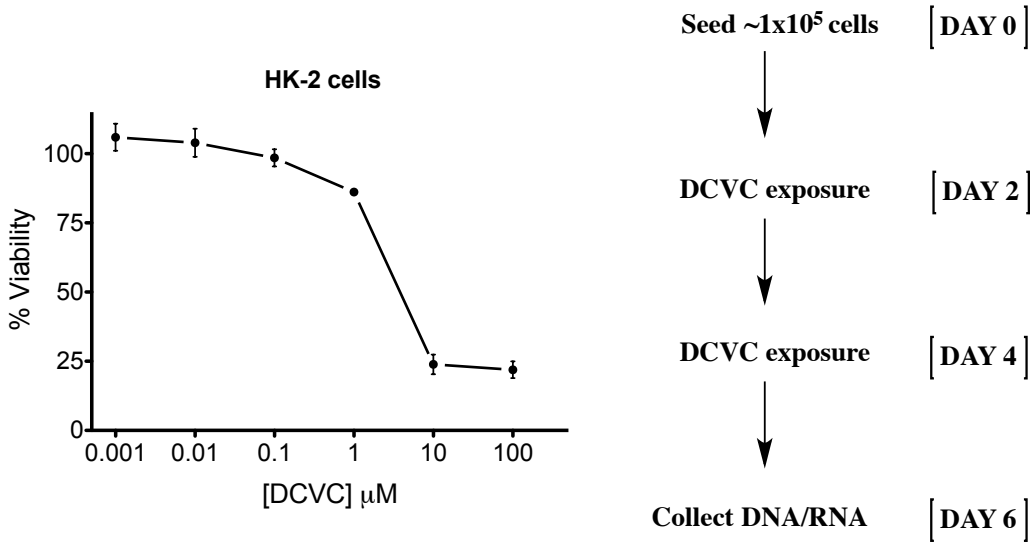

Figure 5.2. Dose response of the metabolite DCVC in HK-2 cells and overview of treatment protocol. Cells are seeded in 24 well plates and treated with DCVC followed by isolation of gDNA for sequencing studies. Values are mean ± SEM; $n \geq 3$ for each measurement.

References

1. Soussi T. Advances in carcinogenesis: a historical perspective from observational studies to tumor genome sequencing and TP53 mutation spectrum analysis. Biochim Biophys Acta. 2011;1816:199–208.

2. Hollstein M, Moriya M, Grollman AP, Olivier M. Analysis of TP53 mutation spectra reveals the fingerprint of the potent environmental carcinogen, aristolochic acid. Mut Res. 2013;753:41–9.

3. Moriya M, Slade N, Brdar B, Medverec Z, Tomic K, Jelakovic B, et al. TP53 Mutational signature for aristolochic acid: an environmental carcinogen. Int J Cancer. 2011;129:1532–6.

4. Ozturk M. p53 mutation in hepatocellular carcinoma after aflatoxin exposure. Lancet. 1991;338:1356–9.

5. Gouas D, Shi H, Hainaut P. The aflatoxin-induced TP53 mutation at codon 249 (R249S): biomarker of exposure, early detection and target for therapy. Cancer Lett. 2009;286:29–37.

6. Pfeifer GP, Denissenko MF, Olivier M, Tretyakova N, Hecht SS, Hainaut P. Tobacco smoke carcinogens, DNA damage and p53 mutations in smoking-associated cancers. Oncogene. 2002;21:7435–51.

7. Desimone MC, Rathmell WK, Threadgill DW. Pleiotropic effects of the trichloroethylene-associated P81S VHL mutation on metabolism, apoptosis, and ATM-mediated DNA damage response. J Natl Cancer I. 2013;105:1355–64.

8. Watson IR, Takahashi K, Futreal PA, Chin L. Emerging patterns of somatic mutations in cancer. Nat Rev Genet. 2013;14:703–18.

9. Brauch H, Weirich G, Hornauer M, Storkel S, Wohl T, Bruning T. Trichloroethylene exposure and specific somatic mutations in patients with renal cell carcinoma. J Natl Cancer I. 1999;91:854–61.

10. Bruning T, Weirich G, Hornauer MA, Höfler H, Brauch H. Renal cell carcinomas in trichloroethene (TRI) exposed persons are associated with somatic mutations in the von Hippel-Lindau (VHL) tumour suppressor gene. Arch Toxicol. 1997;71:332–5.

11. Bruning T, Bolt H. Renal toxicity and carcinogenicity of trichloroethylene: Key results, mechanisms, and controversies. Crit Rev Toxicol. 2000;30:253–85.

12. Shiao Y-H. Genetic Signature for Human Risk Assessment: Lessons From Trichloroethylene. Environ Mol Mutagen. 2009;50:68–77.

13. Charbotel B, Gad S, Caïola D, Béroud C, Fevotte J, Bergeret A, et al. Trichloroethylene exposure and somatic mutations of the VHL gene in patients with Renal Cell Carcinoma. J

Occup Med Toxicol. 2007;2:13.

14. Mardis ER. Cancer genomics identifies determinants of tumor biology. Genome Biol. 2010;11:211.

15. Helleday T, Eshtad S, Nik-Zainal S. Mechanisms underlying mutational signatures in human cancers. Nat Rev Genet. 2014.

16. Berger MF, Hodis E, Heffernan TP, Deribe YL, Lawrence MS, Protopopov A, et al. Melanoma genome sequencing reveals frequent PREX2 mutations. Nature. 2012;485:502–6.

17. Alexandrov LB, Nik-Zainal S, Wedge DC, Campbell PJ, Stratton MR. Deciphering signatures of mutational processes operative in human cancer. Cell Rep. 2013;3:246–59.

18. Cancer Genome Atlas Research Network. Comprehensive molecular characterization of clear cell renal cell carcinoma. Nature. 2013;499:43–9.

19. Farber LJ, Furge K, Teh BT. Renal cell carcinoma deep sequencing: recent developments. Curr Oncol Rep. 2012;14:240–8.

20. Varela I, Tarpey P, Raine K, Huang D, Ong CK, Stephens P, et al. Exome sequencing identifies frequent mutation of the SWI/SNF complex gene PBRM1 in renal carcinoma. Nature. 2011;469:539–42.

21. Sato Y, Yoshizato T, Shiraishi Y, Maekawa S, Okuno Y, Kamura T, et al. Integrated molecular analysis of clear-cell renal cell carcinoma. Nat Genet. 2013;45:860–7.

22. Hoang ML, Chen C-H, Sidorenko VS, He J, Dickman KG, Yun BH, et al. Mutational signature of aristolochic acid exposure as revealed by whole-exome sequencing. Sci Transl Med. 2013;5:197ra102.

23. Poon SL, Pang ST, McPherson JR, Yu W, Huang KK, Guan P, et al. Genome-wide mutational signatures of aristolochic acid and its application as a screening tool. Sci Transl Med. 2013;5:197ra101.

24. Olivier M, Weninger A, Ardin M, Huskova H, Castells X, Vallée MP, et al. Modelling mutational landscapes of human cancers in vitro. Sci Rep. 2014;4:4482.

25. Jo WJ, Loguinov A, Wintz H, Chang M, Smith AH, Kalman D, et al. Comparative Functional Genomic Analysis Identifies Distinct and Overlapping Sets of Genes Required for Resistance to Monomethylarsonous Acid (MMA(III)) and Arsenite (As-III) in Yeast. Toxicol Sci. 2009;111:424–36.

26. Gaytán BD, Vulpe CD. Functional toxicology: tools to advance the future of toxicity testing. Front Genet. 2014;5:110.

27. Moore LE, Boffetta P, Karami S, Brennan P, Stewart PS, Hung R, et al. Occupational

trichloroethylene exposure and renal carcinoma risk: evidence of genetic susceptibility by reductive metabolism gene variants. Cancer Res. 2010;70:6527–36.

28. Rusyn I, Chiu WA, Lash LH, Kromhout H, Hansen J, Guyton KZ. Trichloroethylene: Mechanistic, epidemiologic and other supporting evidence of carcinogenic hazard. Pharmacol Therapeut. 2013.

29. Dalgliesh GL, Furge K, Greenman C, Chen L, Bignell G, Butler A, et al. Systematic sequencing of renal carcinoma reveals inactivation of histone modifying genes. Nature. 2010;463:360–3.

30. Pena-Llopis S, Vega-Rubín-de-Celis S, Liao A, Leng N, Pavía-Jiménez A, Wang S, et al. BAP1 loss defines a new class of renal cell carcinoma. Nat Genet. 2012;44:751–9.

31. Garcia-Closas M, Rothman N, Figueroa JD, Prokunina-Olsson L, Han SS, Baris D, et al. Common genetic polymorphisms modify the effect of smoking on absolute risk of bladder cancer. Cancer Res. 2013;73:2211–20.

32. Gibson JE. An integrated summary of commentary on the National Academy of Sciences report on "Toxicity testing in the 21st century: a vision and a strategy". Hum Exp Toxicol. 2010;29:33–5.

33. Schmitt MW, Kennedy SR, Salk JJ, Fox EJ, Hiatt JB, Loeb LA. Detection of ultra-rare mutations by next-generation sequencing. P Natl Acad Sci Usa. 2012;109:14508–13.

34. Besaratinia A, Li H, Yoon J-I, Zheng A, Gao H, Tommasi S. A high-throughput next-generation sequencing-based method for detecting the mutational fingerprint of carcinogens. Nucleic Acids Res. 2012;40:e116.

Appendix 1: Cadmium sensitive and resistant genes identified

ORF	Standard Name	5 generations			15 generations			Number of Significant
		25% IC20	50% IC20	IC20	25% IC20	50% IC20	IC20	
		1 μM	2 μM	4 μM	1 μM	2 μM	4 μM	
YAL002W	*VPS8*	-0.8	-1.8	-2.5	-3.6	-5.1	-3.7	6
YKL041W	*VPS24*	-1	-1.15	-1.5	-2.05	-3.8	-4.15	6
YNR006W	*VPS27*	-1.15	-1.3	-1.8	-2.8	-4.45	-4.05	6
YPR173C	*VPS4*	-1	-1.1	-1.55	-2.5	-4	-3.9	6
YFL025C	*BST1*	0.6	1.35	1.3		1.7	5.5	5
YGL095C	*VPS45*	-1.6	-1.6	-2.1	-2.8	-3.1		5
YLR119W	*SRN2*		-0.7	-1.3	-1.6	-4.1	-5.1	5
YNR005C	*YNR005C*		-0.7	-1.15	-0.7	-3.3	-4.7	5
YOR036W	*PEP12*	-1.4	-1.5	-2.4	-2.7	-3.1		5
YOR089C	*VPS21*		-1.3	-1.5	-3.25	-3.75	-4.7	5
YPL065W	*VPS28*		-0.9	-1.35	-2.1	-3.25	-2.9	5
YPL084W	*BRO1*		-1.7	-2.1	-1.8	-3.8	-3.8	5
YCL008C	*STP22*		-1	-1.6	-2.3	-2.7		4
YDR323C	*PEP7*	-1.2	-1.5	-1.7	-2.1			4
YDR456W	*NHX1*		-0.8	-1.6	1.8	-1.7		4
YDR495C	*VPS3*	-1.3	-1.35	-2.05		-1.9		4
YGL007W	*BRP1*		-1.1		-1.3	-2.05	-3.2	4
YGR272C	*YGR272C*	0.8	1	1.2			4.7	4
YHR108W	*GGA2*			-1	-1	-2.75	-2.65	4
YIL052C	*RPL34B*		0.9	1.2		1.75	3.8	4
YIL154C	*IMP2'*		0.9	0.9		1.45	3.2	4
YJL053W	*PEP8*		-0.85	-1.4		-3.35	-3.8	4
YJL056C	*ZAP1*	1.1	1.55	1.3			6.4	4
YJL154C	*VPS35*		-1.4	-1.9		-3.8	-3.25	4
YJR102C	*VPS25*			-1.4	-2.05	-2.85	-3.2	4
YKR035C	*OPI8*		-1.3	-1.7	-1.3	-2.45		4
YLR025W	*SNF7*			-0.8	-2.85	-3.4	-2.75	4
YLR360W	*VPS38*		-1.1	-2.05		-3.15	-4	4
YML097C	*VPS9*		-2.4	-2.2	-3.7	-3.2		4
YML115C	*VAN1*		1		1.05	3	4.45	4
YMR275C	*BUL1*		-1.2	-2.1	-1.5	-4.5		4
YOR068C	*VAM10*		-1	-1.15		-2	-2.4	4
YOR322C	*LDB19*			-0.9	-2.1	-3.55	-3.45	4
YPL057C	*SUR1*		-1		-2.15	-4.7	-4.75	4
YPL120W	*VPS30*		-1.1	-1.5		-4.1	-5.6	4
YPR065W	*ROX1*		-1.15		-1.85	-4.05	-4.3	4
YAR003W	*SWD1*				-1.2	-2.6	-3.4	3
YAR014C	*BUD14*		0.7			1	2.1	3

YAR018C	*KIN3*		1.6			1.5	3.5	3
YBL024W	*NCL1*		-0.8			-2.5	-2.5	3
YBR031W	*RPL4A*		0.7			1	1.85	3
YBR036C	*CSG2*				-2.6	-4.3	-5.3	3
YBR208C	*DUR1,2*				-1.2	-1.7	-2.6	3
YCL005W	*LDB16*				3.2	0.9	3.7	3
YCR008W	*SAT4*		0.7			1	1.8	3
YDL117W	*CYK3*		1.1			1.6	3	3
YDL226C	*GCS1*			-2.1		-1.6	-2.8	3
YDR072C	*IPT1*				-1.35	-3.05	-4.05	3
YDR098C	*GRX3*				-1	-3.45	-2.45	3
YDR289C	*RTT103*			1.3		1.2	3.6	3
YDR290W	*YDR290W*		0.8	0.9			2.1	3
YDR455C	*YDR455C*		-0.7	-1.6		-2		3
YDR484W	*VPS52*		-1.2		-1.7	-2.05		3
YDR516C	*EMI2*				-1.3	-2.55	-3.15	3
YER017C	*AFG3*			1.1		2.1	6.15	3
YER092W	*IES5*				-1.15	-1.9	-2.3	3
YGL071W	*AFT1*	-1.3	-1	-1.2				3
YGL212W	*VAM7*			-1.65		-1.95	-3.1	3
YHR013C	*ARD1*				-2.75	-3.5	-3.5	3
YHR045W	*YHR045W*				-0.9	-2.3	-2.8	3
YHR111W	*UBA4*		0.8			1.95	3.55	3
YJR043C	*POL32*				-1.2	-1.95	-3.2	3
YKL032C	*IXR1*				-1.6	-2.25	-3.3	3
YKL048C	*ELM1*		1.2			2.85	5.15	3
YKL113C	*RAD27*			-1.1	-1.4	-3.3		3
YKR035W-A	*DID2*			-0.9		-2.35	-3	3
YKR052C	*MRS4*				-1.8	-3.45	-3.55	3
YLR023C	*IZH3*				-1	-2.7	-3.8	3
YLR047C	*FRE8*				-1.1	-5.5	-5.3	3
YLR131C	*ACE2*				1.3	2.8	4.5	3
YLR148W	*PEP3*	-1.2	-1.5	-1.7				3
YLR417W	*VPS36*			-1.5	-2.2	-2.95		3
YMR015C	*ERG5*				-1.5	-3	-3	3
YMR228W	*MTF1*			1.8		1.1	3.55	3
YMR258C	*YMR258C*				-0.8	-2.05	-3	3
YMR263W	*SAP30*				-1.2	-1.8	-2.4	3
YMR267W	*PPA2*			0.8		2.1	5.85	3
YMR312W	*ELP6*		0.9	0.8			2.5	3
YNL119W	*NCS2*				1.4	2.1	4.65	3
YNL120C	*YNL120C*			1.5		1.8	4.15	3
YNL325C	*FIG4*			-1.1		-2.65	-4.05	3
YOL050C	*YOL050C*				-1	-1.75	-2.6	3

YOL100W	*PKH2*				-1	-2.3	-3	3
YOR158W	*PET123*			1.25		2	5.55	3
YOR258W	*HNT3*				3.2	2.2	4.5	3
YPL002C	*SNF8*			-1.4	-1.6	-2		3
YPL205C	*YPL205C*			1.3		1.5	3.9	3
YPL226W	*NEW1*				-1.1	-2.1	-2.7	3
YPR044C	*OPI11*		1.4			2.1	4	3
YPR064W	*YPR064W*				-0.8	-3.1	-4.5	3
YPR106W	*ISR1*		0.8			1.6	1.7	3
YAL058C-A	*YAL058C-A*					1.3	3.05	2
YAL058W	*CNE1*					1.1	2.5	2
YBL013W	*FMT1*				3.5		4.5	2
YBL017C	*PEP1*					-1.6	-3.7	2
YBL031W	*SHE1*					1.3	2.05	2
YBL038W	*MRPL16*				1.4		5.4	2
YBL057C	*PTH2*					-1.1	-1.8	2
YBL061C	*SKT5*					1.6	3.2	2
YBL066C	*SEF1*					-0.7	-1.7	2
YBL082C	*ALG3*					1	2	2
YBL083C	*YBL083C*					1.45	2.25	2
YBR015C	*MNN2*					1.2	2.85	2
YBR026C	*ETR1*				1.5		3.4	2
YBR027C	*YBR027C*					1.1	1.8	2
YBR084C-A	*RPL19A*				1.5		3.7	2
YBR099C	*YBR099C*				-1.2	-1.45		2
YBR103W	*SIF2*			1.2			1.9	2
YBR151W	*APD1*					-1	-1.9	2
YBR171W	*SEC66*					2.05	2.8	2
YBR174C	*YBR174C*					-1.9	-2.7	2
YBR175W	*SWD3*				-1.1	-2.5		2
YBR187W	*GDT1*					-2	-4.5	2
YBR275C	*RIF1*					-2	-2.4	2
YBR298C	*MAL31*					-1.85	-2.5	2
YBR300C	*YBR300C*			-1.1			-3.7	2
YCL001W-A	*YCL001W-A*					-1.65	-2.75	2
YCL010C	*SGF29*					-1.7	-2.7	2
YCR007C	*YCR007C*				3.9		4	2
YCR009C	*RVS161*			-1.1		-3.05		2
YCR025C	*YCR025C*					-1.5	-3.7	2
YCR026C	*NPP1*					-2.1	-3.2	2
YCR027C	*RHB1*					-2.5	-3.5	2
YCR028C	*FEN2*		0.7			1.4		2
YCR049C	*YCR049C*					-1.2	-3.3	2
YCR063W	*BUD31*					1.6	5.4	2

YCR068W	*ATG15*					-1.7	-4	2
YCR079W	*PTC6*					-1.45	-2.95	2
YCR087C-A	*LUG1*					-1.1	-2.85	2
YCR087W	*YCR087W*					-1.2	-2	2
YDL002C	*NHP10*					-1.4	-2	2
YDL010W	*YDL010W*				3.7		3.9	2
YDL025C	*YDL025C*					-1.6	-2.75	2
YDL061C	*RPS29B*					-1.6	-3.2	2
YDL066W	*IDP1*					1.75	3.1	2
YDL070W	*BDF2*				2.1		3	2
YDL082W	*RPL13A*				1.2		4.4	2
YDL095W	*PMT1*					1.45	4.4	2
YDL198C	*GGC1*			1.1			4.1	2
YDL225W	*SHS1*					1	1.9	2
YDR028C	*REG1*			0.8			5.8	2
YDR057W	*YOS9*					-1.7	-2.4	2
YDR073W	*SNF11*					-1.3	-3.5	2
YDR079W	*PET100*				1		2	2
YDR080W	*VPS41*			-1.85		-1.7		2
YDR146C	*SWI5*					1.1	2.5	2
YDR149C	*YDR149C*					1.2	1.85	2
YDR159W	*SAC3*			0.9			6.1	2
YDR175C	*RSM24*				2		5.9	2
YDR186C	*YDR186C*					-1.75	-3	2
YDR241W	*BUD26*					1.9	5.2	2
YDR245W	*MNN10*					2.4	5.5	2
YDR253C	*MET32*					1	1.9	2
YDR291W	*HRQ1*				4		3.2	2
YDR295C	*HDA2*					-1.1	-4.5	2
YDR322W	*MRPL35*				2.9		5.55	2
YDR363W-A	*SEM1*		1.2			1.5		2
YDR392W	*SPT3*				-1.9	-3.3		2
YDR395W	*SXM1*					-2.25	-4.25	2
YDR417C	*YDR417C*					1.6	5.15	2
YDR418W	*RPL12B*					1.8	5.7	2
YDR463W	*STP1*				-1.2	-1.8		2
YDR466W	*PKH3*					0.8	1.65	2
YDR469W	*SDC1*					-2.3	-3.7	2
YDR471W	*RPL27B*					0.9	1.9	2
YDR476C	*YDR476C*					-1.3	-2.7	2
YDR497C	*ITR1*					-1.3	-2.65	2
YDR507C	*GIN4*					1.7	4.4	2
YDR525W	*API2*					1.55	3.6	2
YEL003W	*GIM4*					1.4	3.8	2

YEL028W	*YEL028W*				3.7		4.2	2
YEL036C	*ANP1*					2	5.25	2
YER119C-A	*YER119C-A*					1.4	2.7	2
YER120W	*SCS2*					1.1	1.7	2
YER122C	*GLO3*					1.8	5.2	2
YER167W	*BCK2*					1.6	2.95	2
YGL031C	*RPL24A*					1.1	1.4	2
YGL148W	*ARO2*				-1.1	-2.95		2
YGL214W	*YGL214W*					-1.3	-3.1	2
YGL240W	*DOC1*					2	6.9	2
YGL250W	*YGL250W*					-1.85	-3.4	2
YGR056W	*RSC1*					2.1	5.65	2
YGR085C	*RPL11B*					1.5	3.1	2
YGR101W	*PCP1*					1.9	6.4	2
YGR106C	*YGR106C*					1.1	2.4	2
YGR122W	*YGR122W*					-1.9	3.3	2
YGR148C	*RPL24B*					1.6	2.95	2
YGR162W	*TIF4631*					2.25	4.6	2
YGR206W	*MVB12*					-1.9	-3.6	2
YGR242W	*YGR242W*				2.5		2.9	2
YGR285C	*ZUO1*					1.9	7.6	2
YHL009C	*YAP3*					1.3	3.35	2
YHL011C	*PRS3*			1.4			4.85	2
YHR011W	*DIA4*			1.2			7.15	2
YHR012W	*VPS29*		-1			-3.3		2
YHR029C	*YHI9*				3.6		3.9	2
YHR030C	*SLT2*					-1.9	-5.5	2
YHR034C	*PIH1*					2.4	4.8	2
YHR039C	*MSC7*					-1.7	-3.3	2
YHR060W	*VMA22*	-1.15			-2.1			2
YHR064C	*SSZ1*					1.6	8.8	2
YHR066W	*SSF1*					1.55	3.1	2
YHR104W	*GRE3*					-1.3	-2.2	2
YHR129C	*ARP1*					1.4	2	2
YHR134W	*WSS1*					1.1	1.9	2
YHR142W	*CHS7*					1.5	4.5	2
YHR153C	*SPO16*				1.9		1.9	2
YIL015C-A	*YIL015C-A*			1.2			5.75	2
YIL018W	*RPL2B*			0.8			5.15	2
YIL148W	*RPL40A*					-2.15	-2.9	2
YJL046W	*YJL046W*				2.9		3.5	2
YJL062W	*LAS21*					1.9	4.75	2
YJL080C	*SCP160*					1.95	4.55	2
YJL099W	*CHS6*					1.4	3.8	2

YJL101C	*GSH1*					-1.2	-2.75	2
YJL149W	*YJL149W*					-1.4	-3.4	2
YJL168C	*SET2*					1.2	5.15	2
YJL169W	*YJL169W*					1.2	3.4	2
YJL175W	*YJL175W*				-1.9	-2.3		2
YJL177W	*RPL17B*					1.15	2.25	2
YJL183W	*MNN11*					2.55	5.1	2
YJL192C	*SOP4*					1.25	2.35	2
YJL204C	*RCY1*		-0.9			-1.2		2
YJR032W	*CPR7*					1.75	2.8	2
YJR044C	*VPS55*					-0.8	-2.6	2
YJR054W	*YJR054W*	0.6					2	2
YJR059W	*PTK2*					-2	-3.2	2
YJR073C	*OPI3*					1.25	2.55	2
YJR075W	*HOC1*					1.1	1.6	2
YJR079W	*YJR079W*	4.1	3					2
YJR083C	*ACF4*					-1.1	-1.8	2
YJR111C	*YJR111C*					1.2	1.5	2
YJR117W	*STE24*					-1.1	-3.25	2
YKL037W	*YKL037W*					1.8	4.3	2
YKL073W	*LHS1*					1.7	5.45	2
YKL076C	*PSY1*					1.5	2.45	2
YKL114C	*APN1*	0.9					6.05	2
YKL119C	*VPH2*	-0.9			-3.9			2
YKL121W	*YKL121W*				-0.9	-1.7		2
YKL133C	*YKL133C*				2.8		3.2	2
YKL134C	*1-Oct*					2.7	7.5	2
YKL190W	*CNB1*					-2.1	-3.2	2
YKR006C	*MRPL13*					1.2	2.9	2
YKR014C	*YPT52*					-1.85	-3	2
YKR041W	*YKR041W*				3.9		3.3	2
YKR047W	*YKR047W*					1.1	2.45	2
YKR048C	*NAP1*					1.4	3.7	2
YKR072C	*SIS2*					1	1.8	2
YLL021W	*SPA2*					1.3	2.2	2
YLL045C	*RPL8B*					1.35	3.2	2
YLR020C	*YEH2*					-1.6	-2.45	2
YLR034C	*SMF3*					-4.5	-4.3	2
YLR036C	*YLR036C*				1.7		1.7	2
YLR055C	*SPT8*				-2.65	-3.6		2
YLR111W	*YLR111W*					1.45	1.7	2
YLR139C	*SLS1*			0.9			3.4	2
YLR149C	*YLR149C*			1.2			7.55	2
YLR203C	*MSS51*				3.1		4	2

YLR214W	*FRE1*				-2	-2.75		2
YLR228C	*ECM22*					-1.3	-2.3	2
YLR319C	*BUD6*					1.1	2.45	2
YLR334C	*YLR334C*				0.8		1.6	2
YLR373C	*VID22*					1.7	3.85	2
YLR374C	*YLR374C*					1.5	2.3	2
YLR375W	*STP3*					0.7	1.2	2
YLR380W	*CSR1*					-1.5	-1.9	2
YLR399C	*BDF1*		1.2				7.1	2
YLR425W	*TUS1*					1.65	3.5	2
YML009C	*MRPL39*				4.2		3	2
YML010C-B	*YML010C-B*			1			2.4	2
YML014W	*TRM9*					1.8	3.2	2
YML117W	*NAB6*					0.9	1.7	2
YML119W	*YML119W*				2.2		3.4	2
YMR010W	*YMR010W*					-1	-1.7	2
YMR058W	*FET3*					-1.5	-4.8	2
YMR072W	*ABF2*			1.2			2.75	2
YMR075C-A	*YMR075C-A*					1.05	3.15	2
YMR193C-A	*YMR193C-A*					1.1	2.45	2
YMR204C	*INP1*				2.4		2.2	2
YMR214W	*SCJ1*					-1.5	-5.3	2
YMR273C	*ZDS1*					0.9	1.7	2
YMR284W	*YKU70*				1.8		2.5	2
YMR294W	*JNM1*					0.9	2.1	2
YMR299C	*DYN3*				1.9		1.6	2
YMR304W	*UBP15*					1.3	4	2
YMR319C	*FET4*					1.8	4.15	2
YNL047C	*SLM2*				3.7		4.1	2
YNL054W	*VAC7*					-3	-5.1	2
YNL070W	*TOM7*					1.5	4.55	2
YNL079C	*TPM1*					1.2	2.05	2
YNL091W	*NST1*					1.7	2.55	2
YNL109W	*YNL109W*					1.1	1.9	2
YNL197C	*WHI3*					1.7	3.9	2
YNL231C	*PDR16*					-2.2	-3.8	2
YNL233W	*BNI4*					0.7	1.6	2
YNL235C	*YNL235C*					-1.5	-2.6	2
YNL271C	*BNI1*					1.8	3.5	2
YNL283C	*WSC2*					1.1	1.9	2
YNL294C	*RIM21*					-1.8	2.8	2
YNL300W	*YNL300W*					1.1	1.85	2

YNL322C	*KRE1*					1.1	2.95	2
YNR007C	*ATG3*					0.95	2.1	2
YNR040W	*YNR040W*					0.95	1.3	2
YNR051C	*BRE5*					-1.9	-4	2
YOL001W	*PHO80*					-1.65	-3.3	2
YOL003C	*PFA4*					1	1.6	2
YOL039W	*RPP2A*					1.15	1.6	2
YOL060C	*MAM3*					-1.2	-1.8	2
YOL072W	*THP1*			1.2			5.4	2
YOL089C	*HAL9*					1.2	3.9	2
YOL118C	*YOL118C*				3.5		3.6	2
YOR002W	*ALG6*					1.35	2.2	2
YOR006C	*YOR006C*					1.6	3.05	2
YOR014W	*RTS1*					2.1	6.75	2
YOR052C	*YOR052C*					-0.8	-1.9	2
YOR054C	*VHS3*				3.3		3.8	2
YOR065W	*CYT1*					2	5.3	2
YOR067C	*ALG8*					1	1.6	2
YOR091W	*TMA46*			0.8			2.8	2
YOR106W	*VAM3*		-0.9	-1.9				2
YOR132W	*VPS17*			-1.1			-1.7	2
YOR150W	*MRPL23*			0.9			3.6	2
YOR191W	*RIS1*					-2	-3.2	2
YOR234C	*RPL33B*				3.4		3.9	2
YOR309C	*YOR309C*					1.8	3.25	2
YOR312C	*RPL20B*					1.4	3.4	2
YOR327C	*SNC2*					0.9	2	2
YPL056C	*YPL056C*					-2.45	-3.2	2
YPL061W	*ALD6*					1.4	3.5	2
YPL115C	*BEM3*					0.8	1.95	2
YPL154C	*PEP4*					-0.9	-2.3	2
YPL158C	*YPL158C*					1.4	3.45	2
YPL179W	*PPQ1*					-1.7	-2.5	2
YPL181W	*CTI6*				-1.3	-1.7		2
YPL182C	*YPL182C*				-1.5	-2		2
YPL227C	*ALG5*					1.05	1.95	2
YPL268W	*PLC1*			1.2			4.85	2
YPR043W	*RPL43A*					1.3	3.55	2
YPR053C	*YPR053C*					-1.5	-2.2	2
YPR087W	*VPS69*					1.75	3.15	2
YPR133W-A	*TOM5*					2.4	5.55	2
YPR140W	*TAZ1*				1.4		2.1	2
YPR179C	*HDA3*					-1.3	-4.4	2
YPR189W	*SKI3*					-1.3	-2.95	2

YAL011W	*SWC3*						1.6	1
YAL013W	*DEP1*				-1.2			1
YAL020C	*ATS1*		0.7					1
YAL026C	*DRS2*				-1.2			1
YAL040C	*CLN3*						4.4	1
YAL042W	*ERV46*						-1.9	1
YBL012C	*YBL012C*						-2.1	1
YBL019W	*APN2*				0.9			1
YBL022C	*PIM1*						4.5	1
YBL027W	*RPL19B*						1.6	1
YBL046W	*PSY4*						3.3	1
YBL062W	*YBL062W*						3.05	1
YBL065W	*YBL065W*				4.2			1
YBL080C	*PET112*						1.4	1
YBL087C	*RPL23A*			1.6				1
YBL089W	*AVT5*					-1.5		1
YBL090W	*MRP21*						6.1	1
YBL107C	*YBL107C*	1.4						1
YBR006W	*UGA2*						-3.7	1
YBR020W	*GAL1*						2.2	1
YBR023C	*CHS3*						3.35	1
YBR057C	*MUM2*				1.4			1
YBR069C	*TAT1*						4.35	1
YBR075W					1.8			1
YBR077C	*SLM4*						2.2	1
YBR106W	*PHO88*						4.9	1
YBR107C	*IML3*						2	1
YBR126C	*TPS1*			1.2				1
YBR134W					1.9			1
YBR138C					3.7			1
YBR149W	*ARA1*				1.7			1
YBR156C	*SLI15*	-1.4						1
YBR159W	*IFA38*						3.2	1
YBR162C	*TOS1*					-1.9		1
YBR163W	*DEM1*						3.4	1
YBR216C	*YBP1*						-1.5	1
YBR231C	*SWC5*						2.7	1
YBR238C							2	1
YBR251W	*MRPS5*						4.85	1
YBR255W							-1.9	1
YBR259W					1.1			1
YBR266C	*SLM6*						4.4	1
YBR267W	*REI1*						3.65	1
YBR268W	*MRPL37*						4.9	1

YBR269C	*FMP21*						-2.1	1
YBR281C	*DUG2*						-3.2	1
YBR284W							-3.3	1
YBR286W	*APE3*						-3.8	1
YBR292C							-3.45	1
YBR295W	*PCA1*						-3.1	1
YBR296C	*PHO89*						-1.8	1
YBR297W	*MAL33*						-3.3	1
YCL037C	*SRO9*						2.4	1
YCL057W	*PRD1*						-1.3	1
YCL058C	*FYV5*						2.6	1
YCR017C	*CWH43*						1.8	1
YCR024C	*SLM5*						1.4	1
YCR028C-A	*RIM1*						2.7	1
YCR031C	*RPS14A*						-2.15	1
YCR034W	*FEN1*		1.1					1
YCR036W	*RBK1*					-1.7		1
YCR044C	*PER1*						3.95	1
YCR050C						-2.75		1
YCR059C	*YIH1*						-2.95	1
YCR065W	*HCM1*						2.6	1
YCR066W	*RAD18*						2.2	1
YCR085W							-3	1
YCR086W	*CSM1*					-1.1		1
YCR101C					1.4			1
YDL006W	*PTC1*						3.2	1
YDL032W							2.7	1
YDL035C	*GPR1*						2.4	1
YDL037C	*BSC1*						-2.4	1
YDL044C	*MTF2*						5.1	1
YDL045W-A	*MRP10*						5.3	1
YDL052C	*SLC1*					1.1		1
YDL056W	*MBP1*						4	1
YDL062W							2.6	1
YDL074C	*BRE1*					-1.9		1
YDL081C	*RPP1A*						4.1	1
YDL090C	*RAM1*					-2.1		1
YDL096C	*OPI6*						2	1
YDL115C	*IWR1*						4.1	1
YDL136W	*RPL35B*						2	1
YDL142C	*CRD1*						2.45	1
YDL146W	*LDB17*						2.7	1
YDL151C	*BUD30*						5.6	1
YDL160C	*DHH1*						5.25	1

YDL162C							1.9	1
YDL167C	*NRP1*						-2	1
YDL175C	*AIR2*				0.9			1
YDL188C	*PPH22*				0.9			1
YDL190C	*UFD2*						1.7	1
YDL191W	*RPL35A*						4.9	1
YDL202W	*MRPL11*						4.9	1
YDL215C	*GDH2*				0.7			1
YDR004W	*RAD57*						2.1	1
YDR049W							2.5	1
YDR065W							5.6	1
YDR071C	*PAA1*						-1.75	1
YDR100W	*TVP15*			2				1
YDR101C	*ARX1*					1.1		1
YDR105C	*TMS1*		-1.3					1
YDR108W	*GSG1*						-1.8	1
YDR112W	*IRC2*	-0.8						1
YDR114C							5.8	1
YDR115W							4.6	1
YDR121W	*DPB4*					1.1		1
YDR122W	*KIN1*				4.1			1
YDR124W					1.3			1
YDR126W	*SWF1*						3.2	1
YDR140W	*MTQ2*						3	1
YDR144C	*MKC7*						1.5	1
YDR150W	*NUM1*					-0.9		1
YDR156W	*RPA14*						2.1	1
YDR162C	*NBP2*						4.6	1
YDR173C	*ARG82*						3.75	1
YDR221W	*GTB1*				1.6			1
YDR226W	*ADK1*						3.4	1
YDR237W	*MRPL7*						3.15	1
YDR268W	*MSW1*						5.8	1
YDR276C	*PMP3*						-2.4	1
YDR296W	*MHR1*						7	1
YDR298C	*ATP5*						5.4	1
YDR310C	*SUM1*						-2.2	1
YDR314C	*RAD34*				1			1
YDR332W	*IRC3*						3	1
YDR337W	*MRPS28*						3.1	1
YDR347W	*MRP1*						5.75	1
YDR348C							2.6	1
YDR349C	*YPS7*		1.45					1
YDR359C	*VID21*						6.3	1

YDR360W	*OPI7*						2.4	1
YDR363W	*ESC2*						2.9	1
YDR384C	*ATO3*				2.3			1
YDR388W	*RVS167*					-1.9		1
YDR400W	*URH1*				1.6			1
YDR403W	*DIT1*						1.9	1
YDR405W	*MRP20*						2.7	1
YDR414C	*ERD1*		-1.2					1
YDR440W	*DOT1*				0.7			1
YDR443C	*SSN2*						-1.7	1
YDR462W	*MRPL28*						2.4	1
YDR474C							1.6	1
YDR477W	*SNF1*		-0.9					1
YDR486C	*VPS60*					-1.7		1
YDR525W-A	*SNA2*						-1.5	1
YDR534C	*FIT1*						-1.2	1
YEL007W							2	1
YEL013W	*VAC8*						1.9	1
YEL037C	*RAD23*					-1.3		1
YEL042W	*GDA1*						2.05	1
YEL043W							1.7	1
YEL048C							1.7	1
YEL050C	*RML2*						3.65	1
YEL054C	*RPL12A*						2.3	1
YEL065W	*SIT1*						-2.2	1
YEL067C				-1.9				1
YER007C-A	*TMA20*					-1.5		1
YER020W	*GPA2*						1.7	1
YER040W	*GLN3*						4.15	1
YER050C	*RSM18*						5.2	1
YER077C							4.45	1
YER087W							5.1	1
YER095W	*RAD51*						2.9	1
YER117W	*RPL23B*						2.4	1
YER139C							2.05	1
YER145C	*FTR1*						-3.65	1
YER151C	*UBP3*						-3.8	1
YER153C	*PET122*						1.7	1
YER154W	*OXA1*						2.15	1
YER164W	*CHD1*						-2	1
YER177W	*BMH1*						2.45	1
YFL014W	*HSP12*				1.1			1
YFL016C	*MDJ1*			0.9				1
YFL023W	*BUD27*						4.8	1

YFL036W	*RPO41*						6.4	1
YFL041W	*FET5*				1.9			1
YFR009W	*GCN20*						-2.2	1
YFR010W	*UBP6*					-2.4		1
YFR016C					1.2			1
YFR021W	*ATG18*						-2.6	1
YFR026C					1.3			1
YFR036W	*CDC26*			-1.4				1
YFR040W	*SAP155*						3.25	1
YFR048W	*RMD8*						-3.4	1
YGL003C	*CDH1*						2.2	1
YGL012W	*ERG4*						4	1
YGL013C	*PDR1*						1.9	1
YGL016W	*KAP122*						2.3	1
YGL019W	*CKB1*						3.2	1
YGL025C	*PGD1*					-1.9		1
YGL028C	*SCW11*						2.8	1
YGL046W							3.2	1
YGL064C	*MRH4*						3.15	1
YGL066W	*SGF73*					-1.5		1
YGL076C	*RPL7A*						4.5	1
YGL084C	*GUP1*						4.2	1
YGL129C	*RSM23*						1.6	1
YGL135W	*RPL1B*						3.9	1
YGL143C	*MRF1*						2.8	1
YGL147C	*RPL9A*						3	1
YGL149W		-1.1						1
YGL163C	*RAD54*					-1.8		1
YGL168W	*HUR1*		-1.1					1
YGL218W							5.2	1
YGL220W							2.35	1
YGL246C	*RAI1*						3.8	1
YGL257C	*MNT2*				1.4			1
YGR023W	*MTL1*				1.7			1
YGR049W	*SCM4*				1.2			1
YGR057C	*LST7*						2.2	1
YGR063C	*SPT4*						3.75	1
YGR064W							3.75	1
YGR072W	*UPF3*						-2.3	1
YGR076C	*MRPL25*						2.95	1
YGR078C	*PAC10*						3.5	1
YGR081C	*SLX9*					1.4		1
YGR102C							4.15	1
YGR135W	*PRE9*					-1.2		1

YGR143W	*SKN1*		-0.8					1
YGR150C							2.1	1
YGR152C	*RSR1*						1.4	1
YGR157W	*CHO2*				2.1			1
YGR163W	*GTR2*						2.8	1
YGR165W	*MRPS35*						2.9	1
YGR166W	*KRE11*						4.7	1
YGR171C	*MSM1*						1.9	1
YGR200C	*ELP2*						3	1
YGR209C	*TRX2*						-1.6	1
YGR215W	*RSM27*						5.3	1
YGR219W							4.8	1
YGR220C	*MRPL9*						3.35	1
YGR229C	*SMI1*						3.2	1
YGR234W	*YHB1*						1.5	1
YGR257C	*MTM1*						3.7	1
YGR270W	*YTA7*						3.05	1
YGR295C	*COS6*				1.8			1
YHL013C	*OTU2*						1.65	1
YHL025W	*SNF6*				-3			1
YHL027W	*RIM101*						4.9	1
YHL034C	*SBP1*						1.8	1
YHL041W				-1.5				1
YHL044W							2.85	1
YHR008C	*SOD2*						6.6	1
YHR010W	*RPL27A*						3.85	1
YHR032W					1.1			1
YHR079C-B					1.2			1
YHR081W	*LRP1*						2.5	1
YHR100C							4.8	1
YHR120W	*MSH1*						3.9	1
YHR132C	*ECM14*					-1.5		1
YHR143W	*DSE2*						2.25	1
YHR147C	*MRPL6*						2.6	1
YHR151C					1.6			1
YHR168W	*MTG2*						2.2	1
YHR171W	*ATG7*				1.3			1
YHR200W	*RPN10*					-1.75		1
YHR206W	*SKN7*			1				1
YHR207C	*SET5*						2.3	1
YIL005W	*EPS1*						-2.55	1
YIL017C	*VID28*						3.8	1
YIL023C	*YKE4*						-1.6	1
YIL060W							2.95	1

YIL067C							3.35	1
YIL093C	*RSM25*						3.65	1
YIL112W	*HOS4*						1.9	1
YIL140W	*AXL2*						1.6	1
YIL141W							1.9	1
YIR017C	*MET28*				2.3			1
YIR026C	*YVH1*						3.65	1
YJL022W							3.6	1
YJL023C	*PET130*						3	1
YJL051W	*IRC8*						2.1	1
YJL063C	*MRPL8*						3.25	1
YJL092W	*HPR5*					1.3		1
YJL094C	*KHA1*						-2.8	1
YJL095W	*BCK1*			-1.4				1
YJL098W	*SAP185*					-1.1		1
YJL102W	*MEF2*						6.25	1
YJL121C	*RPE1*						-2.8	1
YJL124C	*LSM1*					-1.6		1
YJL130C	*URA2*			1				1
YJL150W							-2	1
YJL166W	*QCR8*			1.7				1
YJL190C	*RPS22A*						-1.5	1
YJR014W	*TMA22*					-1.45		1
YJR040W	*GEF1*						-2.7	1
YJR049C	*UTR1*						2.7	1
YJR055W	*HIT1*						4.5	1
YJR082C	*EAF6*					0.7		1
YJR113C	*RSM7*						4.05	1
YJR118C	*ILM1*						5.1	1
YJR121W	*ATP2*					-1.4		1
YJR126C	*VPS70*						-2.1	1
YJR144W	*MGM101*						1.5	1
YJR154W					1.9			1
YKL003C	*MRP17*						6.45	1
YKL007W	*CAP1*						1.9	1
YKL023W							-2.95	1
YKL025C	*PAN3*					-1		1
YKL053C-A	*MDM35*						2.45	1
YKL053W							-2.6	1
YKL054C	*DEF1*						7.65	1
YKL056C	*TMA19*					1.3		1
YKL057C	*NUP120*						5.2	1
YKL077W						-1.2		1
YKL080W	*VMA5*			-1.7				1

YKL101W	*HSL1*						1.3	1
YKL106W	*AAT1*				0.6			1
YKL110C	*KTI12*						2.5	1
YKL131W					0.9			1
YKL138C	*MRPL31*						5.3	1
YKL147C					1.6			1
YKL155C	*RSM22*						2.5	1
YKL169C							4.9	1
YKL170W	*MRPL38*						5.8	1
YKL174C	*TPO5*				2.3			1
YKL176C	*LST4*						2.2	1
YKL208W	*CBT1*						1.5	1
YKL213C	*DOA1*					-2.05		1
YKR007W	*MEH1*						1.6	1
YKR010C	*TOF2*					-0.8		1
YKR019C	*IRS4*					-1.25		1
YKR020W	*VPS51*					-2.25		1
YKR024C	*DBP7*						3.25	1
YKR028W	*SAP190*					1.3		1
YKR031C	*SPO14*						-1.8	1
YKR061W	*KTR2*				1.7			1
YKR073C						1.05		1
YKR077W					1.2			1
YKR085C	*MRPL20*						4.65	1
YLL006W	*MMM1*						3.7	1
YLL033W	*IRC19*						4.3	1
YLL038C	*ENT4*						2	1
YLL039C	*UBI4*						-2.4	1
YLL043W	*FPS1*		1.3					1
YLR015W	*BRE2*					-1.95		1
YLR024C	*UBR2*						1.6	1
YLR053C					0.7			1
YLR061W	*RPL22A*						4.5	1
YLR062C	*BUD28*						4.5	1
YLR065C							-1.5	1
YLR067C	*PET309*						2.55	1
YLR068W	*FYV7*					1.9		1
YLR069C	*MEF1*						3.1	1
YLR079W	*SIC1*						3.2	1
YLR091W							5.5	1
YLR110C	*CCW12*					1.6		1
YLR176C	*RFX1*					-1.3		1
YLR177W					1.5			1
YLR178C	*TFS1*				1.4			1

YLR193C	*UPS1*						3.7	1
YLR200W	*YKE2*						2.6	1
YLR205C	*HMX1*						-3	1
YLR220W	*CCC1*				1.9			1
YLR232W						-1.7		1
YLR270W	*DCS1*						2.75	1
YLR286C	*CTS1*						2.7	1
YLR295C	*ATP14*						5.7	1
YLR304C	*ACO1*						3.7	1
YLR312W-A	*MRPL15*						2.1	1
YLR330W	*CHS5*						3.9	1
YLR335W	*NUP2*						-1.9	1
YLR341W	*SPO77*				1.1			1
YLR349W					1.6			1
YLR357W	*RSC2*						4.7	1
YLR358C							4.15	1
YLR361C	*DCR2*						-1.5	1
YLR369W	*SSQ1*						3.05	1
YLR382C	*NAM2*						4.1	1
YLR384C	*IKI3*						2.25	1
YLR386W	*VAC14*					-2.2		1
YLR402W							3.75	1
YLR407W						-1.2		1
YLR412W							2.4	1
YLR418C	*CDC73*						4.45	1
YLR426W							2.2	1
YLR436C	*ECM30*						1.9	1
YLR439W	*MRPL4*						7.3	1
YLR448W	*RPL6B*						2.8	1
YLR451W	*LEU3*					-1		1
YML001W	*YPT7*			-1.1				1
YML007W	*YAP1*					-1.9		1
YML008C	*ERG6*	-0.9						1
YML010W-A				1.2				1
YML013W	*SEL1*					-1.6		1
YML017W	*PSP2*						-2	1
YML019W	*OST6*						1.5	1
YML021C	*UNG1*						-2.8	1
YML028W	*TSA1*						-2.8	1
YML061C	*PIF1*						4.5	1
YML081C-A	*ATP18*					-1.3		1
YML094W	*GIM5*						3.5	1
YML103C	*NUP188*						-3.2	1
YML116W	*ATR1*						-1.3	1

YML121W	*GTR1*						2	1
YML124C	*TUB3*						2.35	1
YMR053C	*STB2*					0.9		1
YMR057C							-2.7	1
YMR060C	*SAM37*						6.35	1
YMR063W	*RIM9*						3.35	1
YMR066W	*SOV1*						6.05	1
YMR073C	*IRC21*						2.5	1
YMR075W	*RCO1*						3.2	1
YMR077C	*VPS20*				-1.7			1
YMR080C	*NAM7*						-3.1	1
YMR089C	*YTA12*						2.55	1
YMR097C	*MTG1*						5.85	1
YMR098C							3.4	1
YMR100W	*MUB1*						2.25	1
YMR102C						-1.05		1
YMR110C	*HFD1*						-2.3	1
YMR114C					2.9			1
YMR116C	*ASC1*					-1.8		1
YMR119W-A					3.5			1
YMR121C	*RPL15B*						2.3	1
YMR123W	*PKR1*		-1.2					1
YMR138W	*CIN4*						1.8	1
YMR139W	*RIM11*						-1.6	1
YMR142C	*RPL13B*						3.1	1
YMR152W	*YIM1*					0.8		1
YMR154C	*RIM13*						2.5	1
YMR158W	*MRPS8*						1.8	1
YMR179W	*SPT21*					1.4		1
YMR188C	*MRPS17*						2.35	1
YMR193W	*MRPL24*						4.5	1
YMR194W	*RPL36A*						1.7	1
YMR219W	*ESC1*						2.2	1
YMR238W	*DFG5*					0.8		1
YMR264W	*CUE1*					0.8		1
YMR287C	*DSS1*						1.95	1
YMR293C							5.15	1
YMR307W	*GAS1*						4.95	1
YMR310C							-1.7	1
YMR311C	*GLC8*				1			1
YMR315W							-1.4	1
YNL005C	*MRP7*						2.7	1
YNL025C	*SSN8*						2.65	1
YNL027W	*CRZ1*					-1.1		1

YNL055C	*POR1*						5.6	1
YNL066W	*SUN4*						2.2	1
YNL067W	*RPL9B*						2.9	1
YNL077W	*APJ1*						-3.3	1
YNL105W					1			1
YNL107W	*YAF9*						4.9	1
YNL115C							-2.6	1
YNL136W	*EAF7*						3.4	1
YNL148C	*ALF1*						2.8	1
YNL170W							2.2	1
YNL175C	*NOP13*						-3.8	1
YNL177C	*MRPL22*						2.75	1
YNL179C							-2.6	1
YNL183C	*NPR1*					1		1
YNL184C							3.05	1
YNL196C							-3.3	1
YNL203C							-2.2	1
YNL205C							-2.6	1
YNL211C							-2.95	1
YNL215W	*IES2*					-1.8		1
YNL225C	*CNM67*					1.5		1
YNL226W							3.15	1
YNL227C	*JJJ1*						3.5	1
YNL228W							3.2	1
YNL246W	*VPS75*						5.1	1
YNL248C	*RPA49*						5.6	1
YNL252C	*MRPL17*						2.3	1
YNL284C	*MRPL10*						3.6	1
YNL291C	*MID1*						-1.7	1
YNL293W	*MSB3*					-0.9		1
YNL299W	*TRF5*			-1				1
YNL314W	*DAL82*					0.8		1
YNL315C	*ATP11*					-2.9		1
YNL324W						-2.7		1
YNL327W	*EGT2*						1.7	1
YNR036C							1.85	1
YNR037C	*RSM19*						2.4	1
YNR048W							-2	1
YOL002C	*IZH2*						-2.2	1
YOL004W	*SIN3*						-3.15	1
YOL009C	*MDM12*						3.25	1
YOL012C	*HTZ1*						2.5	1
YOL023W	*IFM1*						4.3	1
YOL041C	*NOP12*						2.55	1

YOL064C	*MET22*					1.2		1
YOL095C	*HMI1*						1.95	1
YOL115W	*PAP2*						3.3	1
YOL116W	*MSN1*				2.2			1
YOL121C	*RPS19A*						2.9	1
YOL129W	*VPS68*						-1.9	1
YOR001W	*RRP6*						3.4	1
YOR005C	*DNL4*						-1.3	1
YOR030W	*DFG16*						3.25	1
YOR035C	*SHE4*					2		1
YOR039W	*CKB2*						2.75	1
YOR045W	*TOM6*						1.7	1
YOR051C							2.05	1
YOR061W	*CKA2*						1.7	1
YOR076C	*SKI7*						-2.3	1
YOR078W	*BUD21*					1.9		1
YOR085W	*OST3*					1.3		1
YOR092W	*ECM3*				2			1
YOR096W	*RPS7A*						2.9	1
YOR140W	*SFL1*					-0.9		1
YOR186W					1.2			1
YOR189W	*IES4*					-1.2		1
YOR201C	*MRM1*						4	1
YOR205C	*FMP38*						4.6	1
YOR211C	*MGM1*						3	1
YOR251C					1			1
YOR266W	*PNT1*				1.3			1
YOR267C	*HRK1*						-2.4	1
YOR275C	*RIM20*						3.2	1
YOR276W	*CAF20*				2			1
YOR297C	*TIM18*				-1.2			1
YOR304W	*ISW2*					-1.3		1
YOR317W	*FAA1*						-1.4	1
YOR330C	*MIP1*						1.8	1
YOR355W	*GDS1*						2.5	1
YOR364W						-2.1		1
YPL005W	*AEP3*						4.1	1
YPL008W	*CHL1*						3.25	1
YPL013C	*MRPS16*						2.65	1
YPL029W	*SUV3*						2.3	1
YPL040C	*ISM1*						2.25	1
YPL060W	*LPE10*			1.4				1
YPL062W							3.05	1
YPL097W	*MSY1*						3.1	1

YPL101W	*ELP4*						2.4	1
YPL102C							2.2	1
YPL104W	*MSD1*						5.2	1
YPL106C	*SSE1*						3.95	1
YPL110C	*GDE1*				0.9			1
YPL118W	*MRP51*						4.05	1
YPL125W	*KAP120*						5.2	1
YPL135W	*ISU1*			0.8				1
YPL138C	*SPP1*						-2.7	1
YPL139C	*UME1*					-1.2		1
YPL170W	*DAP1*					-2		1
YPL173W	*MRPL40*						3.2	1
YPL180W	*TCO89*						3.3	1
YPL183W-A							3.3	1
YPL213W	*LEA1*						2.7	1
YPL253C	*VIK1*						2.1	1
YPL260W							2.2	1
YPL261C							1.7	1
YPL270W	*MDL2*						1.8	1
YPL271W	*ATP15*			1.8				1
YPR012W					1.8			1
YPR014C					1.6			1
YPR023C	*EAF3*						1.95	1
YPR024W	*YME1*					-2.2		1
YPR028W	*YOP1*				0.9			1
YPR038W	*IRC16*						-1.9	1
YPR047W	*MSF1*						3.2	1
YPR099C							1.85	1
YPR100W	*MRPL51*						1.8	1
YPR101W	*SNT309*						5.9	1
YPR114W						-1.4		1
YPR116W				2				1
YPR120C	*CLB5*						2.65	1
YPR122W	*AXL1*				1.2			1
YPR166C	*MRP2*						2.7	1

Appendix 2: Lead sensitive and resistant genes identified

ORF	Standard Name	5 generations			15 generations			Number of Significant
		25% IC20	50% IC20	IC20	25% IC20	50% IC20	IC20	
		0.25 mM	0.5 mM	1 mM	0.25 mM	0.5 mM	1 mM	
YCR050C			-1	-1.65	-3	-3.5	-2.75	5
YDL226C	*GCS1*		-1.1	-1.6	-4.9	-3.9	-4.5	5
YDR186C			-0.7	-1.45	-3.1	-2.6	-2.9	5
YJL204C	*RCY1*		-1.1	-1.45	-4.5	-5.9	-4	5
YML013W	*SEL1*		-1	-1.1	-5	-4	-3.6	5
YPL178W	*CBC2*		-1.5	-1.1	-4.2	-3.1	-3.9	5
YCR049C				-1	-2	-2.35	-3.2	4
YCR068W	*ATG15*			-0.8	-2.6	-2.15	-3.25	4
YCR073W-A	*SOL2*		-1.4		2.5	3.2	3.3	4
YDL192W	*ARF1*			-1.4	-3.4	-2.3	-3.8	4
YDL202W	*MRPL11*			1.2	2.4	2.6	4.55	4
YDL223C	*HBT1*		-1.2		2.1	2.15	3	4
YDR126W	*SWF1*			-1.6	-3	-2.9	-2.6	4
YDR153C	*ENT5*		-1.6		3.6	4	4.2	4
YDR414C	*ERD1*			1.3	4	3.55	4.25	4
YDR455C				-1.25	-2.3	-2.05	-3.55	4
YER050C	*RSM18*			0.9	3	3	4.65	4
YER092W	*IES5*			0.8	1.4	1.9	2.4	4
YGL012W	*ERG4*	-1.2	-1.2	-1.7	-3.9			4
YGL148W	*ARO2*			-0.9	-4.9	-3.75	-3	4
YGR220C	*MRPL9*			0.7	1.9	1.8	2.75	4
YIL018W	*RPL2B*			0.85	2.6	2.1	4.3	4
YIL093C	*RSM25*			1.1	2.15	2.35	3.65	4
YJL053W	*PEP8*			-1.5	-2.7	-2.7	-3.1	4
YJL154C	*VPS35*			-1.5	-2.95	-2.45	-2.65	4
YKL138C	*MRPL31*			1.2	2.2	2.2	3.6	4
YLL006W	*MMM1*			1.3	1.7	2.95	4.6	4
YLR025W	*SNF7*	-0.7		-0.7	-2.3	-2.45		4
YLR369W	*SSQ1*			0.8	1.2	2.1	2.55	4
YLR417W	*VPS36*	-0.9	-0.8	-1.35	-1.7			4
YMR058W	*FET3*			1	1.6	1.9	1.9	4
YMR188C	*MRPS17*			0.8	1.35	1.45	2.3	4
YNL101W	*AVT4*		-1.7		2.7	2.6	3.1	4
YNL323W	*LEM3*	-1	-1	-1.5	-3.1			4
YOL018C	*TLG2*			-1.6	-3.1	-3.4	-3.4	4
YOL089C	*HAL9*			-1.65	-4.7	-4.1	-2.1	4
YOR068C	*VAM10*			-0.8	-2.4	-2.35	-3.5	4
YOR123C	*LEO1*			0.8	1.95	2.05	3.05	4
YOR132W	*VPS17*			-0.9	-1.8	-1.6	-2.4	4

YOR133W	*EFT1*		-1.2		2.3	3.7	3.5	4
YOR246C				-1.05	-2.2	-2.55	-2.65	4
YPL005W	*AEP3*			1.2	2.9	2.6	4.45	4
YBL038W	*MRPL16*				2.8	3.6	5	3
YBR006W	*UGA2*			-0.6	-1.8		-2.1	3
YBR044C	*TCM62*				2.7	2.6	3.1	3
YBR069C	*TAT1*				2.5	3.25	4.1	3
YBR103W	*SIF2*				1.9	1.8	2.8	3
YBR171W	*SEC66*				1.7	2.2	2.9	3
YBR213W	*MET8*				2.2	2.6	2.9	3
YBR215W	*HPC2*				-1.6	-2	-2.2	3
YBR238C					1.7	1.7	2.3	3
YBR251W	*MRPS5*				2.2	2.2	3.3	3
YBR284W					-1.2	-1.6	-2.1	3
YBR286W	*APE3*				-1.1	-1.2	-2.35	3
YBR291C	*CTP1*				-3.8	-3.5	-3.2	3
YBR292C					-1.7	-1.9	-2.35	3
YBR298C	*MAL31*				-1.9	-3.4	-3.5	3
YBR300C					-1.8	-1.9	-2.85	3
YCL001W-A					-2.5	-3.15	-2.95	3
YCL010C	*SGF29*			-1.2	-3.2	-2.5		3
YCR026C	*NPP1*				-3.8	-3.3	-3.1	3
YCR036W	*RBK1*				-2.25	-2.55	-3.4	3
YCR079W	*PTC6*				-2.3	-2.05	-2.45	3
YCR087C-A	*LUG1*				-2.1	-1.65	-2.15	3
YCR087W					-1.5	-2.2	-2.4	3
YDL056W	*MBP1*				2.25	2.4	3.85	3
YDL133W					-3.9	-3.05	-3.5	3
YDL198C	*GGC1*				1.8	2.2	2.9	3
YDR065W					2.4	2.7	4.5	3
YDR073W	*SNF11*				-1.4	-2	-3.1	3
YDR115W					2.15	1.95	3.2	3
YDR135C	*YCF1*				-3.9	-3.6	-5.6	3
YDR136C	*VPS61*			-1.2	-2.5		-3.1	3
YDR175C	*RSM24*				3.6	4.2	6.05	3
YDR337W	*MRPS28*				2.15	2.2	3.6	3
YDR347W	*MRP1*				1.9	2.2	4	3
YDR363W-A	*SEM1*				2.6	3	3.65	3
YDR377W	*ATP17*				2.1	2.8	3.45	3
YDR392W	*SPT3*				1.8	2.3	3.2	3
YDR458C	*HEH2*				2.7	3	3	3
YDR484W	*VPS52*			-1.3	-3.1		-2.7	3
YEL003W	*GIM4*				1.5	2.6	2.55	3
YEL008W					1.6	1.5	1.6	3

YEL050C	*RML2*				2.85	3.2	4.15	3
YER077C					2.5	2.4	3.95	3
YER084W					-1.7	-1.8	-1.7	3
YER087W					2.5	2.5	4.25	3
YER122C	*GLO3*				1.9	3.05	4.15	3
YFL013C	*IES1*				1.9	2.1	2.5	3
YFL013W-A					2.4	2.7	2.5	3
YFR018C					1.2	3.7	3.4	3
YGL064C	*MRH4*				2	2.5	3.75	3
YGL133W	*ITC1*				-2.1	-2.2	-3	3
YGL179C	*TOS3*				3.6	4.4	4	3
YGL253W	*HXK2*			-1.2	-1.6	-1.6		3
YGR076C	*MRPL25*				2.5	2.5	3.3	3
YGR078C	*PAC10*				3.1	3.6	3.7	3
YGR092W	*DBF2*				2.8	2.75	3.85	3
YGR102C					2.3	2.2	3.5	3
YGR150C					2	1.9	2.6	3
YGR257C	*MTM1*				1.6	1.7	2.9	3
YGR289C	*MAL11*				-2.1	-2.3	-2.2	3
YHR011W	*DIA4*				2.8	2.6	4.45	3
YHR034C	*PIH1*				2.4	3.3	4.3	3
YHR037W	*PUT2*				2.5	3.2	2.9	3
YHR111W	*UBA4*				1.7	2.05	2.45	3
YHR159W					2.3	2.6	3.4	3
YHR193C	*EGD2*				1.3	1.8	2.3	3
YHR200W	*RPN10*				-1.9	-2.7	-2.8	3
YIL015C-A					2.2	3	4.1	3
YIL060W					2.3	2.15	3.25	3
YIL139C	*REV7*		-1.3		2.2	2.3		3
YIL148W	*RPL40A*				-2.3	-2.8	-2.9	3
YIL154C	*IMP2'*				-3.4	-4.95	-3.05	3
YIR023W	*DAL81*				2.5	2.55	3.25	3
YJL052W	*TDH1*				2.4	2.3	2.8	3
YJL102W	*MEF2*				1.9	3	4.3	3
YJR043C	*POL32*				-2.85	-3.05	-3.9	3
YJR074W	*MOG1*				-2.65	-2.4	-2.7	3
YJR140C	*HIR3*				-1.75	-1.6	-2.1	3
YKL077W					2.1	2	2.5	3
YKL113C	*RAD27*				-3	-2.6	-2.7	3
YKL174C	*TPO5*		-1.3			5.1	4.6	3
YLR023C	*IZH3*				1.9	2.3	2.5	3
YLR047C	*FRE8*				-1.6	-2.25	-2.5	3
YLR055C	*SPT8*				2.55	2.95	4.15	3
YLR091W					2.35	2.8	3.8	3

YLR121C	*YPS3*				1.8	2.2	2.3	3
YLR131C	*ACE2*				2.2	2.25	2.8	3
YLR133W	*CKI1*				2.7	2.8	3.3	3
YLR149C					2.8	2.7	4.3	3
YLR174W	*IDP2*				1.2	1.3	1.4	3
YLR200W	*YKE2*				2.2	3.1	3.85	3
YLR304C	*ACO1*			1.6		2.3	4	3
YLR315W	*NKP2*				2.7	2.6	3.6	3
YLR382C	*NAM2*				2.1	2.9	3.85	3
YLR391W				-1.2	-2	-2.6		3
YLR448W	*RPL6B*				2.3	2.75	2.2	3
YLR450W	*HMG2*				2.3	2.6	3.2	3
YML010C-B					2.1	2.2	2.75	3
YML061C	*PIF1*				2	2.9	4	3
YML095C-A					1.8	2.35	2.5	3
YMR016C	*SOK2*				1.4	1.5	1.4	3
YMR021C	*MAC1*	-1.2	-1.5	-1.8				3
YMR022W	*QRI8*				-1.4	-3.3	-2.7	3
YMR057C					1.3	1.2	1.9	3
YMR097C	*MTG1*				2.8	2.8	4	3
YMR184W	*ADD37*		-1.6		1.8	1.9		3
YMR193W	*MRPL24*				2.65	2.9	4.6	3
YMR244C-A			-1.1			2.2	2.7	3
YMR264W	*CUE1*				-1.55	-3.1	-2.85	3
YMR267W	*PPA2*				3.3	3.8	5.15	3
YMR272C	*SCS7*				1.6	2.55	3.6	3
YMR280C	*CAT8*				2.6	2.7	2.8	3
YMR286W	*MRPL33*				2.5	2.2	2.9	3
YMR293C					1.6	2.4	3.5	3
YMR319C	*FET4*			-1.25	-4.85	-3.8		3
YNL177C	*MRPL22*			0.9		1.3	2	3
YNL179C					-3	-1.45	-2.35	3
YNL206C	*RTT106*				-2.3	-2.85	-2.9	3
YNL236W	*SIN4*				2	2.7	3.5	3
YNL252C	*MRPL17*				1.8	1.5	2.3	3
YNL284C	*MRPL10*				1.9	3	4.1	3
YNL294C	*RIM21*		-0.7	-1.3		-1.4		3
YNR024W					1.3	1.9	1.8	3
YNR051C	*BRE5*				-1.75	-1.6	-2.7	3
YOL023W	*IFM1*				2.4	2.4	3.6	3
YOR035C	*SHE4*				2.5	3.5	3.95	3
YOR065W	*CYT1*				2.05	2.4	3.7	3
YOR070C	*GYP1*				-2.2	-3.1	-3.5	3
YOR201C	*MRM1*				2.5	2.4	3.6	3

YOR205C	*FMP38*				1.95	2.2	3.2	3
YOR304W	*ISW2*				-1.9	-2.2	-2.4	3
YOR312C	*RPL20B*			1.1		3	3.6	3
YOR314W					1.9	2.1	2.1	3
YPL035C					3.1	3.6	3.8	3
YPL097W	*MSY1*				2	1.6	2.35	3
YPL118W	*MRP51*				2.95	2.9	4.6	3
YPL259C	*APM1*				-1.1	-1.1	-1.8	3
YPR065W	*ROX1*				1.45	1.2	1.7	3
YPR079W	*MRL1*				-0.8	-1.1	-1.3	3
YPR173C	*VPS4*			-1.3	-2.9	-2.7		3
YAL002W	*VPS8*			-1.5	-2.7			2
YAL009W	*SPO7*				-2.5	-2.4		2
YAL026C	*DRS2*				-2.5	-2.4		2
YBL013W	*FMT1*					6	6.6	2
YBL046W	*PSY4*				-1.9	-2.9		2
YBL061C	*SKT5*					3	3.6	2
YBL062W					2.3	2.9		2
YBL065W						6.6	6.7	2
YBL082C	*ALG3*					1.3	1.3	2
YBL090W	*MRP21*					3	4	2
YBR026C	*ETR1*					2.2	3	2
YBR037C	*SCO1*					2.4	3	2
YBR058C	*UBP14*					1.7	1.7	2
YBR084C-A	*RPL19A*					2.4	2.4	2
YBR134W						2.4	3	2
YBR138C						4.1	4.5	2
YBR149W	*ARA1*					2.4	2.4	2
YBR156C	*SLI15*					2.9	3	2
YBR163W	*DEM1*				2		2.9	2
YBR170C	*NPL4*					3.9	3.1	2
YBR187W	*GDT1*				-2.2		-1.9	2
YBR268W	*MRPL37*					2.3	4.2	2
YBR281C	*DUG2*				-1		-2.3	2
YBR290W	*BSD2*			-0.8	-1.1			2
YBR296C	*PHO89*				-1.95		-1.7	2
YCL008C	*STP22*			-1.55	-2.3			2
YCL030C	*HIS4*					2.7	2.6	2
YCR006C						2.2	2.2	2
YCR007C						2.65	4.3	2
YCR034W	*FEN1*				-2.5	-2.4		2
YCR063W	*BUD31*					3.5	4.9	2
YCR094W	*CDC50*			-2.1			-3.8	2
YDL010W						4.5	4.7	2

YDL032W				1			2.2	2
YDL044C	*MTF2*				2.5		3.4	2
YDL061C	*RPS29B*					-1.8	-2.7	2
YDL070W	*BDF2*					2.1	2.3	2
YDL082W	*RPL13A*					2.7	2.9	2
YDR072C	*IPT1*				0.9	1.5		2
YDR105C	*TMS1*		-1.4		2			2
YDR114C						2.9	3.4	2
YDR122W	*KIN1*					5.3	4.8	2
YDR237W	*MRPL7*					3.1	4.05	2
YDR268W	*MSW1*					3.3	4.7	2
YDR291W	*HRQ1*					4.6	4.7	2
YDR322W	*MRPL35*					4.2	5.2	2
YDR336W						2.3	2.2	2
YDR359C	*VID21*			0.9			4	2
YDR384C	*ATO3*					2.9	2.8	2
YDR385W	*EFT2*					2.2	2.6	2
YDR388W	*RVS167*					3.1	4.4	2
YDR391C						1.9	2.1	2
YDR400W	*URH1*					1.8	1.7	2
YDR405W	*MRP20*			0.9			2.3	2
YDR415C						1.2	1.1	2
YDR450W	*RPS18A*					2.5	3.4	2
YDR495C	*VPS3*			-1.7	-2.3			2
YDR507C	*GIN4*				1.2		2.9	2
YEL012W	*UBC8*					3.7	3.6	2
YEL028W						5.1	5.3	2
YER007C-A	*TMA20*				-1.7		-2.3	2
YER017C	*AFG3*					2.3	3.25	2
YER020W	*GPA2*			-1	-1.6			2
YER072W	*VTC1*			-1.1			-2.35	2
YER167W	*BCK2*				1.1		1.4	2
YER169W	*RPH1*				2.5	3		2
YER177W	*BMH1*			-1.3	-1.2			2
YFL023W	*BUD27*			-1.1	-3.2			2
YFL036W	*RPO41*					3.1	4.5	2
YFR008W	*FAR7*				-1.4		-1.6	2
YGL071W	*AFT1*		-0.9	-1.75				2
YGL215W	*CLG1*					2	2.2	2
YGL220W					2.2		2.4	2
YGR063C	*SPT4*					2.5	3.3	2
YGR064W						2.7	3.2	2
YGR070W	*ROM1*					3	2.9	2
YGR130C					-2.2	-1.4		2

YGR162W	*TIF4631*				2.1		2.85	2
YGR183C	*QCR9*				2	2		2
YGR215W	*RSM27*				2.5		3.85	2
YGR263C	*SAY1*				2.7	2.4		2
YGR282C	*BGL2*					2.3	2.4	2
YHL025W	*SNF6*		1.1	1.2				2
YHR012W	*VPS29*		-1.1	-1.3				2
YHR029C	*YHI9*					3.5	3.4	2
YHR030C	*SLT2*				-3.5	-1.9		2
YHR038W	*RRF1*				3		3.3	2
YHR073W	*OSH3*				-1.5	-1.7		2
YHR120W	*MSH1*					2.6	3.9	2
YHR153C	*SPO16*					2.4	2.3	2
YHR178W	*STB5*					-2.7	-2.9	2
YHR206W	*SKN7*			1.1			1.5	2
YIL030C	*SSM4*					-1.7	-2.3	2
YIL035C	*CKA1*					1.8	2.5	2
YIL067C					-2.3	-1.7		2
YIL107C	*PFK26*					1.4	1.7	2
YIL110W	*MNI1*					2.3	3.2	2
YIL112W	*HOS4*					1.5	2.15	2
YIR028W	*DAL4*					4.9	4.1	2
YJL046W						3.4	3.4	2
YJL094C	*KHA1*				-1.3		-1.4	2
YJL101C	*GSH1*				-1.75		-1.7	2
YJL128C	*PBS2*					1.5	2.1	2
YJL179W	*PFD1*					1.6	1.7	2
YJL183W	*MNN11*				2.7	2.8		2
YJL197W	*UBP12*				-1.4		-2.2	2
YJL214W	*HXT8*					4.6	4	2
YJR040W	*GEF1*				-1.6		-2.85	2
YJR102C	*VPS25*			-1.1	-2.2			2
YJR117W	*STE24*					-1.7	-2.65	2
YKL023W					-1.35		-2.15	2
YKL133C						3.4	3.6	2
YKL135C	*APL2*				-1.5		-2.4	2
YKL136W					-1.7		-2.65	2
YKL170W	*MRPL38*			1.1			2.9	2
YKL221W	*MCH2*					2.6	2.7	2
YKR014C	*YPT52*			-0.8	-1.2			2
YKR020W	*VPS51*				-2.65	-2.3		2
YKR031C	*SPO14*					-1.5	-2.8	2
YKR041W						3.8	3.5	2
YKR061W	*KTR2*					1.6	1.4	2

YKR078W			-1		1.3			2
YKR082W	*NUP133*				2.1		2.7	2
YKR085C	*MRPL20*				1.7		2.6	2
YLL023C						3.5	3.2	2
YLL027W	*ISA1*			1.35			2.2	2
YLL033W	*IRC19*				3.1		3.6	2
YLL038C	*ENT4*					-1	-1.3	2
YLL043W	*FPS1*		1.1	1.45				2
YLL057C	*JLP1*					3.1	3.2	2
YLR006C	*SSK1*					1.1	1.5	2
YLR036C						2.3	2.4	2
YLR052W	*IES3*					2.5	3.1	2
YLR068W	*FYV7*					2.4	2.4	2
YLR087C	*CSF1*					-2.2	-2.5	2
YLR093C	*NYV1*					2.1	2.3	2
YLR178C	*TFS1*					1.9	2	2
YLR188W	*MDL1*					2.7	2.8	2
YLR203C	*MSS51*					3.8	4.1	2
YLR216C	*CPR6*				1.1		1.1	2
YLR228C	*ECM22*					-1.7	-2.1	2
YLR286C	*CTS1*					1.9	2.1	2
YLR334C						1.3	1.5	2
YLR349W						1.5	1.7	2
YLR370C	*ARC18*				2.3		2.4	2
YLR380W	*CSR1*					-1.4	-2	2
YLR402W						3	4.3	2
YLR425W	*TUS1*					2.1	2.7	2
YLR441C	*RPS1A*					2.2	2.8	2
YML009C	*MRPL39*					5	5.2	2
YML010W-A					1.8		2.5	2
YML048W-A					2	1.6		2
YML070W	*DAK1*					3.6	3.4	2
YML097C	*VPS9*			-1.95	-2.6			2
YML119W						2.8	2.6	2
YMR052C-A				-1.65	-2.55			2
YMR052W	*FAR3*			-0.85			-2.1	2
YMR072W	*ABF2*				2.1		2.9	2
YMR073C	*IRC21*				1.9		3.3	2
YMR089C	*YTA12*				2		2.45	2
YMR098C						3.1	4.25	2
YMR116C	*ASC1*			-1.7		-2.2		2
YMR119W-A						2.8	2.5	2
YMR166C			-1.9			2		2
YMR170C	*ALD2*				-1.1		-0.9	2

YMR204C	*INP1*					2.6	2.6	2
YMR228W	*MTF1*					2.2	1.7	2
YMR262W			-1.3			1.6		2
YMR284W	*YKU70*					2.2	2.6	2
YMR299C	*DYN3*					2	2.1	2
YMR304W	*UBP15*					3.3	3.8	2
YMR312W	*ELP6*					1.8	2.95	2
YNL016W	*PUB1*					1.7	2.2	2
YNL047C	*SLM2*					3.6	3.7	2
YNL070W	*TOM7*			-1.4	-2.85			2
YNL077W	*APJ1*					-1.9	-2.4	2
YNL105W						1.35	1.55	2
YNL115C					-1.3		-1.85	2
YNL119W	*NCS2*					3.4	3.6	2
YNL120C						3	3.55	2
YNL136W	*EAF7*					2.2	2.7	2
YNL140C						4.6	4.4	2
YNL205C					-1.6		-1.7	2
YNL211C					-1.7		-1.7	2
YNL264C	*PDR17*		-1.3				-3.2	2
YNL305C						3.8	3.7	2
YOL002C	*IZH2*					-1.2	-2.25	2
YOL027C	*MDM38*					2	2.7	2
YOL118C						4	3.8	2
YOR021C					1.8	2.1		2
YOR054C	*VHS3*					3.5	3.6	2
YOR061W	*CKA2*				-1.3	-1.5		2
YOR089C	*VPS21*			-1.6	-1.95			2
YOR092W	*ECM3*					4.1	4.2	2
YOR137C	*SIA1*				1.6	1.5		2
YOR164C						-2.2	-3.2	2
YOR352W						2.6	2.3	2
YOR364W			-1.5		2.3			2
YPL018W	*CTF19*		-1.2	-1.4				2
YPL104W	*MSD1*				2		4	2
YPL140C	*MKK2*				1.9	1.4		2
YPL157W	*TGS1*					3.4	4.1	2
YPL173W	*MRPL40*					2.3	3.3	2
YPR047W	*MSF1*				2		3.5	2
YPR064W					1.1		1.1	2
YPR087W	*VPS69*				-2.3	-3.1		2
YPR099C				0.8			1.4	2
YPR101W	*SNT309*					3.6	4.2	2
YPR128C	*ANT1*					2	2.4	2

YPR140W	*TAZ1*					2.9	2.7	2
YPR196W						1.8	1.8	2
YBL007C	*SLA1*						3.15	1
YBL010C			-1.2					1
YBL019W	*APN2*					1.3		1
YBL022C	*PIM1*				-3.7			1
YBL051C	*PIN4*	0.8						1
YBL067C	*UBP13*						-2.9	1
YBL072C	*RPS8A*				-1.7			1
YBL079W	*NUP170*						1.7	1
YBL081W						2		1
YBL083C				-1				1
YBR035C	*PDX3*					-2.8		1
YBR056W					1.4			1
YBR113W					2			1
YBR114W	*RAD16*				2			1
YBR129C	*OPY1*					1.4		1
YBR131W	*CCZ1*			-1.1				1
YBR162C	*TOS1*						1.9	1
YBR164C	*ARL1*				-1.6			1
YBR173C	*UMP1*					1.7		1
YBR216C	*YBP1*						1.3	1
YBR225W					-1.2			1
YBR246W							-1.4	1
YBR295W	*PCA1*						-1.8	1
YBR297W	*MAL33*						-2	1
YBR299W	*MAL32*					2.6		1
YCL037C	*SRO9*					2.1		1
YCL045C							-1.4	1
YCR001W					1.6			1
YCR008W	*SAT4*				-1.3			1
YCR020W-B	*HTL1*						6.1	1
YCR027C	*RHB1*						-3.2	1
YCR028C-A	*RIM1*						2.55	1
YCR045C					-1.5			1
YCR082W	*AHC2*					1.2		1
YCR085W					-0.9			1
YCR086W	*CSM1*				-1.5			1
YCR101C						2.5		1
YDL002C	*NHP10*				1.2			1
YDL006W	*PTC1*			-2.05				1
YDL020C	*RPN4*				-1.7			1
YDL040C	*NAT1*				-3.3			1
YDL073W					1.7			1

YDL090C	*RAM1*				1.9			1
YDL160C	*DHH1*				-2.5			1
YDL216C	*RRI1*					1.9		1
YDR006C	*SOK1*				-1			1
YDR083W	*RRP8*					-2.6		1
YDR098C	*GRX3*					-1.7		1
YDR144C	*MKC7*						1.5	1
YDR146C	*SWI5*						1.2	1
YDR159W	*SAC3*		-1.4					1
YDR173C	*ARG82*						2.6	1
YDR194C	*MSS116*						3.1	1
YDR269C							-1.6	1
YDR276C	*PMP3*						1.8	1
YDR283C	*GCN2*					2		1
YDR296W	*MHR1*						3.8	1
YDR298C	*ATP5*						4.6	1
YDR314C	*RAD34*					1.8		1
YDR348C							1.3	1
YDR350C	*ATP22*						2.9	1
YDR354W	*TRP4*					1.7		1
YDR389W	*SAC7*						-2.4	1
YDR393W	*SHE9*						2.4	1
YDR403W	*DIT1*					1.7		1
YDR422C	*SIP1*		-1.3					1
YDR456W	*NHX1*			-1.2				1
YDR462W	*MRPL28*						2	1
YDR465C	*RMT2*					2		1
YDR512C	*EMI1*						3.3	1
YEL009C	*GCN4*			-1.5				1
YEL023C						2		1
YER031C	*YPT31*				-1.9			1
YER051W	*JHD1*					2.2		1
YER059W	*PCL6*					-2.4		1
YER066C-A						2.3		1
YER120W	*SCS2*					-1.2		1
YER164W	*CHD1*				-1.6			1
YFL010C	*WWM1*				1.1			1
YFL016C	*MDJ1*						2.4	1
YFL041W	*FET5*					2.1		1
YFR026C						1.8		1
YFR034C	*PHO4*					-2.3		1
YGL016W	*KAP122*						1.5	1
YGL020C	*GET1*		-1.8					1
YGL025C	*PGD1*						2.8	1

YGL035C	*MIG1*				-1.5			1
YGL046W				-1.1				1
YGL066W	*SGF73*						3.3	1
YGL087C	*MMS2*						2.1	1
YGL127C	*SOH1*				2			1
YGL136C	*MRM2*						2.2	1
YGL138C						2.3		1
YGL167C	*PMR1*		-1.3					1
YGL168W	*HUR1*		-0.9					1
YGL200C	*EMP24*		-1.3					1
YGL218W							3.2	1
YGL226C-A	*OST5*					2.5		1
YGL227W	*VID30*					1.6		1
YGL229C	*SAP4*					2.2		1
YGL240W	*DOC1*						4.2	1
YGL244W	*RTF1*						2.6	1
YGR007W	*MUQ1*						-2.4	1
YGR072W	*UPF3*						-1.3	1
YGR097W	*ASK10*					2.6		1
YGR101W	*PCP1*						3.8	1
YGR104C	*SRB5*						3	1
YGR122W				-1.1				1
YGR143W	*SKN1*				1.8			1
YGR200C	*ELP2*						2.4	1
YGR209C	*TRX2*						-1.2	1
YGR213C	*RTA1*						-1.3	1
YGR219W							2.9	1
YGR228W					-1.4			1
YGR229C	*SMI1*				-2.6			1
YGR230W	*BNS1*				1.8			1
YGR231C	*PHB2*					2.2		1
YGR233C	*PHO81*						2.5	1
YGR272C							3.6	1
YGR295C	*COS6*					1.9		1
YHL007C	*STE20*					-1.8		1
YHL009C	*YAP3*				-1.8			1
YHL014C	*YLF2*				-1.6			1
YHL034C	*SBP1*				-2			1
YHR001W-A	*QCR10*						-1.1	1
YHR004C	*NEM1*				-2.1			1
YHR010W	*RPL27A*						2.5	1
YHR014W	*SPO13*				1.5			1
YHR045W						-1.8		1
YHR060W	*VMA22*			-1.5				1

YHR064C	*SSZ1*						2.8	1
YHR079C-B						2.4		1
YHR116W	*COX23*						1.7	1
YHR142W	*CHS7*					2.2		1
YHR147C	*MRPL6*						2.15	1
YHR182W			-2					1
YHR194W	*MDM31*						3.2	1
YIL017C	*VID28*						3.1	1
YIL032C					1.3			1
YIL036W	*CST6*						4.5	1
YIL047C	*SYG1*						3.4	1
YIL052C	*RPL34B*				-3.05			1
YIL053W	*RHR2*						1.4	1
YIL098C	*FMC1*						2	1
YIR005W	*IST3*				-2.1			1
YIR024C							1.5	1
YJL004C	*SYS1*				-1.6			1
YJL023C	*PET130*						2.2	1
YJL062W	*LAS21*					2.7		1
YJL080C	*SCP160*					1.3		1
YJL098W	*SAP185*				0.8			1
YJL099W	*CHS6*						2.6	1
YJL108C	*PRM10*				1.4			1
YJL124C	*LSM1*				-3.65			1
YJL131C			-1.3					1
YJL132W					-1.3			1
YJL149W							-1.9	1
YJL172W	*CPS1*				-2.7			1
YJL192C	*SOP4*				-2			1
YJR032W	*CPR7*						3.2	1
YJR044C	*VPS55*					2.2		1
YJR055W	*HIT1*						2.3	1
YJR088C						2.8		1
YJR105W	*ADO1*					2		1
YJR113C	*RSM7*						2.7	1
YJR121W	*ATP2*					-2.1		1
YKL003C	*MRP17*					2.3		1
YKL016C	*ATP7*						2.5	1
YKL025C	*PAN3*				-1.5			1
YKL040C	*NFU1*				-1			1
YKL041W	*VPS24*				-1.8			1
YKL048C	*ELM1*						3.5	1
YKL053W							-1.5	1
YKL061W							-1	1

YKL066W						3.4		1
YKL068W	*NUP100*					1.2		1
YKL087C	*CYT2*			-0.9				1
YKL096W-A	*CWP2*		-1.6					1
YKL098W							-2.3	1
YKL110C	*KTI12*						2.6	1
YKL114C	*APN1*				2.3			1
YKL134C	*39356*						3.1	1
YKL150W	*MCR1*					1.4		1
YKL166C	*TPK3*					2.1		1
YKL169C							2.7	1
YKL207W							-1.4	1
YKR019C	*IRS4*				-1.6			1
YKR028W	*SAP190*						2.3	1
YKR052C	*MRS4*					-1.9		1
YKR077W						1.5		1
YKR095W	*MLP1*				-1.3			1
YLL021W	*SPA2*						1.4	1
YLR043C	*TRX1*					1.1		1
YLR044C	*PDC1*						1.3	1
YLR053C						1.5		1
YLR057W				-1.2				1
YLR059C	*REX2*						1.3	1
YLR067C	*PET309*			1				1
YLR069C	*MEF1*						3.05	1
YLR079W	*SIC1*				-2.1			1
YLR104W						0.9		1
YLR139C	*SLS1*						2.9	1
YLR148W	*PEP3*			-2.3				1
YLR165C	*PUS5*					1		1
YLR176C	*RFX1*						1.4	1
YLR180W	*SAM1*						1.2	1
YLR214W	*FRE1*				-1.9			1
YLR225C							1.5	1
YLR232W					1			1
YLR257W					1.6			1
YLR262C	*YPT6*		-1.6					1
YLR268W	*SEC22*		-1.5					1
YLR270W	*DCS1*			1.1				1
YLR295C	*ATP14*						3.6	1
YLR297W					1.6			1
YLR312W-A	*MRPL15*						1.3	1
YLR326W						1.3		1
YLR337C	*VRP1*					2.6		1

YLR338W	*OPI9*				2.6			1
YLR357W	*RSC2*						2.4	1
YLR358C							2.9	1
YLR368W	*MDM30*						2.3	1
YLR384C	*IKI3*						2.35	1
YLR418C	*CDC73*						2.9	1
YLR439W	*MRPL4*						2.9	1
YML008C	*ERG6*			-1.4				1
YML013C-A				-1.4				1
YML017W	*PSP2*				-1.1			1
YML021C	*UNG1*						-1.8	1
YMR004W	*MVP1*				-1.3			1
YMR029C	*FAR8*				-1.1			1
YMR063W	*RIM9*			-1.1				1
YMR064W	*AEP1*						3.5	1
YMR066W	*SOV1*						3.65	1
YMR071C	*TVP18*						-2.5	1
YMR075W	*RCO1*		-1.2					1
YMR135W-A						1.3		1
YMR155W						0.9		1
YMR158W	*MRPS8*						1.9	1
YMR175W	*SIP18*				1.5			1
YMR194W	*RPL36A*					-1.4		1
YMR205C	*PFK2*					-2.5		1
YMR214W	*SCJ1*						-2.1	1
YMR258C							-1.9	1
YMR261C	*TPS3*				1.8			1
YMR275C	*BUL1*			-1.4				1
YMR276W	*DSK2*		-1.1					1
YMR282C	*AEP2*						2.95	1
YMR287C	*DSS1*						1.8	1
YMR294W-A						2.7		1
YMR310C					1.4			1
YNL005C	*MRP7*						1.9	1
YNL022C			-0.8					1
YNL055C	*POR1*						4.2	1
YNL058C					1.8			1
YNL097C	*PHO23*						2.4	1
YNL100W						1.7		1
YNL121C	*TOM70*						1.8	1
YNL127W	*FAR11*				-1.2			1
YNL130C	*CPT1*						1.5	1
YNL175C	*NOP13*						-2.7	1

YNL184C							2.1	1
YNL198C					-1.1			1
YNL204C	*SPS18*				-1.4			1
YNL229C	*URE2*				1.4			1
YNR036C							1.5	1
YNR037C	*RSM19*						1.9	1
YOL009C	*MDM12*						2.5	1
YOL064C	*MET22*						-2.6	1
YOL101C	*IZH4*					1.3		1
YOL115W	*PAP2*				-2.9			1
YOR009W	*TIR4*					1		1
YOR014W	*RTS1*						2.5	1
YOR019W						2		1
YOR030W	*DFG16*			-1.2				1
YOR036W	*PEP12*			-2				1
YOR043W	*WHI2*						1.4	1
YOR044W	*IRC23*				1.3			1
YOR091W	*TMA46*						1.7	1
YOR106W	*VAM3*		-2.2					1
YOR150W	*MRPL23*			1				1
YOR199W							2.8	1
YOR211C	*MGM1*						2.6	1
YOR234C	*RPL33B*					4.2		1
YOR251C							1.5	1
YOR293W	*RPS10A*	-1.3						1
YOR309C						1.7		1
YOR330C	*MIP1*			0.8				1
YPL002C	*SNF8*			-1.3				1
YPL051W	*ARL3*				-2			1
YPL052W	*OAZ1*				1.5			1
YPL065W	*VPS28*			-1.3				1
YPL101W	*ELP4*						2.55	1
YPL102C						1.8		1
YPL170W	*DAP1*					-1.6		1
YPL182C							2.2	1
YPL253C	*VIK1*						1.8	1
YPL261C				-0.6				1
YPL274W	*SAM3*					3.7		1
YPR012W						1.6		1
YPR014C						1.5		1
YPR067W	*ISA2*						2.5	1
YPR090W							-1.95	1
YPR131C	*NAT3*						2.8	1
YPR166C	*MRP2*						2.3	1

Appendix 3: Zinc sensitive and resistant genes identified

ORF	Standard Name	5 generations			15 generations			Number of Significant
		25% IC20	50% IC20	IC20	25% IC20	50% IC20	IC20	
		0.625 mM	1.25 μM	2.5 mM	0.625 mM	1.25 μM	2.5 mM	
YJL056C	*ZAP1*	1.55	1.8	1.4	5.1	4.9	4.6	6
YML097C	*VPS9*	-2.3	-2.75	-2.4	-2.8	-2.15	-3.3	6
YCR044C	*PER1*		1.8	1.4	3.4	3.9	4.85	5
YAL053W	*FLC2*		-1.6	-2.8		-1.7	-4.5	4
YBL038W	*MRPL16*			1.2	1.35	2.15	4.4	4
YDR495C	*VPS3*	-2.15	-2.35	-1.65	-2			4
YKL041W	*VPS24*	-1.1		-2.8		-1.35	-4.8	4
YMR238W	*DFG5*		-2.65	-2.5		-1.75	-4.25	4
YOR036W	*PEP12*	-2.7	-2.5		-2.4	-2.6		4
YOR089C	*VPS21*		-2	-1.8		-2.5	-3.65	4
YOR270C	*VPH1*	-2.9	-2.9	-3.8		-1.9		4
YAL002W	*VPS8*			-2.8		-1.1	-3.2	3
YBL061C	*SKT5*				1.8	1.3	4.7	3
YBR023C	*CHS3*				1.7	2	2.9	3
YBR069C	*TAT1*				1.3	2.05	3.8	3
YCL007C		-3.5	-3.5	-2.1				3
YCL010C	*SGF29*			-1		-1	-2.7	3
YDL226C	*GCS1*			-1.85		-1.85	-4	3
YDR455C				-2.7		-0.6	-3.8	3
YEL051W	*VMA8*	-2.95	-3.2	-1.5				3
YGL095C	*VPS45*	-3.1		-2.2	-2.1			3
YGL148W	*ARO2*			-1.5		-1.45	-3.1	3
YGR063C	*SPT4*			1.1		1.45	3.95	3
YHR060W	*VMA22*	-3.4	-4.15	-2.1				3
YHR142W	*CHS7*				1.55	2.05	3.55	3
YJL099W	*CHS6*				0.9	1.2	2.7	3
YJL204C	*RCY1*			-1.65		-1.05	-3.75	3
YJR059W	*PTK2*			0.9		1	2.3	3
YKL080W	*VMA5*	-3.4	-3.8	-3.35				3
YKL119C	*VPH2*	-3.05	-3.5	-2.2				3
YLL033W	*IRC19*			1.6		1.4	2.8	3
YMR193W	*MRPL24*			1		1.4	2.9	3
YMR243C	*ZRC1*			-3.2		-1.1	-5.5	3
YNL322C	*KRE1*		-1.7	-1.45		-1.25		3
YNR006W	*VPS27*			-2.6		-0.7	-3.9	3
YOL001W	*PHO80*		-1.5	-2.5		-4.35		3
YOR061W	*CKA2*			1		0.7	1.75	3
YPL118W	*MRP51*			0.8		1.4	2.65	3
YPL179W	*PPQ1*			-1.75		-1.25	-4.5	3

YPL182C				1.2		-1.1	-3.1	3
YPR173C	*VPS4*			-3.4		-2.4	-3.8	3
YBR036C	*CSG2*					-1	-2.3	2
YBR068C	*BAP2*					-0.8	-2.55	2
YBR131W	*CCZ1*			-3.65		-4.05		2
YBR287W	*ZSP1*			-4.35			-4.2	2
YBR290W	*BSD2*					0.75	2	2
YCR028C	*FEN2*					1.1	2.55	2
YCR049C				-2.1			-1.5	2
YDR065W				1.4			3.2	2
YDR098C	*GRX3*					-2.1	-3.75	2
YDR202C	*RAV2*			-1.7			-3	2
YDR203W				-1.55			-3.9	2
YDR241W	*BUD26*			1.2			2.75	2
YDR245W	*MNN10*			1.7			3.5	2
YDR323C	*PEP7*	-2.8	-3.5					2
YDR359C	*VID21*			1.35			2.9	2
YDR363W-A	*SEM1*			1.4			3.35	2
YDR377W	*ATP17*			1.6			3.2	2
YDR484W	*VPS52*			-2.3			-3.6	2
YDR507C	*GIN4*					0.9	1.8	2
YEL036C	*ANP1*			2			3.3	2
YEL050C	*RML2*					1.4	3.15	2
YER077C				1.2			2.4	2
YER111C	*SWI4*	-1.4		1.3				2
YER122C	*GLO3*					1.6	2.4	2
YER123W	*YCK3*			-1.55			-2.1	2
YER145C	*FTR1*			-1.3			-2.1	2
YER177W	*BMH1*		-0.8	-0.9				2
YFR010W	*UBP6*			1.8			-2.5	2
YFR034C	*PHO4*					1.5	4.2	2
YGL076C	*RPL7A*	1.1		1.65				2
YGL124C	*MON1*			-3.1		-2.35		2
YGL167C	*PMR1*	-2.3	-2.1					2
YGR064W						1.3	3.85	2
YGR215W	*RSM27*			1.1		1.6		2
YGR220C	*MRPL9*					0.9	1.6	2
YHL011C	*PRS3*			1.2			3	2
YHL014C	*YLF2*			-1.4			-1.6	2
YHR011W	*DIA4*			1.4			3.45	2
YHR045W						-0.8	-3.6	2
YHR104W	*GRE3*			-1.1			-2.5	2
YHR111W	*UBA4*					1.2	1.9	2
YIL015C-A						2	3.35	2

YIL053W	*RHR2*					0.7	1.6	2
YIL060W						1.1	2.8	2
YIL154C	*IMP2'*			-1.95			-4	2
YIR023W	*DAL81*					1.7	3.3	2
YJL095W	*BCK1*			1.35	1.5			2
YJL128C	*PBS2*			1.1			2	2
YJR033C	*RAV1*			-2.55		-2.45		2
YJR040W	*GEF1*			-1.6			-4.2	2
YJR083C	*ACF4*			-1			-1.7	2
YJR102C	*VPS25*			-2.15			-3.4	2
YJR129C				-1.6			-2.2	2
YKL077W						0.7	2.6	2
YKL121W				-1.3			-2.8	2
YKL147C				-1.1			-1.6	2
YKL160W	*ELF1*					0.6	1.8	2
YKR019C	*IRS4*			-1.6			-1.5	2
YKR035W-A	*DID2*			-2.3			-1.4	2
YKR052C	*MRS4*					-1.25	-4.4	2
YLL006W	*MMM1*			1.7			3.1	2
YLL045C	*RPL8B*			0.8			1.95	2
YLR006C	*SSK1*			1.1			1.4	2
YLR025W	*SNF7*			-1.05			-4	2
YLR047C	*FRE8*					-0.95	-3.45	2
YLR111W						1.05	2.25	2
YLR148W	*PEP3*	-3.1		-2.1				2
YLR174W	*IDP2*			-1			1.2	2
YLR358C				1.3			2.75	2
YLR369W	*SSQ1*			1.1			2.15	2
YLR370C	*ARC18*					0.9	2.85	2
YLR380W	*CSR1*					-1.05	-2.55	2
YLR382C	*NAM2*			1.3		1.2		2
YLR417W	*VPS36*			-1.9			-3.25	2
YLR425W	*TUS1*					1	3.2	2
YML013W	*SEL1*					-1.6	-2.8	2
YML115C	*VAN1*					1.5	2.5	2
YML122C				1.6			3.1	2
YML123C	*PHO84*					1	3.85	2
YMR016C	*SOK2*					1	1.7	2
YMR058W	*FET3*			-0.8			-2.1	2
YMR228W	*MTF1*					1.1	2.05	2
YMR267W	*PPA2*					2.3	4.9	2
YNL051W	*COG5*					-0.8	-2.1	2
YNL236W	*SIN4*			2.6			2.8	2
YNL259C	*ATX1*			-1			-3.95	2

YNL323W	*LEM3*			-2.5		-2.4		2
YNL329C	*PEX6*					-0.9	-1.6	2
YOR035C	*SHE4*					1.25	4.15	2
YOR070C	*GYP1*			-1.65			-2.5	2
YOR201C	*MRM1*					1.9	2.9	2
YOR205C	*FMP38*			1		1.5		2
YOR331C		-1.6		-1.9				2
YPL005W	*AEP3*			1.3		1.5		2
YPL057C	*SUR1*					-0.85	-1.9	2
YPL065W	*VPS28*			-1.15			-4.6	2
YPL157W	*TGS1*			1.7			3.35	2
YPL170W	*DAP1*					-1.45	-4.85	2
YPL181W	*CTI6*			1			-2.8	2
YPR065W	*ROX1*			-1.6			-2.15	2
YPR106W	*ISR1*					0.8	1.9	2
YPR153W				-1			-1.7	2
YAL009W	*SPO7*						-2.4	1
YAL019W	*FUN30*			-1.2				1
YAL022C	*FUN26*			-0.8				1
YAL026C	*DRS2*						-4.3	1
YAL040C	*CLN3*			-1.7				1
YAL047C	*SPC72*			1.7				1
YAL048C	*GEM1*						1	1
YAL058C-A				-1.4				1
YAL058W	*CNE1*			-1.7				1
YBL013W	*FMT1*						4.7	1
YBL039C	*URA7*						2.1	1
YBL051C	*PIN4*						-2.1	1
YBL054W							-1.6	1
YBL062W							3.5	1
YBL065W							6.5	1
YBL071C							1.8	1
YBL082C	*ALG3*						2	1
YBL083C							1.8	1
YBL087C	*RPL23A*			1.6				1
YBL090W	*MRP21*						3.1	1
YBR035C	*PDX3*					-1.65		1
YBR037C	*SCO1*						2.2	1
YBR042C							1.2	1
YBR044C	*TCM62*						1.9	1
YBR075W							1.9	1
YBR114W	*RAD16*						1.8	1
YBR125C	*PTC4*						-1.3	1
YBR138C							3.9	1

YBR149W	*ARA1*						2.3	1
YBR156C	*SLI15*						1.9	1
YBR163W	*DEM1*						2.3	1
YBR170C	*NPL4*						3	1
YBR171W	*SEC66*						2.55	1
YBR173C	*UMP1*						1.9	1
YBR175W	*SWD3*						-1.8	1
YBR187W	*GDT1*						2.9	1
YBR207W	*FTH1*						-2	1
YBR208C	*DUR1,2*						-1.7	1
YBR213W	*MET8*						2.3	1
YBR216C	*YBP1*						1.3	1
YBR221C	*PDB1*					-1		1
YBR229C	*ROT2*			-1.05				1
YBR238C							1.4	1
YBR251W	*MRPS5*					1.35		1
YBR260C	*RGD1*					0.7		1
YBR268W	*MRPL37*						2.5	1
YBR286W	*APE3*		-1.2					1
YBR288C	*APM3*			-1.7				1
YBR291C	*CTP1*			-1.5				1
YBR292C				-0.7				1
YBR298C	*MAL31*			-1.45				1
YBR300C				-1.4				1
YCL001W-A				-1.9				1
YCL005W	*LDB16*						4.2	1
YCL008C	*STP22*			-2.1				1
YCL030C	*HIS4*						2.7	1
YCL046W							1.9	1
YCL058C	*FYV5*						3.55	1
YCL062W				-1.2				1
YCR001W							1.7	1
YCR006C							3	1
YCR007C							2.8	1
YCR011C	*ADP1*						2	1
YCR020C-A	*MAK31*						1	1
YCR024C	*SLM5*						1.6	1
YCR026C	*NPP1*			-1.3				1
YCR045C				-1.3				1
YCR050C				-2.4				1
YCR051W				-1.1				1
YCR060W	*TAH1*			-1.2				1
YCR063W	*BUD31*						3	1
YCR068W	*ATG15*			-1.1				1

YCR071C	*IMG2*			-1.7				1
YCR073W-A	*SOL2*						3.9	1
YCR079W	*PTC6*			-1				1
YCR081W	*SRB8*						-3.3	1
YCR082W	*AHC2*						1.5	1
YCR086W	*CSM1*			-1				1
YCR087C-A	*LUG1*			-1.2				1
YCR087W				-0.9				1
YCR095C	*OCA4*						2.3	1
YCR101C							2.7	1
YDL006W	*PTC1*			-1.6				1
YDL010W							4.3	1
YDL041W						-1.3		1
YDL044C	*MTF2*						2.5	1
YDL065C	*PEX19*					-0.9		1
YDL066W	*IDP1*						1.7	1
YDL070W	*BDF2*						1.8	1
YDL075W	*RPL31A*			1.6				1
YDL118W							-2.6	1
YDL130W	*RPP1B*						1.9	1
YDL133W							-2.2	1
YDL151C	*BUD30*						3.1	1
YDL182W	*LYS20*						-1.2	1
YDL194W	*SNF3*						1.8	1
YDL202W	*MRPL11*						3.4	1
YDL223C	*HBT1*						2.25	1
YDR006C	*SOK1*						-1	1
YDR008C				-1.6				1
YDR011W	*SNQ2*						-1.2	1
YDR025W	*RPS11A*						3.1	1
YDR028C	*REG1*			1				1
YDR057W	*YOS9*						-1.9	1
YDR069C	*DOA4*			2.25				1
YDR072C	*IPT1*						-2.55	1
YDR080W	*VPS41*			-1.75				1
YDR100W	*TVP15*			2.1				1
YDR101C	*ARX1*					0.9		1
YDR105C	*TMS1*						2.4	1
YDR122W	*KIN1*						3.8	1
YDR138W	*HPR1*			2.25				1
YDR140W	*MTQ2*			1.5				1
YDR153C	*ENT5*						3.3	1
YDR159W	*SAC3*						2.7	1
YDR161W				1.4				1

YDR162C	*NBP2*			-2				1
YDR175C	*RSM24*						4.4	1
YDR186C							-4.45	1
YDR194C	*MSS116*			1.75				1
YDR258C	*HSP78*						-1.4	1
YDR269C							-5.35	1
YDR270W	*CCC2*						-4.2	1
YDR271C							-4.7	1
YDR290W							1.6	1
YDR291W	*HRQ1*						4.6	1
YDR298C	*ATP5*						2.2	1
YDR322W	*MRPL35*						3.7	1
YDR335W	*MSN5*						-2.2	1
YDR337W	*MRPS28*			1.1				1
YDR371W	*CTS2*			-2.8				1
YDR378C	*LSM6*			1.5				1
YDR384C	*ATO3*						2.4	1
YDR385W	*EFT2*						2.9	1
YDR388W	*RVS167*						3.1	1
YDR393W	*SHE9*			1.2				1
YDR401W							2.5	1
YDR403W	*DIT1*						1.9	1
YDR414C	*ERD1*						2.6	1
YDR417C							3.1	1
YDR435C	*PPM1*						1.9	1
YDR441C	*APT2*						1.6	1
YDR443C	*SSN2*						-1.1	1
YDR447C	*RPS17B*						1.6	1
YDR450W	*RPS18A*						2.4	1
YDR456W	*NHX1*			-2.25				1
YDR457W	*TOM1*						1.7	1
YDR458C	*HEH2*						3.3	1
YDR462W	*MRPL28*						1.4	1
YDR474C							-1.5	1
YDR477W	*SNF1*					1.3		1
YDR486C	*VPS60*			-1.5				1
YDR530C	*APA2*						1	1
YEL003W	*GIM4*						1.7	1
YEL008W							1.6	1
YEL012W	*UBC8*						3.1	1
YEL027W	*CUP5*	-2.3						1
YEL028W							5.2	1
YEL044W	*IES6*			1.6				1
YEL054C	*RPL12A*						1.4	1

YEL065W	*SIT1*						-1.6	1
YER020W	*GPA2*			-1				1
YER041W	*YEN1*						-1.85	1
YER047C	*SAP1*						2.6	1
YER050C	*RSM18*						2.95	1
YER051W	*JHD1*						2.7	1
YER084W							-2	1
YER092W	*IES5*						1.85	1
YER098W	*UBP9*						-1	1
YER110C	*KAP123*						1.1	1
YER156C				-1.35				1
YER169W	*RPH1*						2.5	1
YFL010C	*WWM1*						1.1	1
YFL011W	*HXT10*						1.8	1
YFL013C	*IES1*						2.4	1
YFL013W-A							2.3	1
YFL015C							1.2	1
YFL025C	*BST1*						2.3	1
YFL036W	*RPO41*						2.9	1
YFL040W							1.3	1
YFR007W							-1.9	1
YFR016C							1.2	1
YFR018C							3.6	1
YFR024C-A	*LSB3*						1.3	1
YFR026C							2.1	1
YFR033C	*QCR6*			-0.9				1
YFR036W	*CDC26*			-1.2				1
YFR044C	*DUG1*						1.9	1
YFR048W	*RMD8*						2.4	1
YGL025C	*PGD1*					1.2		1
YGL038C	*OCH1*			2.55				1
YGL064C	*MRH4*					1.3		1
YGL071W	*AFT1*			-1.9				1
YGL082W							-2.1	1
YGL087C	*MMS2*						1.95	1
YGL138C							2.3	1
YGL149W				-2.9				1
YGL153W	*PEX14*						-1.4	1
YGL179C	*TOS3*						3.1	1
YGL212W	*VAM7*			-2.25				1
YGL215W	*CLG1*						2.2	1
YGL220W				-3				1
YGL226C-A	*OST5*						3	1
YGL229C	*SAP4*						2	1

YGR041W	*BUD9*						2.2	1
YGR070W	*ROM1*						2.7	1
YGR081C	*SLX9*					1		1
YGR102C							2.55	1
YGR122W				0.8				1
YGR130C							-2	1
YGR133W	*PEX4*					-1.4		1
YGR162W	*TIF4631*						2.55	1
YGR181W	*TIM13*					-1		1
YGR184C	*UBR1*						-2.8	1
YGR192C	*TDH3*						2.25	1
YGR200C	*ELP2*						2.7	1
YGR209C	*TRX2*						-2.55	1
YGR237C							-1.4	1
YGR240C	*PFK1*						2.9	1
YGR242W							2.3	1
YGR263C	*SAY1*						2.2	1
YGR282C	*BGL2*						2.65	1
YGR284C	*ERV29*						1.9	1
YGR295C	*COS6*						1.7	1
YHL020C	*OPI1*						-2.6	1
YHL039W							2.2	1
YHR010W	*RPL27A*			0.8				1
YHR013C	*ARD1*						-3.6	1
YHR014W	*SPO13*						1.5	1
YHR029C	*YHI9*						3.4	1
YHR034C	*PIH1*						3.05	1
YHR037W	*PUT2*						2.4	1
YHR061C	*GIC1*					0.7		1
YHR100C				1.65				1
YHR108W	*GGA2*						-2.5	1
YHR120W	*MSH1*			1.2				1
YHR151C				-1.4				1
YHR153C	*SPO16*						1.8	1
YHR179W	*OYE2*						-2.6	1
YHR200W	*RPN10*						-2.1	1
YHR206W	*SKN7*						1.4	1
YIL009C-A	*EST3*						3.5	1
YIL018W	*RPL2B*						2.2	1
YIL035C	*CKA1*						2.3	1
YIL036W	*CST6*						5.05	1
YIL052C	*RPL34B*			1				1
YIL067C							2.3	1
YIL069C	*RPS24B*						1.4	1

YIL090W	*ICE2*	2.1						1
YIL092W					1.2			1
YIL093C	*RSM25*						2.7	1
YIL098C	*FMC1*						-2.2	1
YIL107C	*PFK26*						1.7	1
YIL112W	*HOS4*						1.3	1
YIL139C	*REV7*						2.5	1
YIL148W	*RPL40A*			-1.6				1
YIL152W				-1.2				1
YIL153W	*RRD1*						2.55	1
YIL155C	*GUT2*			-0.9				1
YIL170W				-1.1				1
YIR028W	*DAL4*						4.1	1
YIR033W	*MGA2*			-2.35				1
YIR037W	*HYR1*						1.35	1
YJL024C	*APS3*			-1.4				1
YJL027C							-2	1
YJL029C	*VPS53*			-1.7				1
YJL062W	*LAS21*						3.1	1
YJL080C	*SCP160*						2	1
YJL094C	*KHA1*						-2.7	1
YJL121C	*RPE1*						3	1
YJL127C	*SPT10*						3	1
YJL130C	*URA2*						-1.6	1
YJL132W							-1.9	1
YJL136C	*RPS21B*						2.1	1
YJL149W							-2.2	1
YJL150W							-1.5	1
YJL154C	*VPS35*			-0.9				1
YJL155C	*FBP26*						-3.25	1
YJL168C	*SET2*						1.75	1
YJL172W	*CPS1*			2.5				1
YJL175W		2.1						1
YJL183W	*MNN11*						3.3	1
YJL193W							-2.2	1
YJL214W	*HXT8*						3.7	1
YJR015W							-1.5	1
YJR032W	*CPR7*						2.8	1
YJR074W	*MOG1*						-3.2	1
YJR088C							3.7	1
YJR118C	*ILM1*			1.2				1
YJR120W							-1.9	1
YJR145C	*RPS4A*			-1.5				1
YKL001C	*MET14*						2.4	1

YKL016C	*ATP7*			1.1				1
YKL025C	*PAN3*						-2.3	1
YKL054C	*DEF1*			1.6				1
YKL064W	*MNR2*			-1.4				1
YKL066W							2.8	1
YKL073W	*LHS1*						3.8	1
YKL074C	*MUD2*						1.3	1
YKL098W							-3.4	1
YKL113C	*RAD27*						-3.1	1
YKL133C							3	1
YKL174C	*TPO5*						4.1	1
YKL190W	*CNB1*						-1.4	1
YKL191W	*DPH2*						1.1	1
YKL197C	*PEX1*						-1.4	1
YKR020W	*VPS51*			-1.7				1
YKR024C	*DBP7*			1.9				1
YKR028W	*SAP190*						1.9	1
YKR031C	*SPO14*						-1.4	1
YKR035C	*OPI8*			-2.8				1
YKR040C				-1.1				1
YKR042W	*UTH1*					0.8		1
YKR046C	*PET10*						-1.6	1
YKR047W						0.8		1
YKR048C	*NAP1*					0.9		1
YKR061W	*KTR2*						1.6	1
YKR072C	*SIS2*						1.1	1
YKR078W							2.3	1
YKR082W	*NUP133*						2.5	1
YLL002W	*RTT109*			1.7				1
YLL007C							1.5	1
YLL014W		2.3						1
YLL023C							3.3	1
YLL027W	*ISA1*			1.3				1
YLL029W							-4	1
YLL043W	*FPS1*			2.15				1
YLL048C	*YBT1*						1	1
YLL051C	*FRE6*						1.5	1
YLR014C	*PPR1*			0.9				1
YLR020C	*YEH2*						-1.3	1
YLR021W	*IRC25*			1				1
YLR023C	*IZH3*						-1.5	1
YLR035C	*MLH2*			1.2				1
YLR036C							2.2	1
YLR041W				1				1

YLR044C	*PDC1*						2.05	1
YLR048W	*RPS0B*						3.5	1
YLR052W	*IES3*						2.9	1
YLR053C							1.5	1
YLR055C	*SPT8*						1.7	1
YLR061W	*RPL22A*			1.5				1
YLR062C	*BUD28*			1.1				1
YLR068W	*FYV7*						3.25	1
YLR069C	*MEF1*			1.5				1
YLR072W				0.9				1
YLR085C	*ARP6*						2.1	1
YLR091W				1.4				1
YLR108C							2.4	1
YLR110C	*CCW12*					1.1		1
YLR119W	*SRN2*						-3.45	1
YLR121C	*YPS3*						1.9	1
YLR126C							-2.1	1
YLR133W	*CKI1*						3.1	1
YLR146C	*SPE4*			1.1				1
YLR149C				1.35				1
YLR150W	*STM1*			0.95				1
YLR151C	*PCD1*			1				1
YLR168C				0.9				1
YLR169W							1.5	1
YLR172C	*DPH5*						1.2	1
YLR180W	*SAM1*			1.2				1
YLR190W	*MMR1*			1.3				1
YLR192C	*HCR1*			1.1				1
YLR193C	*UPS1*			0.8				1
YLR200W	*YKE2*						2.45	1
YLR203C	*MSS51*						3.9	1
YLR214W	*FRE1*			1				1
YLR225C				1.2				1
YLR226W	*BUR2*			1.5				1
YLR227C	*ADY4*			0.8				1
YLR228C	*ECM22*						-1.6	1
YLR231C	*BNA5*						1.7	1
YLR232W							-2.4	1
YLR240W	*VPS34*			2				1
YLR244C	*MAP1*			1.5				1
YLR261C	*VPS63*						2.6	1
YLR286C	*CTS1*						1.9	1
YLR295C	*ATP14*			1.6				1
YLR297W							1.8	1

YLR315W	*NKP2*						2.6	1
YLR322W	*VPS65*			1.6				1
YLR324W	*PEX30*			1.2				1
YLR330W	*CHS5*			1.7				1
YLR335W	*NUP2*						2.7	1
YLR349W							1.5	1
YLR368W	*MDM30*			1.1				1
YLR384C	*IKI3*						2.25	1
YLR386W	*VAC14*			1.5				1
YLR396C	*VPS33*		-1.9					1
YLR402W							3.6	1
YLR403W	*SFP1*			2.25				1
YLR422W							1.2	1
YLR436C	*ECM30*						1.2	1
YLR448W	*RPL6B*			1				1
YLR450W	*HMG2*						3.7	1
YLR451W	*LEU3*					-0.9		1
YML001W	*YPT7*			-2.3				1
YML009C	*MRPL39*						3.3	1
YML010C-B							3	1
YML017W	*PSP2*						-1.3	1
YML022W	*APT1*						1.4	1
YML028W	*TSA1*			-1.3				1
YML048W-A							2	1
YML051W	*GAL80*						-1.6	1
YML070W	*DAK1*						3.3	1
YML100W-A				-0.7				1
YML101C	*CUE4*			-0.7				1
YML103C	*NUP188*			-1.2				1
YML106W	*URA5*						1.65	1
YML107C	*PML39*						1.5	1
YML119W							3.4	1
YMR010W							-1.6	1
YMR021C	*MAC1*			-1.9				1
YMR029C	*FAR8*						-1.8	1
YMR052W	*FAR3*						-2.3	1
YMR066W	*SOV1*						2.5	1
YMR073C	*IRC21*						2.5	1
YMR075W	*RCO1*						2.5	1
YMR077C	*VPS20*			-2.05				1
YMR097C	*MTG1*						3.35	1
YMR123W	*PKR1*			-2.3				1
YMR142C	*RPL13B*			1.4				1
YMR158W	*MRPS8*						1.6	1

YMR166C							2.4	1
YMR184W	*ADD37*						2.1	1
YMR194W	*RPL36A*						1	1
YMR204C	*INP1*						2.2	1
YMR209C							-2.65	1
YMR214W	*SCJ1*			-1.4				1
YMR216C	*SKY1*			1.6				1
YMR272C	*SCS7*						2.25	1
YMR275C	*BUL1*					0.8		1
YMR280C	*CAT8*						2.6	1
YMR284W	*YKU70*						2.2	1
YMR286W	*MRPL33*						2.5	1
YMR293C							2.25	1
YMR294W-A							2.2	1
YMR299C	*DYN3*						1.7	1
YMR304W	*UBP15*						4.2	1
YMR307W	*GAS1*			-2.2				1
YMR310C							1.5	1
YMR311C	*GLC8*			-1.3				1
YMR312W	*ELP6*						3.1	1
YNL003C	*PET8*			1.1				1
YNL041C	*COG6*					-1		1
YNL047C	*SLM2*						3.5	1
YNL059C	*ARP5*			2				1
YNL097C	*PHO23*						-3.6	1
YNL101W	*AVT4*						2.1	1
YNL105W							1.7	1
YNL107W	*YAF9*						2.2	1
YNL108C							1.5	1
YNL109W							1.6	1
YNL119W	*NCS2*						3	1
YNL120C							2.75	1
YNL127W	*FAR11*						-2	1
YNL138W	*SRV2*			2.45				1
YNL140C							4.2	1
YNL179C				-0.8				1
YNL183C	*NPR1*						1.3	1
YNL204C	*SPS18*			-1.4				1
YNL205C				-0.9				1
YNL215W	*IES2*			1				1
YNL225C	*CNM67*			1.1				1
YNL231C	*PDR16*						-4.6	1
YNL248C	*RPA49*						2.6	1
YNL271C	*BNI1*						3.05	1

YNL284C	*MRPL10*						3.4	1
YNL288W	*CAF40*						1.1	1
YNL294C	*RIM21*			1				1
YNL305C							3.4	1
YNL315C	*ATP11*					-1.3		1
YNR005C							-2.5	1
YNR024W							1.6	1
YNR051C	*BRE5*						-1.3	1
YOL002C	*IZH2*						-1.6	1
YOL009C	*MDM12*			1.25				1
YOL018C	*TLG2*			-1.6				1
YOL023W	*IFM1*					1.5		1
YOL050C						0.6		1
YOL114C				-1.4				1
YOL115W	*PAP2*						3	1
YOL116W	*MSN1*						1.8	1
YOL118C							3.9	1
YOR006C							2.5	1
YOR030W	*DFG16*			1.5				1
YOR039W	*CKB2*			1.3				1
YOR042W	*CUE5*						-1.3	1
YOR052C							-1.3	1
YOR054C	*VHS3*						2.5	1
YOR065W	*CYT1*						2.1	1
YOR072W							-2.1	1
YOR078W	*BUD21*						2.4	1
YOR085W	*OST3*			-1.6				1
YOR092W	*ECM3*						3.2	1
YOR123C	*LEO1*						2	1
YOR133W	*EFT1*						3.7	1
YOR140W	*SFL1*						-1.9	1
YOR141C	*ARP8*						2.6	1
YOR164C							-2.3	1
YOR183W	*FYV12*						2.5	1
YOR211C	*MGM1*			1.1				1
YOR234C	*RPL33B*						3.7	1
YOR246C							-2.35	1
YOR258W	*HNT3*						3.6	1
YOR297C	*TIM18*			0.9				1
YOR309C							2	1
YOR314W							2	1
YOR316C	*COT1*						-3.6	1
YOR322C	*LDB19*						-2.3	1
YOR352W							2.3	1

YPL002C	*SNF8*			-1.6				1
YPL035C							2.8	1
YPL069C	*BTS1*						2.7	1
YPL084W	*BRO1*						-3.1	1
YPL097W	*MSY1*						1.7	1
YPL101W	*ELP4*						2.55	1
YPL102C							2.45	1
YPL104W	*MSD1*						2.5	1
YPL115C	*BEM3*					0.6		1
YPL125W	*KAP120*						2.5	1
YPL138C	*SPP1*						-2.3	1
YPL161C	*BEM4*			1.2				1
YPL205C							2	1
YPL271W	*ATP15*			2				1
YPL274W	*SAM3*						2.8	1
YPR012W							1.5	1
YPR014C							1.7	1
YPR052C	*NHP6A*						-1.9	1
YPR053C							-1.4	1
YPR059C				-1.3				1
YPR064W				-1.2				1
YPR067W	*ISA2*					1		1
YPR079W	*MRL1*						-1.6	1
YPR116W				2.1				1
YPR123C				-1.75				1
YPR124W	*CTR1*			-1.75				1
YPR133W-A	*TOM5*						2	1
YPR140W	*TAZ1*						2.1	1

Appendix 4: DCVC sensitive and resistant genes identified

ORF	Standard Name	5 generations			Number of Significant
		25% IC20	50% IC20	IC20	
		4.5 μM	9 μM	18 μM	
YIL162W	*SUC2*	-4.2	-4.1	-4	3
YFR036W	*CDC26*	-3.2	-3.8	-3.05	3
YDR112W	*IRC2*	-2.7	-4	-2.95	3
YLR032W	*RAD5*		-2.2	-2.7	2
YCR066W	*RAD18*		-2.1	-2.4	2
YBR171W	*SEC66*		-2	-2.4	2
YAL002W	*VPS8*		-1.8	-2.3	2
YOR304C-A		-2	-2.5	-2.2	3
YML097C	*VPS9*		-2.3	-2.2	2
YKL188C	*PXA2*			-2	1
YMR141C				-2	1
YOR089C	*VPS21*		-1.9	-1.95	2
YGL154C	*LYS5*			-1.8	1
YDR338C				-1.8	1
YKL199C				-1.8	1
YML095C	*RAD10*			-1.8	1
YMR137C	*PSO2*		-1.8	-1.75	2
YGL164C	*YRB30*	-1.6	-1.5	-1.7	3
YAL024C	*LTE1*			-1.7	1
YDR247W	*VHS1*			-1.7	1
YER095W	*RAD51*			-1.7	1
YPL022W	*RAD1*			-1.65	1
YLR218C			-1.5	-1.6	2
YER162C	*RAD4*			-1.6	1
YKR046C	*PET10*	-1.4		-1.5	2
YMR237W	*BCH1*	-1.2		-1.5	2
YGL166W	*CUP2*			-1.4	1
YPL147W	*PXA1*			-1.4	1
YIL146C	*ECM37*			-1.4	1
YKL167C	*MRP49*			-1.4	1
YGL253W	*HXK2*			-1.4	1
YKL215C		-1.3	-1.1	-1.3	3
YKL197C	*PEX1*	-1.4		-1.3	2
YER067W		-1.3		-1.3	2
YKR033C		-1.3		-1.3	2
YOR346W	*REV1*			-1.3	1
YLR210W	*CLB4*			-1.3	1
YOR017W	*PET127*			-1.3	1
YHR110W	*ERP5*			-1.3	1

YDR291W	*HRQ1*			-1.3	1
YMR008C	*PLB1*			-1.2	1
YML109W	*ZDS2*			-1.2	1
YMR283C	*RIT1*			-1.2	1
YKL100C				-1.1	1
YDL034W				1.2	1
YJR154W				1.3	1
YDR463W	*STP1*			1.3	1
YCR082W	*AHC2*		1.5	1.4	2
YOR006C				1.4	1
YDR333C				1.4	1
YPL123C	*RNY1*			1.4	1
YCR001W			1.6	1.5	2
YJR051W	*OSM1*		1.6	1.5	2
YMR238W	*DFG5*		2.1	1.5	2
YMR124W		1.4		1.5	2
YGL198W	*YIP4*	1.4		1.5	2
YDR440W	*DOT1*			1.5	1
YML124C	*TUB3*			1.55	1
YCR060W	*TAH1*	1.2	1.4	1.6	3
YOR085W	*OST3*		1.5	1.6	2
YLR093C	*NYV1*	2.1	1.6	1.6	3
YBL107C			1.7	1.6	2
YPR201W	*ARR3*		1.7	1.6	2
YOR183W	*FYV12*		1.7	1.6	2
YOR137C	*SIA1*	1.7	1.8	1.6	3
YDR217C	*RAD9*	1.6		1.6	2
YLR023C	*IZH3*			1.6	1
YJL208C	*NUC1*	1.6	1.6	1.7	3
YPL197C		1.6	1.6	1.7	3
YGR192C	*TDH3*	1.7	1.9	1.7	3
YGR263C	*SAY1*		2.2	1.7	2
YDR441C	*APT2*	1.9	1.8	1.8	3
YLR202C		2	1.8	1.8	3
YML073C	*RPL6A*		1.8	1.8	2
YGL214W			1.8	1.8	2
YMR286W	*MRPL33*	1.9	2	1.8	3
YHR034C	*PIH1*		2	1.8	2
YKR035C	*OPI8*		2.4	1.8	2
YMR244C-A			2.8	1.8	2
YPL178W	*CBC2*		3	1.8	2
YCR011C	*ADP1*		1.8	1.9	2
YLR042C		2	1.9	1.9	3
YDR465C	*RMT2*		1.9	1.9	2

YEL068C			2	1.9	2
YMR294W-A			2.6	1.9	2
YGL252C	*RTG2*			1.9	1
YPL140C	*MKK2*	2.1	1.6	2	3
YLR057W		2.2	1.6	2	3
YMR272C	*SCS7*	2.3	1.9	2.1	3
YDR255C	*RMD5*	2.1	2.2	2.1	3
YJR130C	*STR2*		2.2	2.1	2
YOR021C		2.3	2.4	2.1	3
YFR018C			3.1	2.1	2
YFL021W	*GAT1*			2.1	1
YJL131C				2.1	1
YMR289W	*ABZ2*	2.5	2.4	2.15	3
YCL046W		1.9	1.9	2.2	3
YDR215C		1.8	2.1	2.2	3
YIL032C			2.1	2.2	2
YOR314W		2.5	2.3	2.2	3
YBR272C	*HSM3*	1.7		2.2	2
YFL025C	*BST1*			2.2	1
YIL090W	*ICE2*	2.1	2.6	2.3	3
YLR133W	*CKI1*		2.7	2.3	2
YHL039W				2.3	1
YML122C			2	2.4	2
YPR116W		2.8	2.2	2.4	3
YHR037W	*PUT2*		2.4	2.4	2
YOR133W	*EFT1*		3.1	2.4	2
YBR298C	*MAL31*	2.2		2.4	2
YDR389W	*SAC7*			2.4	1
YBR159W	*IFA38*	2.4	2	2.5	3
YLR262C	*YPT6*	2.5	2.1	2.5	3
YLR044C	*PDC1*	2.7	2.3	2.5	3
YMR166C			2.4	2.5	2
YBR113W		2.6	2.6	2.5	3
YER169W	*RPH1*	2.5	2.9	2.5	3
YDR153C	*ENT5*		3.1	2.5	2
YGR261C	*APL6*		3.7	2.5	2
YLR169W		2.6	2.3	2.6	3
YDR105C	*TMS1*	2.6	2.7	2.6	3
YGL229C	*SAP4*	2.5	2.4	2.7	3
YGL226C-A	*OST5*	2.5	2.5	2.7	3
YBR114W	*RAD16*	2.7	2.7	2.7	3
YCR006C		2.6	2.8	2.7	3
YGL138C		2.8	3	2.7	3
YBR175W	*SWD3*		3.9	2.7	2

YDL223C	*HBT1*	1.5	2.25	2.8	3
YDR175C	*RSM24*	2.8	2.3	2.8	3
YCR073W-A	*SOL2*	2.5	2.5	2.8	3
YHL011C	*PRS3*	3	2.6	2.8	3
YDR377W	*ATP17*	3.1	2.8	2.8	3
YDR456W	*NHX1*	3.5	2.9	2.8	3
YEL012W	*UBC8*		3.9	2.8	2
YJR044C	*VPS55*	2.8	2.8	2.9	3
YER066C-A		2.7	2.9	2.9	3
YLR450W	*HMG2*	3.3	2.8	3	3
YER002W	*NOP16*	3	3	3	3
YJR088C		3.2	3.1	3	3
YBR213W	*MET8*	3.1	3.1	3.1	3
YDR163W	*CWC15*	3	2.9	3.2	3
YPL157W	*TGS1*		3.8	3.2	2
YHR157W	*REC104*	3.2	3.1	3.3	3
YMR304W	*UBP15*	3.3	2.9	3.4	3
YMR261C	*TPS3*	3.3	2.9	3.5	3
YDR458C	*HEH2*	3.6	3.7	3.8	3
YBR187W	*GDT1*	4	4	4.3	3
YML079W				4.3	1
YEL056W	*HAT2*	-3.5	-3.1		2
YEL043W		-3.3	-2.8		2
YPL138C	*SPP1*	-1.9	-2.1		2
YPL167C	*REV3*		-1.7		1
YKL097C			-1.4		1
YOR253W	*NAT5*		-1.3		1
YMR326C			1.1		1
YNL010W		1.4	1.2		2
YLR121C	*YPS3*	1.6	1.4		2
YLR098C	*CHA4*		1.6		1
YDR314C	*RAD34*		1.6		1
YDR283C	*GCN2*		1.6		1
YJL108C	*PRM10*	1.6	1.7		2
YDR251W	*PAM1*	1.7	1.7		2
YLR192C	*HCR1*	1.7	1.7		2
YBL008W	*HIR1*		1.7		1
YML048W-A		1.7	1.8		2
YHR046C	*INM1*		1.9		1
YFL013W-A			1.9		1
YDR285W	*ZIP1*		1.9		1
YHR160C	*PEX18*		1.9		1
YKL096W-A	*CWP2*		1.9		1
YGR041W	*BUD9*		2		1

YOR161C	*PNS1*		2		1
YOR364W			2		1
YPR044C	*OPI11*		2		1
YJR010C-A	*SPC1*		2		1
YBR037C	*SCO1*		2.1		1
YKL174C	*TPO5*		2.1		1
YMR280C	*CAT8*		2.2		1
YMR262W			2.2		1
YBL062W			2.4		1
YLR335W	*NUP2*	1.6	2.5		2
YFL032W			2.5		1
YPL035C			2.5		1
YGL118C			2.5		1
YNL101W	*AVT4*		2.5		1
YFL019C			2.7		1
YOR086C	*TCB1*	3	2.8		2
YGL071W	*AFT1*	-2.5			1
YOR276W	*CAF20*	-2.2			1
YFL003C	*MSH4*	-1.9			1
YOR054C	*VHS3*	-1.8			1
YIL089W		-1.6			1
YDR057W	*YOS9*	-1.4			1
YLR131C	*ACE2*	1.3			1
YNL058C		1.4			1
YLR099C	*ICT1*	1.4			1
YOR041C		1.4			1
YLR018C	*POM34*	1.4			1
YLR456W		1.5			1
YLR443W	*ECM7*	1.5			1
YLR053C		1.6			1
YLR049C		1.7			1
YGR183C	*QCR9*	1.7			1
YMR175W	*SIP18*	1.8			1
YLR270W	*DCS1*	1.8			1
YBR044C	*TCM62*	1.9			1
YLR257W		2			1
YOR199W		2			1
YIL139C	*REV7*	2.2			1
YOR201C	*MRM1*	2.2			1
YLL009C	*COX17*	2.8			1